

Electronic Thesis and Dissertation Repository

8-22-2013 12:00 AM

Investigating the pathological response to beta amyloid toxicity in rats: the role of age and the antioxidant catalase-SKL

Hayley J. Nell
The University of Western Ontario

Supervisor
Dr. David Cechetto
The University of Western Ontario Joint Supervisor
Dr. Shawn Whitehead
The University of Western Ontario

Graduate Program in Anatomy and Cell Biology
A thesis submitted in partial fulfillment of the requirements for the degree in Master of Science
© Hayley J. Nell 2013

Follow this and additional works at: <https://ir.lib.uwo.ca/etd>



Part of the [Other Neuroscience and Neurobiology Commons](#)

Recommended Citation

Nell, Hayley J., "Investigating the pathological response to beta amyloid toxicity in rats: the role of age and the antioxidant catalase-SKL" (2013). *Electronic Thesis and Dissertation Repository*. 1497.
<https://ir.lib.uwo.ca/etd/1497>

This Dissertation/Thesis is brought to you for free and open access by Scholarship@Western. It has been accepted for inclusion in Electronic Thesis and Dissertation Repository by an authorized administrator of Scholarship@Western. For more information, please contact wlsadmin@uwo.ca.

INVESTIGATING THE PATHOLOGICAL RESPONSE TO BETA AMYLOID
TOXICITY IN RATS: THE ROLE OF AGE AND THE
ANTIOXIDANT CATALASE-SKL

(Thesis format: Monograph)

by

Hayley J. Nell

Graduate Program in Anatomy & Cell Biology

A thesis submitted in partial fulfillment
of the requirements for the degree of
Master of Science

The School of Graduate and Postdoctoral Studies
The University of Western Ontario
London, Ontario, Canada

© Hayley J. Nell 2013

Abstract

Accumulation of beta-amyloid (A β) in the brain is a major contributor to the cellular pathology and cognitive impairment observed in Alzheimer's disease (AD). In part, A β exerts its toxic effects by increasing reactive oxygen species (ROS) and neuroinflammation in the brain. Aging, a major risk factor for AD is also associated with increased production of ROS. This study investigated the age-related pathological response to A β toxicity and examined whether catalase-SKL (CAT-SKL), a genetically engineered derivative of the peroxisomal antioxidant enzyme catalase, is able to reduce A β toxicity. Bilateral intracerebroventricular (icv) injections of the A β_{25-35} peptide was used to model A β toxicity in 3, 6 and 9 months old male Wistar rats. A subset of 6 months old rats undergoing CAT-SKL treatment received CAT-SKL injections intraperitoneally (ip) once a week for four consecutive weeks. Control animals received bilateral icv injections of the reverse physiologically inactive A β_{35-25} peptide. Spatial learning and reference memory were assessed using the Morris Water Maze (MWM); histopathological and immunohistochemical analyses were used to evaluate neuroinflammation, and neuronal degeneration. A β_{25-35} icv administration in animals 6 and 9 months of age resulted in increased microglia activation and decreased number of cholinergic neurons in the basal forebrain and loss of neuronal integrity in the hippocampus in comparison to A β_{25-35} induced pathology in 3 months old animals. CAT-SKL treatment significantly decreased microglia activation and reduced cholinergic neuronal loss in the basal forebrain. A β_{25-35} animals showed deficits in long-term reference memory in the MWM, which was effectively ameliorated in A β_{25-35} animals treated with CAT-SKL. These findings demonstrate the importance of taking into consideration animal age when modeling A β toxicity, and provides support for the use of CAT-SKL in reducing neuroinflammation and long-term reference memory deficits induced by A β_{25-35} in the rat.

Key Words: Alzheimer's disease, A β , Neuroinflammation, Oxidative Stress, H₂O₂, Catalase

Acknowledgements

First, I would like to thank my supervisors Dr. David Cechetto and Dr. Shawn Whitehead for the opportunity to work in their lab in pursuit of my Masters degree and for their support and guidance along the way.

I would like to thank Dr. Stanley Terlecky and Courtney Giordino from Wayne State University for the provision of the CAT-SKL molecule and Dr. Paul Walton for his guidance, suggestions and feedback in regards to the CAT-SKL work. I also thank my supervisory committee members Dr. Lynne-Marie Postovit and Dr. Susanne Schmid for their input and suggestions.

Thank-you to the members of the Cechetto/Whitehead lab both past and present for their support, assistance and friendship; Jeff Hepburn, Zareen Amtul, Sarah Caughlin and especially Lin Wang who's assistance and patience was invaluable. Also, thank-you to the volunteers who spent many hours helping me with cell counts and tissue processing; Fan Liu, Sophia Liu, Cristina Marcello and Christal Huang. Also, I would like to thank Nicole MacLeod for everything she does.

Finally, I would like to thank my family. To my mom and dad who are and have always been my biggest supporters, and to my sister who is always there to cheer me up when I need it the most—I could not have done this without you.

Table of Contents

| | |
|---|------------|
| Abstract | ii |
| Acknowledgements | iii |
| Table of Contents | iv |
| List of Figures | vii |
| List of Tables | ix |
| List of Abbreviations | x |
| Section 1: Introduction | 1 |
| 1.1 Alzheimer’s Disease..... | 2 |
| 1.2 Genetics and Risk Factors..... | 3 |
| 1.3 Vulnerable brain regions in Alzheimer’s disease..... | 4 |
| 1.4 Beta amyloid..... | 6 |
| 1.5 The Amyloid Cascade hypothesis..... | 7 |
| 1.6 Cerebral Amyloid Angiopathy and vascular dysfunction in AD..... | 9 |
| 1.7 Neuroinflammation..... | 10 |
| 1.8 A role for peroxisomes and mitochondrial dysfunction in AD..... | 12 |
| 1.9 Reactive Oxygen Species and Oxidative Stress..... | 14 |
| 1.10 Beta-amyloid and H ₂ O ₂ | 17 |
| 1.11 Catalase-SKL: a targeted antioxidant approach..... | 19 |
| 1.12 Modeling AD in animals..... | 21 |
| 1.13 Rationale..... | 22 |
| 1.14 Hypothesis and Aims..... | 23 |
| Section 2: Methods | 24 |
| 2.1 Animals..... | 25 |
| 2.2 A β preperation..... | 25 |

| | |
|---|-----------|
| 2.3 Surgery..... | 25 |
| 2.4 Treatment groups..... | 26 |
| 2.5 Catalase administration..... | 29 |
| 2.6 Behaviour: Morris Water Maze..... | 29 |
| 2.7 Sacrifice..... | 32 |
| 2.8 Immunohistochemistry..... | 32 |
| 2.9 Dual label immunohistochemistry..... | 33 |
| 2.10 Histological Examination..... | 36 |
| 2.11 Imaging and Quantification..... | 36 |
| 2.12 Statistical Analysis..... | 40 |
| Section 3: Results..... | 41 |
| 3.1 Effect of Age and Aβ₂₅₋₃₅ Toxicity | |
| 3.1.1 Body Weight Changes..... | 42 |
| 3.1.2 Microglia Expression in the MSN/VDB..... | 42 |
| 3.1.3 Cholinergic neurons in the MSN/VDB..... | 44 |
| 3.1.4 Microglia and astroglial reactivity in the thalamus..... | 47 |
| 3.1.5 Astrocyte activation in the hippocampus..... | 47 |
| 3.1.6 Hippocampus integrity: H&E and thionin staining..... | 50 |
| 3.1.7 Leakiness of cerebrovasculature..... | 53 |
| 3.2 CAT-SKL and Aβ₂₅₋₃₅ toxicity | |
| 3.2.1 Body Weight Changes..... | 55 |
| 3.2.2 Microglia expression in CAT-SKL treated animals..... | 59 |
| 3.2.3 Cholinergic neurons in the MSN/VDB..... | 59 |
| 3.2.4 Astrocytes activation in the hippocampus..... | 62 |
| 3.2.5 Neuronal integrity in the hippocampus..... | 62 |
| 3.2.6 Behavior testing: Morris Water Maze..... | 65 |
| Section 4: Discussion..... | 73 |

| | |
|---|------------|
| 4.1 Neuroinflammation..... | 74 |
| 4.2 The basal forebrain cholinergic system..... | 76 |
| 4.3 Neuronal integrity..... | 77 |
| 4.4 CAT-SKL..... | 78 |
| 4.5 Behavior testing: Morris Water Maze..... | 82 |
| 4.6 Limitations and Future Directions..... | 84 |
| Section 5: Summary and Conclusions..... | 86 |
| References..... | 89 |
| Appendix..... | 104 |
| Ethics Approval..... | 105 |
| Curriculum Vitae..... | 107 |

List of Figures

| | |
|--|----|
| Figure 1. Role of A β in the production of reactive oxygen species and the resultant oxidative stress in Alzheimer's diseases..... | 18 |
| Figure 2. Treatment paradigm and time course for CAT-SKL injections, A β administration and behavior testing..... | 30 |
| Figure 3. Immunohistochemical controls..... | 35 |
| Figure 4. Atlas representations of the rat brain..... | 38 |
| Figure 5. Weight loss in 9 month A β_{25-35} treated rats..... | 43 |
| Figure 6. Increase in activated microglia in the medial septal nucleus/vertical diagonal band in response to A β_{25-35} | 45 |
| Figure 7. Age-dependent cholinergic neuronal loss in the basal forebrain..... | 46 |
| Figure 8. Age-related increase in thalamic microglia activation in response to A β_{25-35} | 48 |
| Figure 9. No changes in GFAP immunopositive astrocytes in the thalamus..... | 49 |
| Figure 10. Astrocyte activation in the CA3 region of the hippocampus..... | 51 |
| Figure 11. Neuronal numbers in the CA1 and CA3 subfields of the hippocampus..... | 52 |
| Figure 12. Thionin staining to evaluate neuronal integrity in the CA3 region of the hippocampus..... | 54 |
| Figure 13. Cerebromicrovessels in the CA1 and CA3 subfields of the hippocampus..... | 56 |
| Figure 14. Age-dependent leakiness of cerebromicrovessels in the thalamus.... | 57 |
| Figure 15. Body weight changes..... | 58 |
| Figure 16. CAT-SKL reduces microglia activation in the MSN/VDB and thalamus..... | 60 |
| Figure 17. CAT-SKL prevents cholinergic loss in the MSN/VDB..... | 61 |
| Figure 18. CAT-SKL reduces astrocyte activation in the CA3 region of the hippocampus..... | 63 |
| Figure 19. Neuronal integrity in the CA1 and CA3 regions of the hippocampus.. | 64 |
| Figure 20. Thionin staining in the hippocampus..... | 66 |

| | |
|--|----|
| Figure 21. Spatial learning during the hidden platform Morris Water Maze task..... | 68 |
| Figure 22. Probe trials: Short and long term memory retention | 70 |
| Figure 23. CAT-SKL reduces A β ₂₅₋₃₅ induced impairments in long-term reference memory | 71 |
| Figure 24. Cued learning during the Morris Water Maze..... | 72 |
| Figure 25. Summary of pathology induced by A β ₂₅₋₃₅ toxicity with and without CAT-SKL treatment..... | 81 |

List of Tables

| | |
|--|----|
| Table 1. Treatment groups and corresponding n values..... | 27 |
| Table 2. Treatment groups and corresponding n values for behavior, and immunohistochemical analysis for animals included in the CAT-SKL study..... | 28 |
| Table 3. Overview of the primary antibodies used for immunohistochemistry.... | 34 |

List of Abbreviations

| | |
|-----------------------------------|---------------------------------|
| Aβ | Beta-amyloid |
| AD | Alzheimer's Disease |
| ApoE | Apolipoprotein E |
| APP | Amyloid Precursor Protein |
| ATP | Adenosine triphosphate |
| BACE1 | Beta-site-APP-cleaving enzyme-1 |
| BBB | Blood-Brain-Barrier |
| CAA | Cerebral Amyloid Angiopathy |
| CAT-SKL | Catalase-serine-lysine-leucine |
| ChAT | Choline acetyltransferase |
| CNS | Central Nervous System |
| DAB | Diaminobenzidine |
| ddH₂O | Deionized water |
| FJB | Fluoro Jade B |
| GFAP | Glial Fibrillary Acidic Protein |
| HDB | Horizontal Diagonal band |
| HNE | 4-hydroxy-2-transnonenal |
| H&E | Hematoxylin and Eosin |
| H₂O₂ | Hydrogen Peroxide |
| icv | Intracerebroventricular |

| | |
|--------------------------------|---------------------------------------|
| IHC | Immunohistochemistry |
| ip | Intraperitoneal |
| KANL | Lysine-alanine-asparagine-leucine |
| MSN | Medial Septal Nucleus |
| NM | Nucleus Basalis of Meynert |
| NSAID | Non-Steroidal Anti-Inflammatory Drug |
| PBS(T) | Phosphate Buffered Saline (Triton X) |
| PFA | Paraformaldehyde |
| PS | Presenilin |
| PTS1 | Type 1 peroxisomal targeting sequence |
| ROS | Reactive Oxygen Species |
| RP | Reverse Peptide |
| TNF-α | Tumor necrosis factor α |
| VDB | Vertical Diagonal Band |
| 8-OHdG | 8-hydroxy-2'deoxyguanosine |

Section 1

INTRODUCTION

1.1 Alzheimer's Disease

Alzheimer's disease (AD) is a neurodegenerative disorder and is the most common cause of dementia in the elderly. Clinically, AD manifests itself in the early stages as impairments in learning and memory. As the disease progresses language, judgment, visuo-spatial skills and complex cognition are impaired, compromising the ability of the affected individual to carry out the activities of their day-to-day lives (Forstl and Kurz, 1999; Marcello 2008). AD is an age-related disease with the prevalence rising with increasing age. At present, 5-8% of Canadians over the age of 65 have AD, rising to approximately 30-50% of Canadians over the age of 85 (Smetanin et al., 2009). In 2006, there were 26.6 million cases of AD worldwide, a number predicted to increase to 106.8 million by 2050, due to the aging world population (Brookmeyer, 2007). The number of Canadians impacted by AD will continue to grow each year as the proportion of the population over 65 increases. Therefore, the need to better understand the pathophysiology of this age-related disease, and to find ways to delay the onset and slow the progression of this disease is of utmost importance.

Alzheimer's disease was first described by Alois Alzheimer in 1907 when he presented the progressive symptoms and mental deterioration of his patient Auguste D that left her delusional, aggressive and unable to remember recent events. Following her demise, he noted overt neurofibrillary tangles and neuritic plaques in her brain (Stelzmann et al., 1995). It wasn't until 1984 however, that it was discovered that beta-amyloid peptide ($A\beta$) was the primary protein component of plaques (Glennner and Wong, 1984). Today, the histopathological hallmarks of AD include the presence of extracellular amyloid plaques, intracellular neurofibrillary tangles, inflammation, neuronal degeneration and loss, and synaptic dysfunction and failure (Selkoe, 2001; Querfurth and LaFerla, 2010). Plaques are composed of insoluble extracellular aggregates of $A\beta$, a sticky peptide generated from the proteolytic cleavage of amyloid precursor protein (APP). Neurofibrillary tangles are the result of hyper-phosphorylation of the microtubule stabilizing protein tau (Hardy and Selkoe, 2002).

1.2 Genetics and Risk Factors

The cause of AD is thought to be due to complex interactions between multiple genetic, and environmental factors. Autosomal dominant mutations in the amyloid precursor protein (APP), presenilin-1 and presenilin-2 (PS1, PS2) encoding genes have been identified and are known to cause early-onset (<60 years) familial AD. However, the majority of AD cases are classified as sporadic and late-onset (>60 years) with the familial forms only accounting for 1-10% of AD cases (Campion et al., 1999; Selkoe, 2001). Apart from the earlier age-of onset for autosomal dominant forms of familial AD, both familial and sporadic AD progress in highly similar manners, with the clinical manifestations and pathophysiology of the disease processes usually being indistinguishable between the two types (Selkoe, 2001). Aside from the mutated genes implicated in familial AD, the most important genetic risk factor for AD is inheritance of the E4 allele of apolipoprotein E (apoE), the primary cholesterol transporter in the brain. Inheritance of two apoE4 alleles significantly increases the lifetime risk and lowers the age of onset of AD (Corder et al., 1993; Morishima-Kawashima et al., 2000). The lifetime risk estimate of developing AD for individuals with 2 copies of the apoE4 allele is around 60% by the age of 85, in comparison to those individuals with 2 copies of the apoE3 allele whose risk of developing AD by the age of 85 is around 10% (Genin et al., 2011).

Aging is the most important nongenetic risk factor for late-onset AD. Aging is associated with oxidative stress, glial activation, increased production of inflammatory mediators, decreased antioxidant functioning and accumulation of modified proteins and lipids, all of which take a toll on the brain (Wyss-Coray and Musck, 2002). However, despite all the changes that accompany the aging process, aging alone is not sufficient to initiate the disease process, some precipitating event is required. Risk factors that could be potential triggers for late-onset AD include but are not limited to; traumatic brain injury, diabetes mellitus, obesity, hyperlipidemia, hypertension, transient ischemic attacks, stroke and atherosclerosis (Grammas, 2011; Herrup 2010). Of these many are vascular

risk factors, suggesting that neurovascular dysfunction may contribute to the onset and/or progression of neurodegenerative events in AD (Grammas, 2002; 2011).

1.3 Vulnerable brain regions in Alzheimer's disease

AD causes a large loss in brain weight and volume, with vulnerable neuronal populations and brain areas being affected more than others (Huang and Mucke, 2012). Specifically, AD causes neuronal degeneration and loss in regions of the brain important for memory and learning with areas including the hippocampus, frontal cortex and limbic areas being particularly vulnerable (Marcello et al., 2008; Venkateshappa et al., 2012). Neuronal loss in these regions leads to significant impairments in intellectual abilities that are severe enough to disrupt social and occupational functioning (Gotz et al., 2011). One of the first neuronal populations identified as being vulnerable in AD was neurons synthesizing and releasing acetylcholine. Changes in activity of synthetic choline acetyltransferase and degradative acetylcholinesterase in the limbic and cerebral cortices along with loss of cholinergic cell bodies in the subcortical nuclei that project to these regions has been demonstrated in both human AD brains and in animal models of the disease (Selkoe, 2001). Specifically, degeneration of cholinergic neurons in the basal forebrain, which provides major cholinergic inputs to the hippocampus and neocortex, is thought to be one of the first neuronal populations affected in the disease process (Whitehouse et al., 1982; Coyle et al., 1983; Pearson et al., 1983; Schliebs, 2005). The basal forebrain cholinergic system is comprised of cell bodies in the medial septal nucleus (MSN), the vertical and horizontal bands of Broca (VDB, HDB) and the nucleus basalis of Meynert (NM) (Reviewed by Collerton, 1986; D'Hooge and De Deyn, 2001; Auld et al., 2002). Clinically, basal forebrain cholinergic deficits positively correlate with cognitive impairments and behavioral disturbances in human patients with dementia (Perry et al., 1978; Collerton, 1986; Minger et al., 2000).

Cholinergic deficit has been reported as a result of A β administration, suggesting A β may contribute to cholinergic dysfunction. Both single injections

and chronic intracerebroventricular infusion of A β have been shown to induce degeneration of cholinergic neurons in the basal forebrain and cause memory impairment in rats (Vaucher et al., 2001; Stepanichev et al., 2004). In addition to significant neuronal loss, studies have demonstrated decreases in choline acetyltransferase activity and acetylcholine release in the basal forebrain in response to A β administration; implicating A β as a contributor to basal forebrain cholinergic system neuropathology (Auld et al., 2002). The severe cholinergic degeneration observed in AD patients lead to the development of drugs focusing on enhancing acetylcholine levels. Currently, the only drugs approved to date for treatment of AD in the United States target this neuronal population (Selkoe, 2001; Auld et al., 2002; Donev et al., 2009).

The hippocampus, a region of the brain that plays a key role in cognitive functioning, is one of the brain regions most vulnerable to the aging process, and demonstrates substantial AD pathology. Both in humans and in animal models of AD, the severity of cognitive decline is positively correlated with the extent of structural and functional modifications occurring in the hippocampus (Gallagher and Nicolle, 1993; Landfield, 1988; Hayakawa et al., 2007). In the human AD brain, substantial neuronal loss occurs in the hippocampus, particularly in the CA1 region (West et al., 1993; 2004). However, preclinical AD brains are not associated with significant neuronal loss in the CA1 or any other subdivisions of the hippocampus. Thus, while the hippocampus is one of the first regions of the brain to demonstrate AD pathology, including A β deposition and tau pathology, neuronal loss in the hippocampus only occurs later in the disease process. Mice genetically altered to express the genes associated with familial AD (APP, PS1, PS2), show inflammation and substantial amyloid deposition in the hippocampus, most notably in the CA1, and CA3 hippocampal regions. However, despite the pathology and cognitive decline shown in transgenic mouse models of AD they demonstrate correspondingly little neurodegeneration (Abramowski et al., 2012), suggesting they are models of the earlier, preclinical stages of AD.

1.4 Beta amyloid

A β is a peptide of 37-43 amino acids that is generated by proteolytic cleavage of the amyloid precursor protein (APP) by the action of β - and γ -secretases (Shoji et al., 1992; Haass and Selkoe, 1993). The physiological role of APP, a transmembrane protein, remains poorly understood, however it is thought to be involved in cell-cell interactions and cell-substrate adhesions (Reviewed by Nalivaeva and Turner, 2013). APP is highly conserved in evolution and expressed in all mammals in which it has been sought (Selkoe 2001; Jacobsen et al., 2009). Production of A β is a normal cellular event, and can be detected in both the cerebrospinal fluid and plasma of healthy humans throughout life (Seubert et al., 1992; Shoji et al., 1992). Recent studies have demonstrated that at normal physiological concentrations A β oligomers can positively regulate learning and memory (Lublin and Gandy, 2010). However, altered protein-processing resulting in abnormal A β accumulation has inextricably been tied to the neuropathology of AD. This accumulation can be caused by overproduction of A β as seen in the familial forms of the disease (Citron et al., 1992; Cai et al., 1993; Bentahir et al., 2006), or due to the inability to properly clear A β (Hardy and Selkoe, 2002; Mawuenyega et al., 2010). A β is produced when β -secretase cleaves APP to generate a soluble version of APP (sAPP β) and a 99-amino acid carboxy-terminal fragment that remains membrane bound (Seubert et al., 1993). The carboxy-terminal fragment can then be subsequently cleaved in the middle of the transmembrane domain by γ -secretase to produce A β (Haass et al., 1992; Haass and Selkoe 1993). The cleavage by γ -secretase at the carboxy-terminus is heterogeneous and dictates the length of the A β peptide produced. Following the non-amyloidogenic pathway APP is cleaved within the A β domain by α -secretase, which precludes A β generation (Esch et al., 1990; Sisodia 1992; Eckman and Eckman, 2007). β -Secretase activity has been attributed to one protease, namely beta-site APP-cleaving enzyme 1 (BACE1) (Cai et al., 2001) whereas a set of four proteins is required to form the γ -secretase complex. Presenilin along with the additional cofactors nicastrin, anterior-pharynx-defective

phenotype (APH-1) and PS-enhancer (PEN-2) together form the proteolytic γ -secretase complex (De Strooper, 2003).

A β has the ability to spontaneously aggregate into multiple coexisting physical forms. Among these are A β oligomers (2-6 peptides) which can fuse to form intermediate amyloid assemblies. A β can also form fibrils, which make up the β -pleated sheets that go on to become insoluble fibers of advanced amyloid plaques (Querfurth and LaFerla, 2010). Soluble A β oligomers identified in the brains of AD patients include A β_{1-40} and A β_{1-42} . Of the A β species, A β_{1-40} is more abundantly produced, however A β_{1-42} is considered the more toxic species as it is particularly prone to aggregation, and thus much more likely to form oligomers (Selkoe 2001; Walsh and Selkoe 2007; Querfurth and Laferla, 2010). Enzymatic cleavage of A β_{1-40} by brain proteases can also produce the truncated A β fragments A β_{25-35} and A β_{25-40} (Kaneko et al., 2001). A β_{25-35} is the shortest A β peptide sequence that can form β -sheet aggregated structures and retains biological activity comparable to full length A β (Yankner et al., 1989; Pike et al., 1995; Millucci et al., 2009). These truncated A β_{25-35} fragments are present in the brains of AD patients, but not in age-matched controls (Kubo et al., 2002). The A β_{25-35} fragment is a useful tool for studying A β toxicity as it induces similar toxicity to that of the full length A β fragments, while its shorter length allows for better solubility and rapid aggregation into soluble oligomers (Kowall et al., 1992; Millucci et al., 2009).

1.5 The Amyloid Cascade hypothesis

According to the amyloid cascade hypothesis the progressive accumulation and deposition of neurotoxic A β in amyloid plaques in the brain is thought to be an initiating factor in the pathogenesis of AD (Hardy and Allsop, 1991; Hardy and Higging, 1992; Hardy and Selkoe 2002). There are several major pieces of evidence implicating A β as playing a causative role in AD. One of the first was localization of the APP gene to chromosome 21. Those individuals with Down syndrome (trisomy of chromosome 21) demonstrate a neuropathology essentially identical to that seen in AD as a result of increased APP expression

and consequently higher A β levels (Eckman and Eckman, 2007, Walsh and Selkoe, 2007). In the brains of Down syndrome patients the accumulation of A β precedes tau pathology and neuronal loss. The brains of AD patients also consistently show higher levels of both soluble and insoluble A β_{1-40} and A β_{1-42} in comparison to the normally aged brain, with A β deposition preceding tau pathology and neurodegenerative changes (Morishima-Kawashima et al., 2000; Eckman and Eckman, 2010). This provides convincing evidence in support of the involvement of A β in AD, and further suggests that A β is one of the initiating factors in the pathogenesis of AD.

Additionally, the genes identified as playing a role in familial forms of AD, including the APP and presenilin genes, all increase the production and accumulation of A β . Numerous studies have since demonstrated that mice genetically engineered to overexpress human APP show a time-dependent increase in extracellular A β and demonstrate cognitive decline and neuropathological changes that mimic what is seen in human AD patients (Yamada and Nabeshima, 2000; Gotz et al., 2004). A β peptides have also been shown to be toxic to hippocampal and cortical neurons both in culture and *in vivo* (Pike et al. 1991; Lambert et al. 1998; Hoshi et al., 2003; Deshpande et al. 2006). The precise molecular mechanisms by which A β exerts its toxicity is still unclear however, the addition of toxic forms of A β in neuronal culture results in membrane damage, calcium ion influx, oxidative free radical production and damage, inflammation and apoptosis (Tabner et al., 2005; Deshpande et al. 2006).

Despite the evidence for the contribution of A β to AD pathology, accumulation of A β has also been reported in the brains of the elderly whose cognitive functioning is still intact (Dickson et al., 1992; Aizenstein et al., 2008). Moreover, amyloid plaque load determined histopathologically and radiologically, does not correlate well with severity of dementia (Walsh and Selkoe, 2007; Huang and Mucke 2012). This lack of correlation between plaque load and cognitive impairment was further substantiated by studies in APP transgenic mice where

memory impairment and changes in neuron function are observed well before the first signs of amyloid plaque deposition (Walsh and Selkoe, 2007). This led to a conundrum regarding the exact role of A β in the disease process, as A β plaque burden was not coinciding with cognitive deficits yet A β was inextricably tied to the disease process. In 1995, a study by Oda et al., suggested that soluble complexes of A β , rather than A β fibrils were the toxic A β species. Further support for the idea that soluble A β oligomers had neurotoxic properties came in 1998, when a group demonstrated that A β oligomers rapidly inhibit long-term potentiation, an experimental paradigm representative of memory and synaptic plasticity (Oda et al., 1995; Lambert et al., 1998; Marcello et al., 2008). Their work and the subsequent studies of others led to an update on the amyloid cascade hypothesis that suggested early A β protein assemblies of various types, including protofibrils, soluble oligomers and A β derived diffusible ligands may be the true neurotoxic forms of A β (Tabner et al., 2005; Krafft and Klein, 2010). This has since been supported by the finding that compared to the normally aged brain, the AD brain has higher levels of soluble A β and moreover, the extent of synaptic loss and severity of cognitive decline correlates with the amount of soluble A β in the brain (Eckman and Eckman, 2007; Zussy et al., 2013).

1.6 Cerebral amyloid angiopathy and vascular dysfunction in AD

Epidemiological, clinical, pathological and neuroimaging studies have implicated neurovascular dysfunction as playing a role in the pathogenesis of AD (Dickstein et al., 2010). Studies in humans and animal models of AD suggest that cerebrovascular dysfunction may precede cognitive decline and the onset of neurodegenerative changes and exacerbate underlying AD pathology (Bell and Zlokovic, 2009; Merlini et al., 2011; Murray et al., 2011). In particular, elevated levels of A β have been closely linked to vascular changes, and implicated in the vascular pathology of AD. A β plaques accumulate on and around cerebral capillaries (Bell and Zlokovic, 2010) and 70-90% of AD patients show amyloid deposition in the small arterioles, venules and capillaries within the cerebral cortex (Selkoe, 2001; Humpel, 2011).

Amyloid deposition in and along the walls of the cerebral blood vessels leads to a condition called cerebral amyloid angiopathy (CAA). CAA has been linked to cognitive impairment, and the incidence of CAA increases with age, with 10-40% of the elderly population without AD showing amyloid deposition in the microvessels of the brain (Bell and Zlokovic, 2009). CAA can lead to narrowing of the blood vessels resulting in hypoperfusion, capillary abnormalities, disruption and breakdown of the blood-brain barrier and micro-aneurysms (Dickstein et al., 2010; Querfurth and LaFerla, 2010; Humpel, 2011). CAA has also been shown to be a significant cause of cerebral hemorrhage in the elderly population (Bell and Zlokovic, 2009). Mouse models of AD harboring APP mutations also demonstrate CAA, with A β deposits in the neocortical, hippocampal and thalamic vessel walls (Calhoun et al., 1999; Miao et al., 2005).

1.7 Neuroinflammation

A β deposition and intracellular tau accumulation are capable of triggering pathological cascades in the brain that set it down a destructive path to cell death and a diseased state. Such is the case with the brain's dysregulated inflammatory and oxidative response to A β toxicity. It has been well established that neuroinflammation is involved in the pathogenesis of AD (Akiyama et al., 2000; Wyss-Coray and Mucke, 2002; Tuppo and Arias, 2005). In the AD brain, up-regulated inflammatory mechanisms are co-localized with those regions of the brain exhibiting high levels of AD pathology. Moreover, in regions of the brain showing low levels of AD pathology, inflammatory mediators are absent or minimal (Lue et al., 1996). Common neuroinflammatory events include; up-regulation of inflammatory cytokines and chemokines, activation of the complement system, release of reactive oxygen species (ROS) and activation and proliferation of microglia and astrocytes (Akiyama et al., 2000). A β is thought to be one of the key contributors to the chronic inflammatory response in the AD brain. Evidence for this comes from analysis of human AD brains where inflammatory mediators are most highly expressed in the vicinity of A β deposits and from studies that have demonstrated A β aggregates activate a variety of

inflammatory pathways, including A β -mediated activation of microglia and astrocytes as well as the complement pathway (Akiyama et al., 2000; Bamberger and Landreth, 2002; Wyss-Coray and Mucke, 2002). At what point inflammation arises in the course of AD had not yet been fully resolved. However, A β and inflammation appear to work in a self-propagating cycle, with inflammation stimulating the production of A β , and A β activating and promoting the release of inflammatory mediators (Grammas, 2011).

Microglia and astrocytes are the cell mediators of inflammation in the brain. Changes in microglia morphology from a ramified (resting) state to that of the amoeboid (active) state, along with astrocytosis, involving increases in number and size of astrocytes have been demonstrated in AD (Glass et al., 2010). Astrocytes are the most common cells in the brain and perform many essential functions under normal physiological conditions including maintaining the functional connectivity of neuronal synapses, regulating the activity of neurons and providing nutrients to the nervous tissue. The precise role of astrocytes in the inflammatory process is not fully understood, however, they have been shown to secrete pro-inflammatory products in response to A β toxicity, and accumulate around A β deposits in the brain. Microglia are the 'macrophages' of the brain, serving as the immunocompetent defense cells orchestrating the central nervous system (CNS) immune response. Activated microglia surround and invade A β plaques in both the human AD brain and in APP transgenic mice that develop A β plaques (Reviewed by Akiyama et al, 2000; Herrup, 2010). Initially, this neuroinflammatory response is involved in the clearance of A β from the brain, with the phagocytic microglia actively engulfing and degrading A β . However, after prolonged activation microglia have been shown to release a variety of pro-inflammatory mediators, and potentially neurotoxic substances. These include secretion of the cytokines interleukin-1, interleukin-6 and tumor necrosis factor α , secretion of the chemokines interleukin-8, and macrophage inflammatory protein-1 α along with cell surface expression of MHC class II, and activation of the complement pathway (Akiyama et al, 2000; Tuppo and Arias, 2005; Dumont and Beal 2010; Querfurth and LaFerla, 2010). Inflammatory cells

also have the potential to produce large amounts of ROS, including superoxide radicals and hydrogen peroxide (H₂O₂). An increased level of ROS leads to oxidative stress, further exacerbating the neuroinflammatory process (Akiyama et al., 2000; Massaad 2011).

The substantial evidence implicating inflammation in the pathogenesis of AD lead to the idea that therapeutic strategies targeting inflammation would be beneficial in slowing the onset and progression of AD. In support of this, retrospective studies demonstrated that nonsteroidal anti-inflammatory drugs (NSAIDs) lower the lifetime risk of AD by 30-60% and further slow the progression of the disease (Herrup, 2010; Querfurth and LaFerla, 2010). While these results were initially encouraging, numerous randomized clinical trials of NSAIDs have failed to show any evidence for the reduction of AD pathology or the slowing of cognitive decline (Herrup, 2010; Querfurth and LaFerla, 2010). In part, this failure of prospective human trials of NSAIDs could be attributed to the fact that these trials were only begun after the disease had already progressed and AD symptoms were already manifest (Herrup, 2010). Instead targeting inflammatory pathways at the initial or preclinical stages of the disease might be more effective, as this would aid in preventing or slowing the progression of the disease, rather than attempting to reverse existing pathology.

1.8 A role for peroxisomes and mitochondrial dysfunction in Alzheimer's disease

Closely related to inflammation in the brain, is the role of ROS. There is mounting evidence that oxidative stress resulting from free radical damage plays a role in the pathology of AD and other neurodegenerative diseases. When considering the role of oxidative stress in AD, one has to examine the organelles primarily responsible for the production and elimination of ROS—the mitochondria and peroxisomes. Mitochondria are considered the powerhouses of the cell due to their role in adenosine triphosphate (ATP) production however they are also involved in many other cellular functions including calcium regulation, alteration of reduction-oxidation potential of cells, free radical

scavenging, and apoptosis. During the process of ATP production, a subset of electrons transferred through the respiratory chain form ROS. Under normal physiological conditions these ROS are kept in check by the endogenous antioxidant enzymes including superoxide dismutase, catalase, glutathione reductase, and glutathione peroxidase. However, with aging mitochondrial changes occur, resulting in a decline in electron transport chain function and an increase in free radical production. A β has also been shown to interact with mitochondria, inhibiting key mitochondrial enzymes, having detrimental effects on mitochondrial functioning. A β associated mitochondrial dysfunction has been reported in AD postmortem brains, in transgenic mouse models of AD and in cellular A β toxicity work. Consequently, dysfunctional mitochondria release free radicals, which in both the aging and AD brain cause substantial oxidative stress (Pagani and Eckert, 2010; Swerdlow, 2011; Leuner et al., 2012; Mao et al., 2012).

Peroxisomes are subcellular organelles present in almost all eukaryotic cells, including neurons and glial cells in the brain. They perform a variety of anabolic and catabolic functions including the β -oxidation of very long chain fatty acids, biosynthesis of plasmalogens, and the metabolism of saturated and polyunsaturated fatty acids. Additionally, they play a role in both the production and removal of ROS in the cell under both physiological and pathological conditions. A decline in peroxisomal function has been associated with cellular aging and in age related neurodegenerative diseases, with a resultant increase in oxidative stress and neuroinflammation as a consequence (Lizard et al., 2011; Titorenko and Terlecky, 2011). Evidence for peroxisomal dysfunction in AD comes from *in vitro* and *in vivo* work. *In vitro*, A β toxicity was shown to result in a loss of peroxisomes in primary rat hippocampal neurons. Moreover, treatment of A β challenged hippocampal neurons with a peroxisomal proliferator was shown to protect them from A β toxicity by reducing neuronal death, indicating that proper peroxisomal functioning may be neuroprotective (Santos et al., 2005). In a transgenic mouse model of AD significant peroxisomal alterations were observed in rats 3 months of age, when no apparent neuroanatomical or

cytological signs of the disease were present, suggesting peroxisomal dysfunction may be one of the earlier contributors to the disease process (Cimini et al., 2009). Peroxisome-related dysfunction has also been reported in the postmortem brain tissue of patients with AD (Kou et al., 2011). The exact contribution that mitochondrial and peroxisomal dysfunction plays in aging and AD is yet to be elucidated, however it is clear that impairment in these organelles leads to increased levels of free radicals and resultant oxidative stress.

1.9 Reactive Oxygen Species and Oxidative Stress

Oxidative stress occurs when free radical production exceeds antioxidant defense mechanisms leading to oxidative damage of various cellular components including oxidation of lipids, proteins, and nucleic acids. The brain consumes approximately 20% of the body's total oxygen due to its high metabolic demand and need for ATP. This disproportionately high level of oxygen consumption combined with the brain's abundant lipid content and relative scarcity of antioxidant enzymes compared with other organs leaves the brain particularly susceptible to increased production of ROS and oxidative stress (Markesbery and Carney 1999, Su et al., 2008; Massaad 2011). The aging process is also associated with high levels of ROS, along with a reduction in the ability to defend against oxidative stress (Su et al., 2008; Massaad, 2011).

Regions of the aging brain that have been shown to be particularly susceptible to neurodegeneration demonstrate increased oxidative damage and lowered antioxidant functioning. A study by Venkateshappa et al., showed increased levels of protein oxidation and protein nitration in the hippocampus and frontal cortex compared to the cerebellum with increasing age in the human brain. Moreover, these changes were associated with a decrease in activity of the antioxidant enzymes superoxide dismutase and catalase (Venkateshappa et al., 2012). Age-related alterations in antioxidant enzyme activities have also been demonstrated in rats; with decreases in superoxide dismutase and catalase activities being noted in the cerebral cortex of aging animals (Alper et al., 1998).

Reactive oxygen species are generated in a number of cellular locations, including the aforementioned organelles—peroxisomes and mitochondria. They are produced as a normal consequence of cellular activity, as is the case during aerobic metabolism where ROS are produced in the reduction of molecular oxygen to water and in peroxisomes during β -oxidations of fatty acids (Markesbury & Carney, 1999; Mohsenzadegan & Mirshafiey, 2011; Terlecky et al., 2012). A number of ROS exist including the superoxide anion ($O_2^{\bullet-}$), hydrogen peroxide (H_2O_2), singlet oxygen and the hydroxyl radical ($\bullet OH$) (Markesbury & Carney, 1999; Schrader and Fahimi, 2006). Typically ROS are categorized as neurotoxic molecules, exerting their detrimental effects via oxidation of essential molecules. However, ROS are also necessary for normal cellular functioning and have been shown to play important roles in signaling, synaptic plasticity, and in the immune system where they contribute to an organism's defense against microbial agents (Massaad 2011; Mohsenzadegan & Mirshafiey, 2011).

ROS are usually maintained at low physiological levels by antioxidants and antioxidant enzymes. Some of the enzymatic antioxidants synthesized by cells include superoxide dismutase, glutathione peroxidase, glutathione reductase and catalase (Markesbury and Carney, 1999; Su et al., 2008). Reduction of molecular oxygen yields the superoxide anion, which is converted to H_2O_2 by superoxide dismutase. Hydrogen peroxide can then either be reduced to form the highly reactive hydroxyl radical, or can be broken down by catalase or glutathione peroxidase (Markesbury and Carney, 1999). In addition a number of nonenzymatic antioxidants exist including α -tocopherol (vitamin E), ascorbic acid (vitamin C), glutathione, and carotenoids, all of which assist in maintaining ROS levels. These antioxidants are able to remove and or repair molecules that are oxidized, defending cells against free radical damage. However, when ROS levels exceed the antioxidant capabilities of the cell, oxidative damage results.

The brains high demand for oxygen, coupled with increased levels of ROS accompanying the aging process, set the aging brain up to be particularly vulnerable to oxidative stress. Thus, it comes as no surprise that oxidative stress

contributes to the pathophysiology of AD, an age-related neurodegenerative disease. In fact, evidence indicates that one of the earliest pathological events in AD is oxidative damage to the brain (Tabner et al., 2005). In transgenic mouse models of AD, markers of lipid and protein oxidation are increased prior to amyloid deposition (Resende et al., 2008). The early involvement of oxidative stress in AD is further supported by evidence in Down's syndrome patients where oxidative damage has been shown to precede A β build up (Nunomura et al., 2000; Milton 2001).

Numerous studies have demonstrated oxidative damage in the brains of AD patients, including increased products of lipid peroxidation, protein oxidation and oxidative damage to nucleic acids (Markesbury and Carney, 1999). Two of the major products of lipid peroxidation in the AD brain are 4-hydroxy-2-transnonenal (HNE) and acrolein, both of which are α , β -unsaturated aldehydes, capable of binding to brain proteins and significantly altering their structure and function (Butterfield et al., 2001). HNE has been shown to be elevated in multiple brain regions and in ventricular cerebrospinal fluid in AD patients compared to age matched controls (Sayre et al., 1997; Markesbery and Lovell 1998). Additionally, HNE levels are increased in rat hippocampal neurons in response to A β toxicity (Mark et al., 1997), and HNE has been shown to damage cholinergic neurons and inhibit choline acetyltransferase activity in the basal forebrain (Bruce-Keller et al., 1998). Acrolein is also reported to be increased in the brain in AD compared to age matched controls, and has been shown to be toxic to primary hippocampal cultures (Lovell and Markesbery, 2001). The most commonly oxidized DNA base product as a result of ROS attack is 8-hydroxy-2'-deoxyguanosine (8-OHdG). 8-OHdG levels are elevated in the AD brain and in the cerebral spinal fluid of AD subjects (Lovell and Markesbery, 2001). Moreover, immunohistochemical detection has revealed that 8-OHdG and 8-hydroxyguanosine (8-OHG) markers of oxidatively damage DNA and RNA respectively, are restricted to hippocampal and neocortical neurons in the AD brain, the same neurons known to be vulnerable and to degenerate in AD (Nunomura et al., 1999; Markesbery and Carney, 1999).

1.10 Beta-amyloid and H₂O₂

Of particular relevance to oxidative stress and AD is the contribution of the A β peptide to the generation of ROS (Figure 1). Numerous studies have demonstrated the ability of A β to generate hydrogen peroxide (H₂O₂) in neuronal cell cultures (Behl et al., 1994; Goodman et al., 1994; Manelli and Puttfarcken, 1995). The production of H₂O₂ has been shown to occur early in the A β aggregation process, when oligomers and protofibrils are formed, while mature A β fibrils lack the ability to generate H₂O₂ (Tabner et al., 2005). Included among the amyloidogenic proteins and peptides shown to have the ability to generate H₂O₂ are A β ₁₋₄₀, A β ₁₋₄₂ and A β ₂₅₋₃₅ while controls, including scrambled and reverse peptides were shown to lack any significant H₂O₂ producing ability when tested under the same experimental conditions (Tabner et al., 2005). Hydrogen peroxide is a stable, uncharged and freely diffusible ROS that is an effective oxidant for many biological molecules. Its stability and diffusion properties allow H₂O₂ to move within and between cells with relative ease, enhancing its toxicity (Milton, 2004). Hydrogen peroxide is readily converted into the highly reactive hydroxyl radical in the presence of iron (Fe²⁺) or copper (Cu⁺) (Milton, 2004; Tabner et al., 2005). The reaction of iron with H₂O₂ to produce the hydroxyl radical is termed the Fenton reaction (Markesbury and Carney, 1999). The hydroxyl radical in turn is then capable of damaging carbohydrates, DNA, protein and lipids (Milton, 2004).

The mechanism for the generation or rise in H₂O₂ levels associated with A β toxicity remains unclear. However, it may involve direct formation of ROS by A β with the involvement of metal complexes, via activation of the enzymes that can directly or indirectly generate ROS, or as a result of reduced degradation of H₂O₂ in A β challenged cells (Milton, 2001; 2004; Habib 2010). Nonetheless, the ability of A β to increase H₂O₂ accumulation in cells suggests that H₂O₂ or one of its metabolites plays a role in the cytotoxicity of A β (Behl et al., 1994; Milton, 2004; Varadarajan et al., 2000).

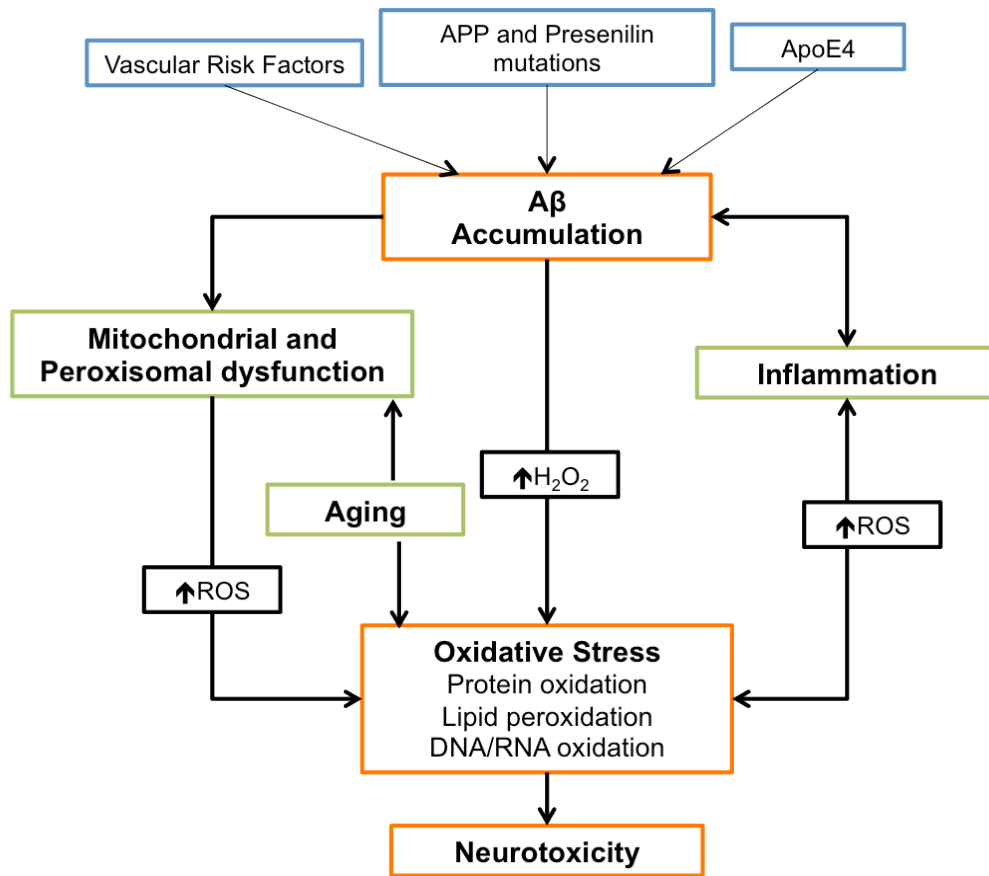


Figure 1. Role of A β in the production of reactive oxygen species (ROS) and the resultant oxidative stress in Alzheimer's disease. Genetic factors including amyloid precursor protein (APP) or presenilin mutations and presence of apolipoprotein E4 (apoE4) allele or other stressors including vascular risk factors (hypertension, transient ischemic attacks, stroke, atherosclerosis) contribute to A β accumulation in the brain. A β toxicity results in increased free radical production (particularly H₂O₂), is associated with mitochondrial and peroxisomal dysfunction and activates inflammatory cells, which in turn release ROS. An increased level of ROS leads to oxidative damage of lipids, proteins and DNA/RNA. Aging also contributes to oxidative stress and has been shown to result in mitochondrial and peroxisomal dysfunction along with increased production of inflammatory mediators and ROS.

The peroxidase enzymes, which remove H_2O_2 , include glutathione peroxidase, thioredoxin dependent peroxidases and catalase, all of which are present in the brain (Milton, 2004). Of these enzymes degradation of H_2O_2 is primarily achieved by catalase in the peroxisomes and glutathione peroxidase, a cytosolic enzyme (Schrader and Fahimi, 2006). In considering the role of oxidative stress in the pathophysiology of AD, the balance between the generation and removal of ROS by antioxidant enzymes is of utmost importance. Modification of the activities of these antioxidant enzymes could be potential pharmacological targets for future AD therapy (modified Milton, 2004).

1.11 Catalase-SKL: a targeted antioxidant approach

Catalase is heme containing tetrameric enzyme, predominantly found in peroxisomes, that catalyzes the conversion of H_2O_2 to water and oxygen. Deficiencies in catalase activity, expression and peroxisomal localization are associated with oxidative stress, aging and human disease (Sheikh et al., 1998; Wood et al., 2006; Terlecky et al., 2006; Koepke et al., 2007). Catalase is targeted to peroxisomes by a type 1 peroxisomal targeting signal (PTS1), with the carboxy-terminus residues, lysine-alanine-asparagine-leucine (KANL). This targeting sequence is different from the classical PTS1 of other peroxisomal enzymes, which have a serine-lysine-leucine (SKL) consensus sequence (Sheikh et al., 1998; Koepke et al., 2007). The PTS1 KANL only poorly targets catalase to peroxisomes, and as cells age it has been shown that catalase is increasingly mislocalized to the cytosol (Koepke et al., 2007). The poor targeting efficiency of the KANL sequence coupled with the mislocalization of catalase to peroxisomes as cells age is associated with accumulation of H_2O_2 in cells and resultant oxidative injury. In order to better target catalase to peroxisomes, a genetically engineered variant of the enzyme, catalase-SKL (CAT-SKL), has been developed (United States patent 7601366). This recombinant enzyme is able to enter cells and traffic to organelles (mostly peroxisomes) where it is able to efficiently metabolize H_2O_2 (Koepke et al., 2007; Young et al., 2007; Price et al., 2009; Undyala et al., 2011). Use of CAT-SKL has been shown to restore

catalase levels and oxidative equilibrium in hypocatalaseemic fibroblasts (Wood et al., 2006), delay the appearance of aging markers in human fibroblasts (Koepeke et al., 2007), reduce tumor necrosis factor α (TNF- α) induced production of inflammatory cytokines in primary human keratinocytes (model of inflammatory skin disease) (Young et al., 2008) and protect cardiac myocytes from hypoxia-reoxygenation and ischemia reperfusion injury (Undyala et al., 2011).

The anti-inflammatory and anti-oxidant properties of CAT-SKL demonstrated *in vitro*, make it a viable candidate for targeting oxidative stress and inflammation *in vivo*. The use of CAT-SKL may therefore be beneficial in reducing A β toxicity since A β mediates its toxicity in part by increasing H₂O₂ levels and triggering neuroinflammatory cascades. The use of catalase to protect cells from A β toxicity has already been demonstrated in cell cultures, with the addition of catalase to the extracellular environment or transfection of cells with catalase decreasing the toxicity induced by A β (Behl et al., 1994; Goodman et al., 1994; Manelli and Puttfracken, 1995; Zhang et al., 1996). This protection was attributed to decreases in H₂O₂ levels both inside and outside the cell (Habib et al., 2010). Furthermore, inhibition of cellular catalase enhances A β ₁₋₄₂ and A β ₂₅₋₃₅ toxicity in both neuronal and non-neuronal cell lines (Milton, 2001).

In cell cultures, A β ₁₋₄₂ and A β ₂₅₋₃₅ have been shown to bind with high affinity to catalase both in peroxisomes and in the cytosol. Specifically, catalase is able to directly bind the cytotoxic region of A β . This A β -catalase binding results in significant inhibition of H₂O₂ breakdown by catalase, leading to ROS accumulation and toxicity in cells (Milton, 1999; Milton, 2001; Habib et al., 2010). Catalase-amyloid interaction also appears to occur in the brains of AD patients, where catalase is associated with senile plaques (Pappolla et al., 1992; Lovell et al., 1995). Thus, increasing catalase levels in the brain may aid in reducing the toxicity induced by the A β peptide, with lowered ROS production, decreased neuroinflammation and reduced neuronal dysfunction as a result.

1.12 Modeling AD in animals

The complex pathophysiology of AD makes modeling the disease in animals a challenge. Nonetheless, a number of transgenic and non-transgenic animal models of AD exist, each with their own strengths and limitations. While these animal models are incapable of simulating all aspects of the disease process, they are of value in aiding our understanding of aspects of the disease. Rodents genetically engineered to overexpress genes associated with AD including APP, PS1/PS2, tau, and apoE isoforms, either individually or in combination, have been particularly informative. These transgenic animals have been shown to develop early AD-like pathology including A β deposits, tau immunoreactivity along with progressive impairments in memory and learning (Reviewed by Yamada and Nabeshima, 2000; Ashe and Zahs, 2010; Jucker, 2010). Non-transgenic animal models involving acute injection or continuous infusion of A β into the rodent brain also exist and have been shown to cause brain dysfunction and learning and memory deficits (Reviewed by Yamada and Nabeshima, 2000).

In our lab a non-transgenic rat model of acute icv administration of A β_{25-35} has been developed and used as a model of AD. A β_{25-35} is the core neurotoxic fragment of A β , retaining many of the same biological and physical properties of the full-length peptide (Yankner et al., 1989; Pike et al., 1995; Millucci et al., 2009). Use of this truncated peptide has been shown to induce neuroinflammation, neuronal cell death, and synaptic loss similar to that seen with A β_{1-40} and A β_{1-42} however, its smaller length allows for better solubility and rapid aggregation into soluble oligomers (Kowall et al., 1992; Milluci et al., 2009). Previous studies in our lab have demonstrated the initial effectiveness of this non-transgenic rat model, with enhanced inflammatory responses, and A β neurotoxicity being observed in the brains of 3 month old rats (Whitehead et al., 2005a,b; Cheng et al., 2006; Whitehead et al., 2007). Other groups have also demonstrated AD-like pathological changes in response to icv A β_{25-35} administration including glial activation, oxidative stress, hippocampal alterations

and memory impairments (Ruan et al., 2010; Zussy et al., 2011; Guo et al., 2012). Zussy et al assessed the time-course and regional effects of single icv injection of A β ₂₅₋₃₅ demonstrating the ability of A β ₂₅₋₃₅ to penetrate through the ependymal cells lining the ventricles and reach the brain vasculature. The injected peptide was found to locate in the septum, hypothalamus, hippocampus, amygdala and various cortical regions and moreover was still present in the brain 3 weeks after injection (Zussy et al., 2011; Zussy et al., 2012).

1.13 Rationale:

Most studies examining the effect of icv injection of A β ₂₅₋₃₅ have done so in 3 months old rats. However, AD is a disease of the elderly and apart from genetic predisposition, aging is the most important risk factor for AD. With age comes increased levels of ROS and decreased antioxidant functioning, amyloid accumulation, glial activation, increased peroxisomal and mitochondrial dysfunction and alterations in lipid and protein activity in the human brain. Each of these age-related changes on their own are not sufficient to cause AD, but together they render the brain vulnerable to further insult. A β toxicity is one such insult thought to drastically alter many of the brain functions already affected by the aging process. Therefore, this study investigated the age-related (3, 6 and 9 month) pathological response to icv administration of A β ₂₅₋₃₅. While the ages of 6 and 9 months are not considered particularly old for a rodent, they are more physiologically relevant ages in terms of animal sexual, skeletal and social maturity than are 3 months old animals (Quinn, 2005; Sengupta, 2011). Thus, the first aim of this study was to determine whether the rodent brain is more vulnerable to A β toxicity at 6 and 9 months than it was at 3 months, with particular focus on neuroinflammatory and neurodegenerative changes.

A number of studies have shown that A β exerts its toxicity in part by facilitating the formation of ROS, in particular H₂O₂, with a resultant increase in oxidative damage. The aging process itself is also associated with an increase in production of free radicals, along with a concurrent decrease in the ability to defend against oxidative stress. One of the key enzymes responsible for

maintaining oxidative balance in cells is catalase. Catalase is an antioxidant enzyme, targeted to peroxisomes, that catalyzes the conversion of H₂O₂ to water and oxygen. A β has been shown to inhibit catalase activity in cells, resulting in increased H₂O₂ levels (Milton, 1999; Milton 2001; Habib et al., 2010). Moreover, addition of catalase to A β challenged cells has been shown to protect cells from A β toxicity by decreasing levels of H₂O₂ and reducing protein and lipid oxidation (Behl et al., 1994; Manelli and Puttfarcken 1995; Sagara et al., 1996). A genetically engineered variant of the enzyme, Catalase-SKL (CAT-SKL), with an enhanced peroxisomal targeting signal that is able to enter tissues and cells and traffic to peroxisomes has been developed. Use of CAT-SKL *in vitro* settings has demonstrated the antioxidant, anti-inflammatory and anti-aging properties of this recombinant enzyme (Koepke et al., 2007; Young et al., 2007; Price et al., 2009; Undyala et al., 2011). Since A β and catalase-amyloid interactions result in increased H₂O₂ levels, and addition of catalase to cell culture alleviates this increase in H₂O₂, the use of catalase *in vivo* could be a targeted approach to reducing the toxicity induced by A β . The second aim of this study was to treat rats with CAT-SKL in an attempt to reduce the oxidative stress and neuroinflammation induced by A β toxicity.

1.14 Hypothesis and Aims:

Aim 1: To investigate the age-related pathological response to A β ₂₅₋₃₅ toxicity

Hypothesis: Rats 6 and 9 months of age will demonstrate a greater pathological response to A β ₂₅₋₃₅ toxicity than 3 months old rats, as evidenced by increased neuroinflammation, cholinergic deficits, neuronal loss, and vascular impairment.

Aim 2: To evaluate whether the targeted antioxidant CAT-SKL is able to reduce A β ₂₅₋₃₅ toxicity

Hypothesis: Catalase-SKL treatment will reduce the toxicity induced by A β ₂₅₋₃₅ administration in the mature rat brain by reducing oxidative stress and inflammation, improving neuronal survival, and attenuating cognitive deficits.

Section 2

METHODS

2.1 Animals

All experimental procedures were carried out in accordance with the guidelines of the Canadian Council on Animal Care and were approved by Western University Animal Use Subcommittee. Male Wistar rats (Charles River, Montreal Quebec) 3, 6 or 9 months of age were housed at a temperature of 22-24°C under a 12h:12h light:dark cycle. Rats were provided food and water *ad libitum*. Animals were randomly assigned to treatment groups and were housed individually following surgery.

2.2 A β preparation

A β_{25-35} or the reverse peptide A β_{35-25} was purchased from Bachem and dissolved in sterile saline at a concentration of either 4.24 μ g/ μ l or 21.2 μ g/ μ l and then stored at -80°C in 30 μ l aliquots. Rats received bilateral intracerebroventricular (icv) injections of either 100nmol or 500nmol of the toxic A β_{25-35} (Bachem, Torrance California) or 100nmol or 500nmol of the reverse peptide A β_{35-25} . Acute administration of A β was as it has been shown by our lab and others to induce progressive pathology in the rodent brain (Whitehead et al., 2005ab; Cheng et al., 2006; Zussy et al., 2011; 2013). A β_{25-35} is the core neurotoxic fragment of the full length A β_{1-42} peptide, retaining many of the same physical and biological properties (Yankner et al., 1989). A β_{25-35} has been shown to induce neurotoxic effects similar to that of the full-length peptide, while its short length allows for better diffusion (Kaminsky and Kosenko, 2008). The reverse, physiologically inactive, A β_{35-25} peptide was used as the control.

2.3 Surgery

Rats were weighed and then anesthetized in a Harvard anesthesia box with 3% Isoflurane (Baxter Corporation, Mississauga Ontario) and oxygen. Once anaesthetized, rats were placed in a David Kopf stereotaxic apparatus, and were maintained under gas anesthesia for the duration of the surgical procedure. The hair on the surface of the rat's head was shaved, and soap, ethanol and iodine were used to clean and sterilize the surgery site. The skull was exposed and the

ear and incisor bars were adjusted so that lambda and bregma were at the same height, orienting the head in a flat-skull position. Bregma was then marked in order to map out the injection sites. Injection sites were identified based on the following coordinates with respect to bregma (Paxinos & Watson, 1986); -0.8mm anterior/posterior, ± 1.4 mm medial/lateral, and -4mm dorsal/ventral (below dura). Once located, small burr holes were made in the parietal bone to allow for insertion of the injection cannula. $A\beta_{25-35}$ or $A\beta_{35-25}$ (details above) was injected bilaterally into the lateral ventricles through a stainless steel cannula attached to a glass Hamilton syringe at a rate of $1\mu\text{l}/30$ seconds. The injection cannula was left in situ for 5 minutes following each injection, and then removed slowly. The surgery site was then sutured closed and rats were administered 0.3ml of the analgesic Temgesic Buprenorphine hydrochloride subcutaneously and 0.03ml of the antibiotic Baytril (Bayer) intramuscularly. Rats body temperature was maintained at 37°C on a heating pad for the duration of the surgical procedure. Following surgery rats were placed under a heat lamp until they could attain and maintain sternal recumbency.

2.4 Treatment Groups

For the age-based part of the study animals 3, 6 and 9 months of age were assigned randomly to the following treatment groups: low dose $A\beta_{25-35}$ (100nmol in $25\mu\text{l}$), high dose $A\beta_{25-35}$ (500nmol in $25\mu\text{l}$), or reverse peptide $A\beta_{35-25}$ (RP) (100nmol in $25\mu\text{l}$). Table 1 lists the number of animals in each of the treatment groups that underwent successful surgeries and were used for further analysis in the aged study. For the CAT-SKL study, six-month old rats received bilateral intracerebroventricular injections of either $A\beta_{25-35}$ (500nmol in $25\mu\text{l}$) or the reverse physiologically inactive $A\beta_{35-25}$ peptide (500nmol in $25\mu\text{l}$). Animals were randomly assigned to one of four treatment groups: $A\beta_{25-35}$ +CAT-SKL ($A\beta$ +CATSKL), reverse peptide $A\beta_{35-25}$ + CAT-SKL (RP+CATSKL), $A\beta_{25-35}$ +saline ($A\beta$) and reverse peptide $A\beta_{35-25}$ +saline (RP). The number of animals in each of the treatment groups is outlined in Table 2.

Table 1. Treatment groups and corresponding n values. Listed are the animals that underwent successful surgeries and were included in the aged component of the study.

| | 3 Months | 6 Months | 9 Months |
|------------------------------------|-----------------|-----------------|-----------------|
| Reverse Peptide | n=6 | n=6 | n=6 |
| Aβ 100nmol | n=6 | n=7 | n=6 |
| Aβ 500nmol | n=6 | n=6 | n=6 |

Table 2. Treatment Groups and Corresponding n values for behavior, and immunohistochemical analysis for animals included in the CAT-SKL study.

| | Behavior | Immunohistochemistry |
|--------------------------------------|-----------------|-----------------------------|
| RP+ Saline | n=8 | n=6 |
| Aβ+ Saline | n=9 | n=6 |
| RP + CAT-SKL | n=9 | n=7 |
| Aβ + CAT-SKL | n=9 | n=7 |

2.5 Catalase Administration

Rats undergoing Catalase-SKL (CAT-SKL) treatment received a total of 4 catalase injections, once per week for 4 sequential weeks (Figure 2A). Animals were weighed immediately prior to injection and were administered 1mg/kg of CAT-SKL by intraperitoneal (ip) injection. Those animals not receiving CAT-SKL injections received ip injections of an equivalent volume of saline. The dose and route of CAT-SKL administration was based on unpublished work from Dr. Terlecky's lab. The recombinant enzyme CAT-SKL was acquired from Dr. Paul Walton and Dr. Stanley Terlecky (United States patent 7601366 and related patents pending). The molecule consists of a reengineered catalase enzyme, with a SKL targeting sequence, along with a cellular delivery molecule (cell penetrating peptide).

2.6 Behavior: Morris Water Maze

The Morris water maze (MWM) consisted of a circular pool (146cm in diameter, 58cm high) in which rats were trained to escape from the water by swimming to a hidden platform. The pool was filled (36cm high) with water and was virtually divided into four equivalent quadrants: north-east (NE), north-west (NW), south-east (SE) and south-west (SW). The water was made opaque using non-toxic blue paint, and was maintained at a temperature of $21\pm 1^{\circ}\text{C}$. A webcam was placed above the pool to monitor the location and swimming activity of the rats. The webcam was connected to a laptop for video recording and behavioral parameters were measured using video-tracking software (ANY-maze[®], Stoelting CO, USA). Animals underwent four days of spatial learning, two probe trials (D12 and D19) and two days of cued learning (D20-D21) (Figure 2B).

Spatial Learning: Spatial learning took place from 8 to 11 (D8-D11) days after icv injections of $\text{A}\beta_{25-35}$ or $\text{A}\beta_{35-25}$. The platform remained in the middle of the southwest quadrant for the duration of the spatial acquisition trials. Distal extra-maze cues were located around the room, with which rats could learn the location of the hidden platform. The spatial acquisition phase consisted of 16

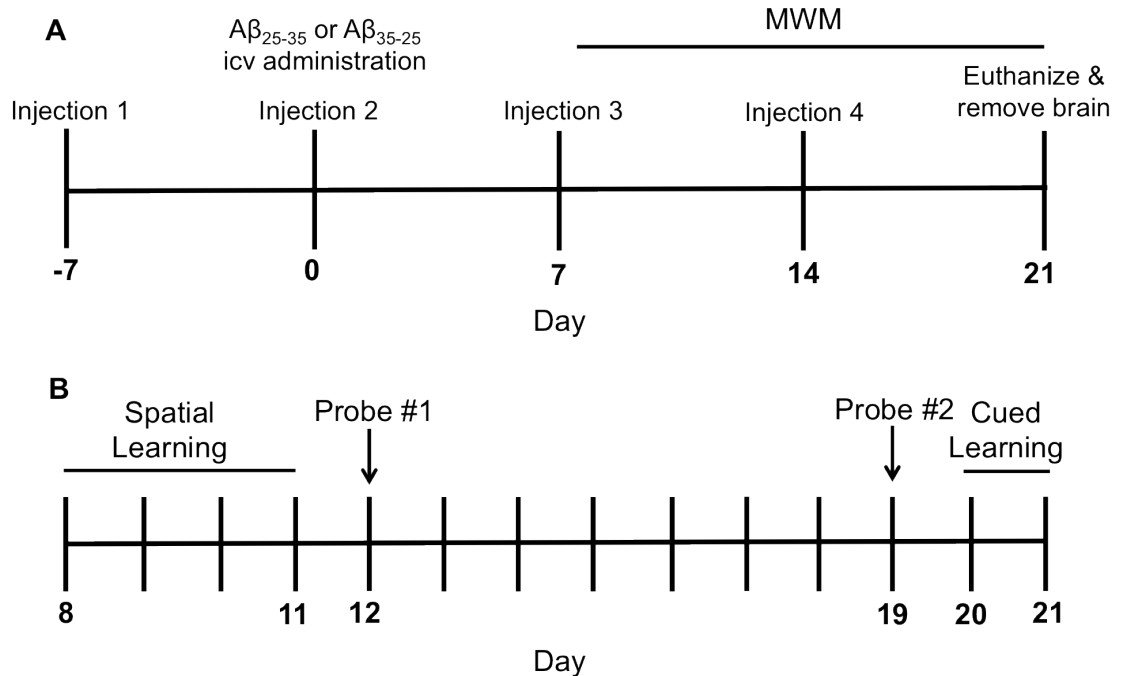


Figure 2. Treatment paradigm and time course for CAT-SKL injections, $A\beta$ administration and behavior testing. (A) CAT-SKL or saline injections were administered intraperitoneal once a week for four consecutive weeks. $A\beta_{25-35}$ or the reverse peptide $A\beta_{35-25}$ was injected intracerebroventricularly (icv) on Day 0 and animals were sacrificed on Day 21. **(B)** Timeline for behavior testing in the Morris Water Maze (MWM). Spatial learning took place from Day 8 to Day 11. Rats underwent two probe trials, one on Day 12 and the second probe trial on Day 19. Cued learning took place on Day 20 and Day 21.

training trials, with 4 trials per day for 4 days with an inter-trial interval of 20 minutes. Rats were released from one of four start locations (N, SE, NW, E) in randomized order and were allowed to swim in search of the platform for 90s. If the rat was unable to locate the platform in that time, they were guided to the platform and allowed to remain on it for 15s before being removed from the pool. Animal behavior, including swimming speed, distance travelled and latency to escape from the pool were monitored using video-tracking software (ANY-maze[®], Stoelting CO, USA).

Probe Trials: Twenty-four hours following the last spatial acquisition trial (D12), rats were subjected to a probe trial where the platform was removed from the pool. Rats were released from a NE start position and were allowed to swim freely in the water for 30s. On the 19th day (D19) rats received an additional probe trial for 30s to determine long-term memory retention. Rats were once again released from the NE start position and were allowed to swim freely for 30s. For both the first (D12) and second (D19) probe trials the amount of time and distance the rat travelled in the quadrant where the platform was previously located was tracked and analyzed. Swimming speed, total path length and path efficiency were also recorded. Time spent and/or distance travelled in the target quadrant was taken as an index of rats' memory capacity. Rats were not trained during the time period between D12 and D19.

Cued Learning: On days 20-21 rats were trained in a non-spatial cued version of the water maze. For cued training rats received 4 trails per day for 2 days, with the location of the hidden platform and the rats start position varying with each trial. The platform location was not predictable based on extra-maze cues, but instead based on the presence of a cue attached to the platform. Swimming speed, distance travelled and the latency to find the platform were recorded. Cued platform learning was used as a control procedure in order to determine if any differences in the MWM could be attributed to either a difference in motivation to escape the water, or an inability to use cues to locate the hidden platform.

2.7 Sacrifice

Twenty-one days following surgery rats were weighed and then euthanized with an overdose of Euthanyl (Pentobarbital Sodium, 240mg/mL) (0.5mL-0.8mL, ip). Animals were perfused transaortically with 0.01M phosphate-buffer saline (PBS) (pH 7.35) for 2 minutes followed by 4% paraformaldehyde (PFA) (pH 7.35) for 7 minutes. Brains were then removed and further fixed for 24 hours in PFA at 4°C after which they were transferred to a 30% sucrose solution until they were ready for slicing. Brains were sliced into 35µm coronal sections using a Leica CM1850 Cryostat (Leica Biosystems) and divided into 6 free-floating series. Series were stored in cryoprotectant (sucrose, ethylene glycol, polyvinylpyrrolidone) at -20°C until they were needed for immunohistochemistry.

2.8 Immunohistochemistry

Day 1: Series representative of each treatment group were processed together to reduce variability between groups. Free-floating coronal sections were washed in 0.1M PBS (6 X 10 minutes), and then incubated with 3% hydrogen peroxide for 10 minutes to block endogenous peroxidase activity. Sections were then washed in 0.1M PBS (3 x 5 minutes), then blocked in 2% horse serum solution (1:200, Vector Laboratories, Burlington, Canada) diluted in PBS with Triton-X (PBST) for 1 hour at room temperature. Sections were then incubated with primary antibodies (Table 3) diluted in 2% horse serum (PBST) for 48 hours at 4°C on a shaker. A mouse monoclonal antibody against Glial fibrillary acidic protein (GFAP; 1:1000; Sigma-aldrich) was used to assess astrocyte activation. Ramified microglia were detected using a mouse monoclonal antibody OX-6 directed against the MHC II receptor (OX-6; 1:1000; Pharmingen). Monoclonal mouse anti-choline acetyltransferase (ChAT; 1: 500; Abcam) was used to detect cholinergic neurons (Table 3).

Day 2: Following incubation with the primary antibody, sections were briefly washed in 0.1M PBS (3 x 5 minutes) and then incubated with biotinylated anti-mouse secondary antibody (1:2000, Vector Laboratories, Burlington, Canada) in

2% horse serum solution for 1 hour at room temperature. Subsequently, sections were washed in PBS (3 x 5 minutes) and incubated for 1 hour at room temperature with Avidin-Biotinylated Complex (ABC) Reagent (Vector Laboratories, Burlington, Canada) for 1 hour. Sections were washed once again in PBS (3 x 5 minutes) and then visualized using 0.05% 3, 3' diaminobenzidine tetrahydrochloride (DAB) (Sigma-aldrich). Sections were incubated with DAB for 1-5min and then washed (0.1M PBS; 3x 5minutes) and mounted onto VWR microscope slides in 0.3% gelatin. Slides were left to air dry, and were then dehydrated in a graded series of ethanol (50%, 70%, 95%, 100%; 5 minutes each) followed by Xylene for 10minutes, after which they were coverslipped using Depex Mounting medium.

2.9 Dual label immunohistochemistry

The same immunohistochemical procedure as described above was used for dual label SMI71&Dysferlin staining with the following amendments:

Day 1: Following incubation with hydrogen peroxide, sections were incubated in proteinase-K working solution for 10 minutes at 37°C. Sections were incubated with primary antibody mouse monoclonal anti-dysferlin (1:200, Abcam) for 24 hours.

Day 2: Sections were washed in 0.175M sodium acetate (3x 5minutes) after incubation with avidin-biotin peroxidase complex, and were then incubated with Nickel-enhanced DAB, followed by washes in 0.175M sodium acetate (3 x5minutes). Sections then underwent a repeat of Day 1 staining as outlined above followed by incubation with anti-SMI71 (1:2000, Covance) primary antibody.

Day 3: Same as Day 2 staining outlined above for immunohistochemistry.

Immunohistochemical controls: As negative controls sections were incubated in parallel but without the primary antibodies. A typical section showed no non-specific binding (Figure 3).

Table 3. Overview of the primary antibodies used for immunohistochemistry.

| Antibody | Host Species | Dilution | Target | Supplier |
|------------------|---------------------|-----------------|---|-----------------|
| ChAT | Mouse monoclonal | 1:500 | Cholinergic neurons | Abcam |
| Dysferlin | Mouse monoclonal | 1:200 | Expressed by leaky endothelial cells | Abcam |
| GFAP | Mouse monoclonal | 1:2000 | Astrocytes | Sigma-Aldrich |
| OX-6 | Mouse monoclonal | 1:1000 | Microglia | Pharmingen |
| SMI71 | Mouse monoclonal | 1:2000 | Endothelial proteins at Blood Brain Barrier | Covance |

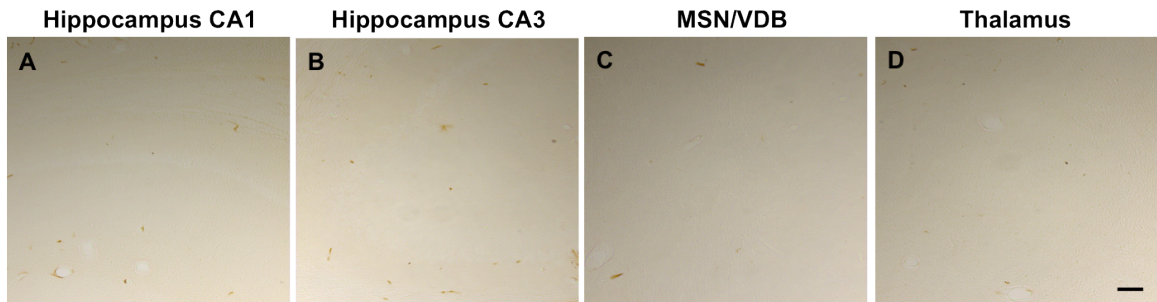


Figure 3. Immunohistochemical controls. (A-D) Representative photomicrographs of the hippocampal CA1 and CA3 subfield, medial septal nucleus/vertical diagonal band (MSN/VDB) and thalamus respectively in a 6 months old $A\beta_{25-35}$ 500nmol administered rat. Sections underwent the same immunohistochemical staining protocol as described but without the primary antibody. Scale bar 100 μ m.

2.10 Histological Examination

Hematoxylin and Eosin (H&E) Staining: Free-floating sections were removed from cryoprotection and washed in 0.1M PBS (6 x 10 minutes). Sections were then mounted onto Superfrost microscope slides using 0.3% gelatin and air-dried in preparation for staining. Sections were placed in Mayer's Hematoxylin solution for 4 minutes, rinsed under tap water for 5 minutes and then dipped in 0.05% Eosin Y solution 9 times and rinsed in deionized water (ddH₂O). Sections were then dehydrated in a graded series of ethanol (50%, 70%, 95%, 100%) followed by 10 minutes in Xylene after which they were coverslipped using Depex mounting medium. Representative sections from each treatment group were processed simultaneously to reduce variability between groups.

Thionin Staining: Free-floating sections were removed from cryoprotection and washed in 0.1M PBS (6 x 10 minutes). Sections were then mounted on Superfrost micro slides using 0.3% gelatin and left to air dry. Sections were then rehydrated in 100% ethanol (4min), 95% ethanol (4min), 70% ethanol (2min), 50% ethanol (2min) and ddH₂O (1min) and then stained in 0.5% thionin for 20-25 seconds. Stained sections were then rinsed in ddH₂O (2x10s) and dehydrated in 50% ethanol (2min), 70% ethanol (2min), 95% ethanol with 6 drops of acetic acid (2.5min), 95% ethanol (5min) and 100% ethanol (5min). Finally, sections were immersed in Xylene for 10 minutes and coverslipped using Depex mounting medium.

2.11 Imaging & Quantification

Stained brain sections were photographed with a Leica DFC295 camera coupled to a Leica DM IRE2 microscope (Leica Microsystems Inc., Concord, Ontario, Canada) with Leica Application Suite Version 4.1.0 image analysis software (Leica Microsystems). Analysis and quantification was carried out using ImageJ 1.45s software (Wayne Rasband, National Institute of Health, Bethesda, Maryland, USA).

Regions of interest: Areas of the brain examined included the anterior cortex, hippocampus, basal forebrain, thalamus, internal capsule, corpus callosum, and the cerebral cortex. Further analysis and quantification was carried out specifically in the medial septal nucleus (MSN) and vertical diagonal band (VDB) of the basal forebrain (Bregma level 0.7mm to 0.2mm), the CA1 and CA3 regions of the hippocampus (Bregma level -3.14mm to -3.8mm), and the posterior thalamic, ventral posteromedial and ventral posterolateral thalamic nuclei (Bregma level -3.14mm to -3.8mm) (Figure 4).

Microglia Cell counts: Images of OX-6 immunoreactive microglia in the MSN/VDB, thalamus, and internal capsule were acquired at 10x magnification. Images were taken from both the left and right side of the brain for the thalamus and internal capsule. Two observers blinded to the treatment groups completed cell counts from images by manually selecting positively stained microglia cells in the predefined region of interest using ImageJ software. Four tissue sections per rat corresponding to the brain region of interest were used for analysis.

Cholinergic neuronal counts: Images of ChAT positive neurons in the MSN/VDB were acquired. Cholinergic neurons were counted by two observers blinded to the treatment groups in five representative brain sections per rat within the same 5000 μm^2 area. Observers manually selected ChAT positive stained cells using ImageJ software in the pre-identified MSN/VDB region of the basal forebrain. Counts were then normalized to that of the control (Reverse Peptide) group within an age group. Cholinergic neuronal numbers were then represented as the % of cholinergic neurons in the MSN/VDB region relative to the control.

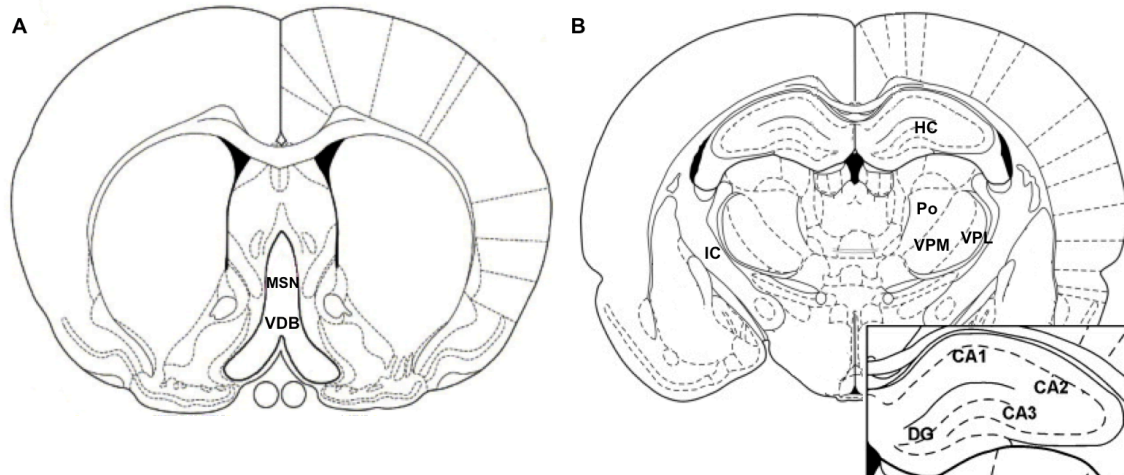


Figure 4. Atlas representations of the rat brain. (A) The basal forebrain medial septal nucleus (MSN) and vertical diagonal band (VDB). **(B)** The internal capsule (IC), the posterior (Po), ventral posterolateral (VPL) and ventral posteromedial (VPM) thalamic nuclei and the hippocampus (HC). Subregions of the hippocampus including the CA1, CA2, CA3 and dentate gyrus (DG) are represented in the bottom right part of the image.

H&E cell counts: Photomicrographs of the left and right CA1 and CA3 region of the hippocampus were taken at 20x magnification in H&E stained sections. The total number of undamaged neurons within the same area were counted using ImageJ software. Two different observers counted the number of undamaged neurons in the CA1 and CA3 region of the hippocampus; the observers completed the counts independently from one another and were blinded to the experimental conditions. Only cells with a neuronal morphology were counted. The number of undamaged neurons per optical field (neuronal density) was determined in four tissue sections per rat.

Thionin cell counts: Images of the left and right CA1 and CA3 regions of the hippocampus of thionin stained sections were acquired. Thionin staining was completed to further evaluate neuronal integrity in the hippocampus. This method gives the opportunity to assess cytoarchitecture as well as degenerative changes in neurons in the regions of interest. The quantification measure, termed % irregular neurons, was defined as the number of irregular neurons over the total number of neurons counted in the region of interest. Damaged neurons were recognized as cells that were severely misshapen and/or with changed nuclei (pyknosis, karyorrhexis and karyolysis). Two different observers, independently from each other and blinded to the experimental groups, completed cell counts of both damaged and undamaged neurons in the CA1 and CA3 regions of the hippocampus for all treatment groups.

Astrocyte Optical Density Measurements: Images of GFAP positive astrocytes from both the left and right side of the CA1 and CA3 regions of the hippocampus and in the thalamus were acquired at 20x magnification. Densitometric analysis of GFAP immunohistochemistry staining was measured in 8-bit converted images using ImageJ software in 4 tissue sections per rat. Optical density measurements of GFAP staining were taken as correlates of astocytosis.

2.12 Statistical Analysis

Statistical analysis was performed using GraphPad Prism 4.0 for Windows. Data was analyzed by performing a one-way or two-way analysis of variance (ANOVA) followed by a Tukey's or Bonferroni posttest respectively. Data is expressed as mean \pm S.E.M, and a $p < 0.05$ was considered statistically significant. In some cases statistical significance between treatment groups was indicated using a lettering system on graphs. Letters shared in common between or among groups indicated no significant differences.

Section 3

RESULTS

3.1 Effects of Age and A β ₂₅₋₃₅ toxicity

3.1.1 Body Weight Changes

Rats were weighed on the day of A β ₂₅₋₃₅ or RP icv administration and once weekly for the following 3 weeks. Changes in weight were calculated as weight on day of sacrifice minus weight on day of surgery. No notable body weight changes were identified between treatment groups for 3 month or 6 month rats. Nine months old rats treated with 500nmol A β ₂₅₋₃₅ showed a significant loss in body weight pre to post treatment in comparison to RP treated animals ($p < 0.05$) (Figure 5).

3.1.2 Neuroinflammation: Microglia Expression in the Medial Septal Nucleus/Vertical Diagonal Band

Microglia are one of the key cellular mediators of inflammation in the brain, and their activation and proliferation play critical roles in both acute and chronic neuroinflammatory responses. In response to A β toxicity, microglia are activated and have been shown to secrete a number of pro-inflammatory molecules. They are also known to cluster around sites of A β deposition in the AD brain (Akiyama et al., 2000). The basal forebrain cholinergic system appears particularly susceptible to A β toxicity, and cholinergic neurons are one of the first neuronal populations affected in the AD brain (Auld et al., 2002). Neuroinflammation, and thus microglia recruitment and activation, has been shown to occur in vulnerable regions of the AD brain. Thus, the basal forebrain, specifically the subdivision that innervates the hippocampus, namely the medial septal nucleus (MSN) and vertical diagonal bands (VDB), was examined in order to determine if this area was susceptible to neuroinflammation in response to A β ₂₅₋₃₅ toxicity. Sections were stained with the microglia marker OX-6 in order to examine microglia reactivity, taken as a correlate of neuroinflammation.

Three months old A β ₂₅₋₃₅ 500nmol rats had an increased number of reactive microglia in the MSN/VDB compared to 3 months old RP animals ($p < 0.05$; Figure 6). There was a significant increase in microglia in the MSN/VDB

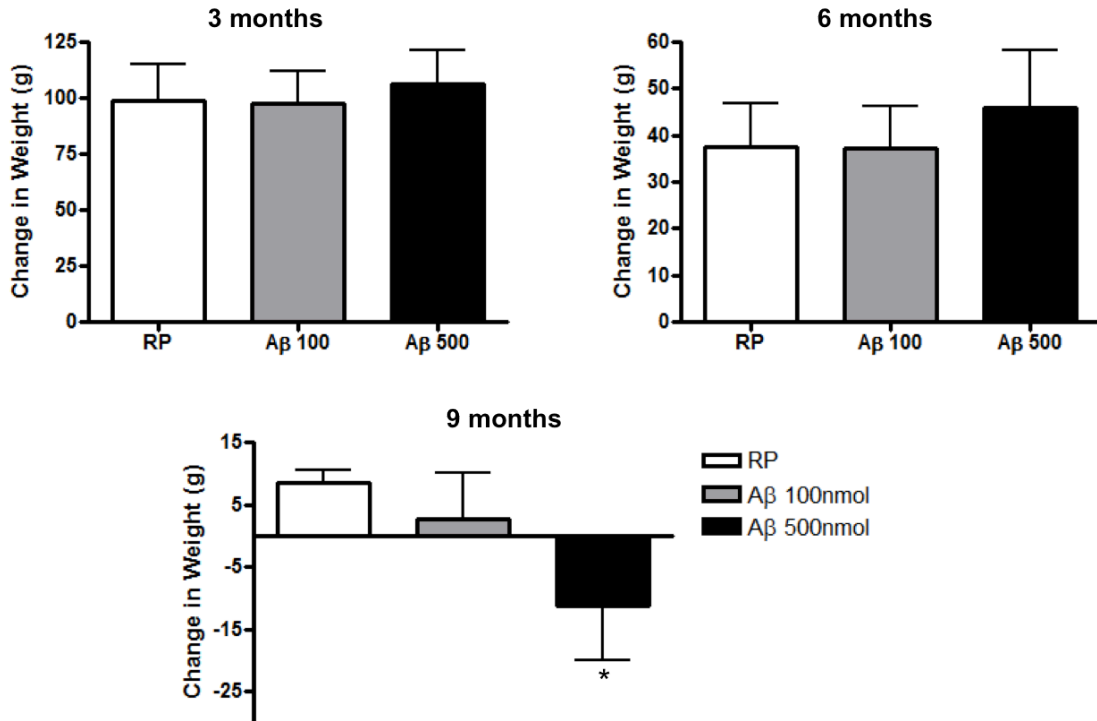


Figure 5. Weight loss in 9 month $A\beta_{25-35}$ treated rats. Changes in body weight for 3, 6, and 9 month RP, $A\beta_{25-35}$ 100nmol and $A\beta_{25-35}$ 500nmol administered rats. Change in weight was calculated as weight on day of perfusion minus weight on day of reverse peptide $A\beta_{35-25}$ or $A\beta_{25-35}$ administration. Data is presented as mean \pm SEM, * p <0.05 vs. the control RP (One-way ANOVA, Tukey's post hoc).

of 6 months A β_{25-35} 500nmol treated rats in comparison to 6 month RP ($p<0.001$) and A β_{25-35} 100nmol ($p<0.001$) groups. Activated microglia were also significantly higher in 9 month A β_{25-35} 500nmol animals in comparison to 9 month RP ($p<0.01$) and A β_{25-35} 100nmol ($p<0.001$) animals. There was also an age-dependent increase in activated microglia, with 6 month A β_{25-35} 500nmol animals showing significantly higher numbers of microglia in the MSN/VDB in comparison to 3 months A β_{25-35} 500nmol animals ($p<0.01$; Figure 6). Therefore, higher doses of A β_{25-35} toxicity resulted in increased activation of microglia in the MSN/VDB in 3, 6 and 9 month animals, and 6 and 9 month animals showed greater microglia activation in the MSN/VDB in response to A β_{25-35} toxicity than 3 month animals.

3.1.3 Cholinergic neurons in the MSN/VDB

Degeneration of cholinergic neurons in the basal forebrain is a well-established hallmark of AD. The known vulnerability of this region to A β toxicity combined with the increased microglia activation observed in the MSN/VDB of the basal forebrain with age and A β_{25-35} toxicity, led to the evaluation of whether cholinergic neuronal loss occurred in this region. Tissue sections containing the MSN/VDB were stained using anti-choline acetyltransferase antibody (ChAT). Choline acetyltransferase is the enzyme responsible for synthesizing acetylcholine and loss of ChAT staining indicates a loss of cholinergic neurons. There were no significant differences in cholinergic neuronal number, shown as a percentage of the control, between treatment groups in 3 months old rats (Figure 7G). At 6 months, the 500nmol A β_{25-35} group showed a significant decrease in cholinergic neurons compared to both the 100nmol A β_{25-35} treated group ($p<0.05$) and the RP group ($p<0.05$; Figure 7H). There was also a significant decrease in number of cholinergic neurons in the MSN/VDB of 9 month 500nmol A β_{25-35} administered rats compared to the 9 month RP group ($p<0.05$; Figure 7I). Therefore, it appears that high doses of A β_{25-35} in 6 and 9 months old rats contribute to cholinergic neuronal loss. No differences in cholinergic neuronal numbers in the MSN/VDB were seen within treatment groups between age groups.

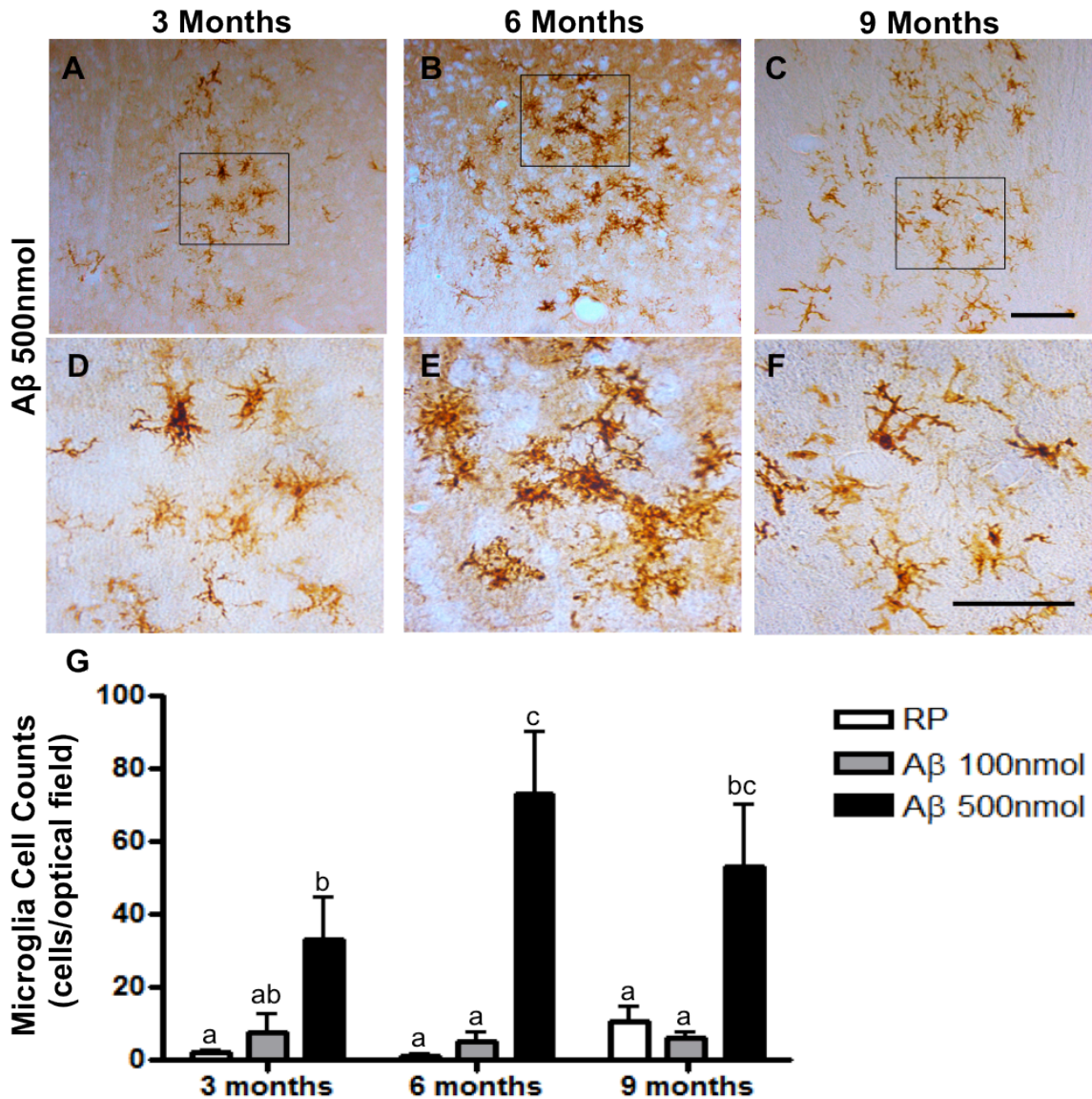


Figure 6. Increase in activated microglia in the Medial Septal Nucleus/Vertical Diagonal Band (MSN/VDB) in response to A β ₂₅₋₃₅. (A-F) Representative photomicrographs of OX-6 immunopositive microglia in the MSN/VDB of 3, 6 and 9 months old A β ₂₅₋₃₅ 500nmol administered rats. Areas boxed in lower power photomicrographs (20x) (A-C) are shown at higher power (40x) in panels (D-F). Scale bar 100 μ m. (G) The number of OX-6-immunoreactive microglia in the MSN/VDB of rats 3, 6 or 9 months of age administered the control RP, A β ₂₅₋₃₅ 100nmol or A β ₂₅₋₃₅ 500nmol. Data are presented as mean \pm SEM, means with different letters are significantly different (Two-way ANOVA, Bonferroni posttest, p <0.05).

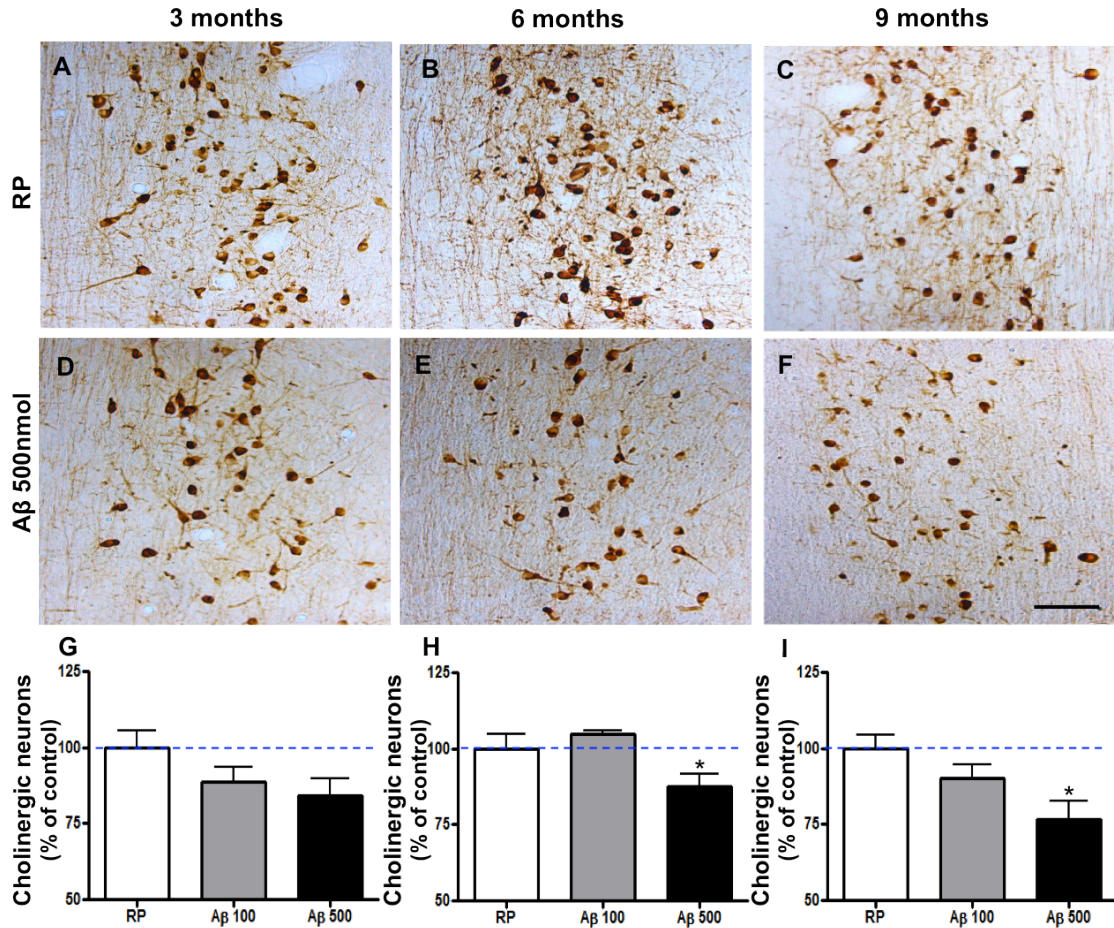


Figure 7. Age-dependent cholinergic neuronal loss in the basal forebrain. (A-F) Representative images of ChAT immunolabeled cholinergic neurons in the medial septal nucleus/vertical diagonal band (MSN/VDB) of the basal forebrain in RP and A β_{25-35} 500nmol administered animals 3, 6 and 9 months of age. Scale bar 100 μ m (G-I) The percent change (relative to RP rats within an age group) of ChAT positive neurons in MSN/VDB in RP, A β_{25-35} 100nmol and A β_{25-35} 500nmol administered rats, 3, 6 or 9 months of age. Data presented as mean \pm SEM, * p <0.05 vs. RP group within an age-group (One-way ANOVA, Tukey's posthoc).

3.1.4 Neuroinflammation: Microglia and astroglial reactivity in the thalamus

A β deposition and neuroinflammation have been shown to occur in almost all thalamic nuclei in both the human AD brain and in animal models of the disease (Braak and Braak, 1990; Miao et al., 2005; Fan et al., 2007). Microglia and astrocyte reactivity was examined in the thalamus in response to A β_{25-35} toxicity. Three months old rats showed little to no microglia activation in the thalamus regardless of treatment. Microglia activation in the thalamus of 6 months old, 500nmol A β_{25-35} animals was significantly greater than 100nmol A β_{25-35} ($p < 0.001$) and RP ($p < 0.001$) treated rats (Figure 8D). There were no significant differences in microglia activation between treatment groups in the thalamus of 9-month old rats. However, baseline levels of microglia in the thalamus of 9 months old animals were elevated compared to that seen in 3 and 6 months old animals. Both 6 and 9 months old rats exposed to 500nmol A β_{25-35} showed significantly greater numbers of activated microglia in the thalamus compared to 3 month A β_{25-35} 500nmol animals ($p < 0.01$ and $p < 0.05$ respectively, Figure 8).

Glial activation in response to A β toxicity has been repeatedly reported in cell culture and in animal models of AD (Akiyama et al., 2000). To determine if there was an increase in activation or proliferation of astrocytes in response to A β toxicity, GFAP immunohistochemistry was performed. GFAP is a marker of astroglial reactivity. Optical density measurements of GFAP immunopositive astrocytes revealed no statistically significant differences in astrocyte density in the thalamus between ages or treatment groups (Figure 9).

3.1.5 Neuroinflammation: Astrocyte activation in the hippocampus

Qualitative analysis and quantitative optical density measurements of GFAP immunolabeled astrocytes in the CA1 and CA3 regions of the hippocampus were completed in order to examine whether A β_{25-35} toxicity resulted in astrogliosis in these hippocampal regions. Qualitative analysis involved blinded assessments of the relative number of astrocytes in the defined hippocampal subregions. Qualitative assessments revealed an increase

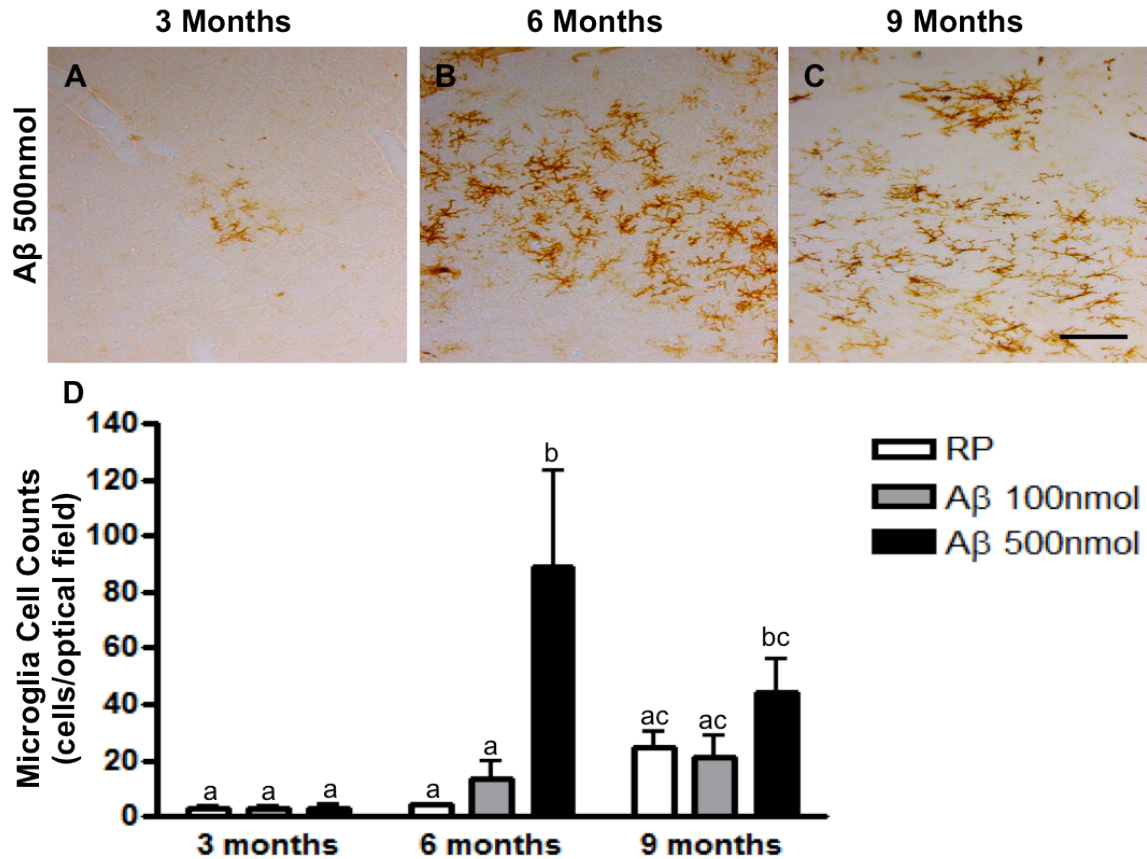


Figure 8. Age-related increase in thalamic microglia activation in response to Aβ₂₅₋₃₅. (A-C) Representative photomicrographs of OX-6 immunopositive microglia in the thalamus of 3, 6 and 9 months old Aβ₂₅₋₃₅ 500nmol rats respectively. Scale bar, 100μm. (D) The number of OX-6 immunoreactive microglia cells in the thalamus (posterior thalamic, ventral posterolateral and ventral posteromedial thalamic nuclei) of RP, Aβ₂₅₋₃₅ 100nmol and Aβ₂₅₋₃₅ 500nmol administered rats 3, 6 or 9 months of age. Data are presented as mean ± SEM, means with different letters are statistically different (Two-way ANOVA, Bonferroni posttest, *p* < 0.05).

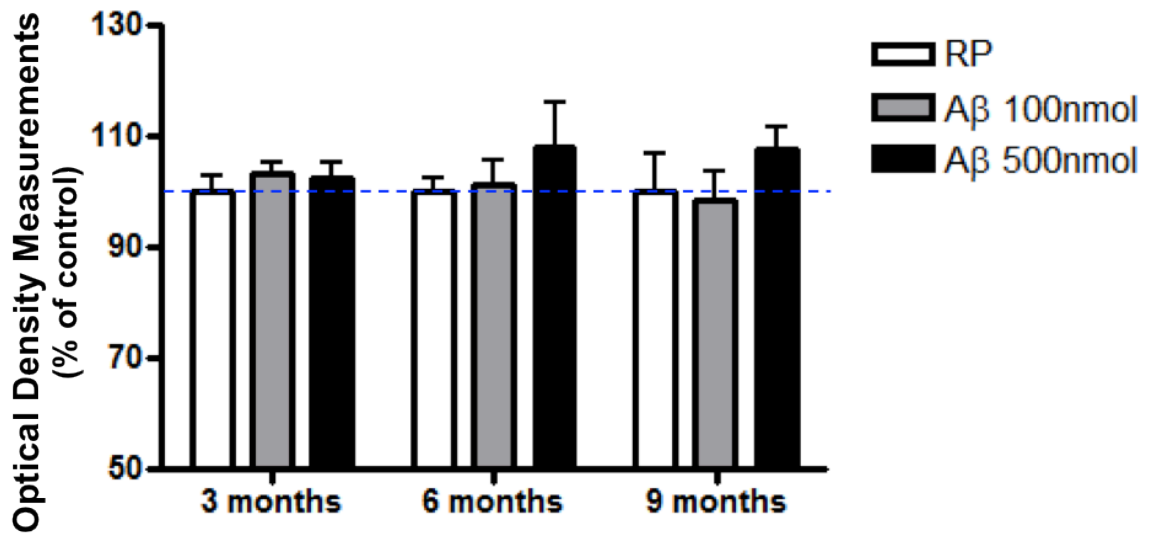


Figure 9. No changes in GFAP immunopositive astrocytes in the thalamus.

(A) Optical density measurements of GFAP immunoreactive astrocytes in the thalamus of RP, A β_{25-35} 100nmol and A β_{25-35} 500nmol administered animals 3, 6 or 9 months of age. Optical density measurements are shown as a percentage of the control RP group within an age group. Data are presented as mean \pm SEM. No statistically significant differences were seen between treatment groups within an age group (Two-way ANOVA, Bonferroni posttest, $p < 0.05$).

in astrocyte density in the CA3 region of the hippocampus in 6 and 9 month 500nmol A β_{25-35} administered animals compared to RP administered animals within an age group (Figure 10D,E, F). However, optical density measurements of GFAP positive astrocytes in the CA3 region of the hippocampus only revealed increased astrocyte density in 6 month A β_{25-35} 500nmol animals compared to 6 month RP animals ($p < 0.05$; Figure 10H). Three-month and 9-month old rats showed no differences in astrocyte density in the CA3 region of the hippocampus between treatment groups (Figure 10G,I). No differences in astrocyte density were detected in the CA1 region of the hippocampus between age groups or treatment groups (Data not shown).

3.1.6 Hippocampus integrity: H&E and thionin staining

Loss of hippocampal neurons occurs in normal aging and in AD, with the CA1 and CA3 regions of the hippocampus being particularly susceptible to A β toxicity (Gallagher and Nicolle, 1993; Landfield, 1988; Hayakawa et al., 2007). Pyramidal neuronal numbers in the CA1 and CA3 region of the hippocampus were measured from sections stained with H&E in rats 3 weeks after icv injections of A β_{25-35} or the reverse A β_{35-25} peptide. Six months old animals receiving 500nmol A β_{25-35} icv injections had a decrease in pyramidal cell counts in the CA3 subfield of the hippocampus compared to 6 months old RP injected rats ($p < 0.05$; Figure 10E). In 9-month animals both 100nmol A β_{25-35} and 500nmol A β_{25-35} icv injections resulted in a decrease in pyramidal cells in the CA3 region compared to 9 month RP injected animals ($p < 0.01$, $p < 0.001$ respectively; Figure 11F). No differences in neuronal counts in the CA3 subfield between treatment groups were identified in 3 months old rats (Figure 11D). Age and treatment had no effect on number of pyramidal neurons in the CA1 hippocampal subfield (Figure 11A-C).

To further evaluate neuronal integrity in the hippocampus and to complement the H&E data, thionin staining was completed. This additional histological stain was completed in order to assess neuronal morphology and changes in neuronal numbers in response to A β_{25-35} toxicity. Total number of

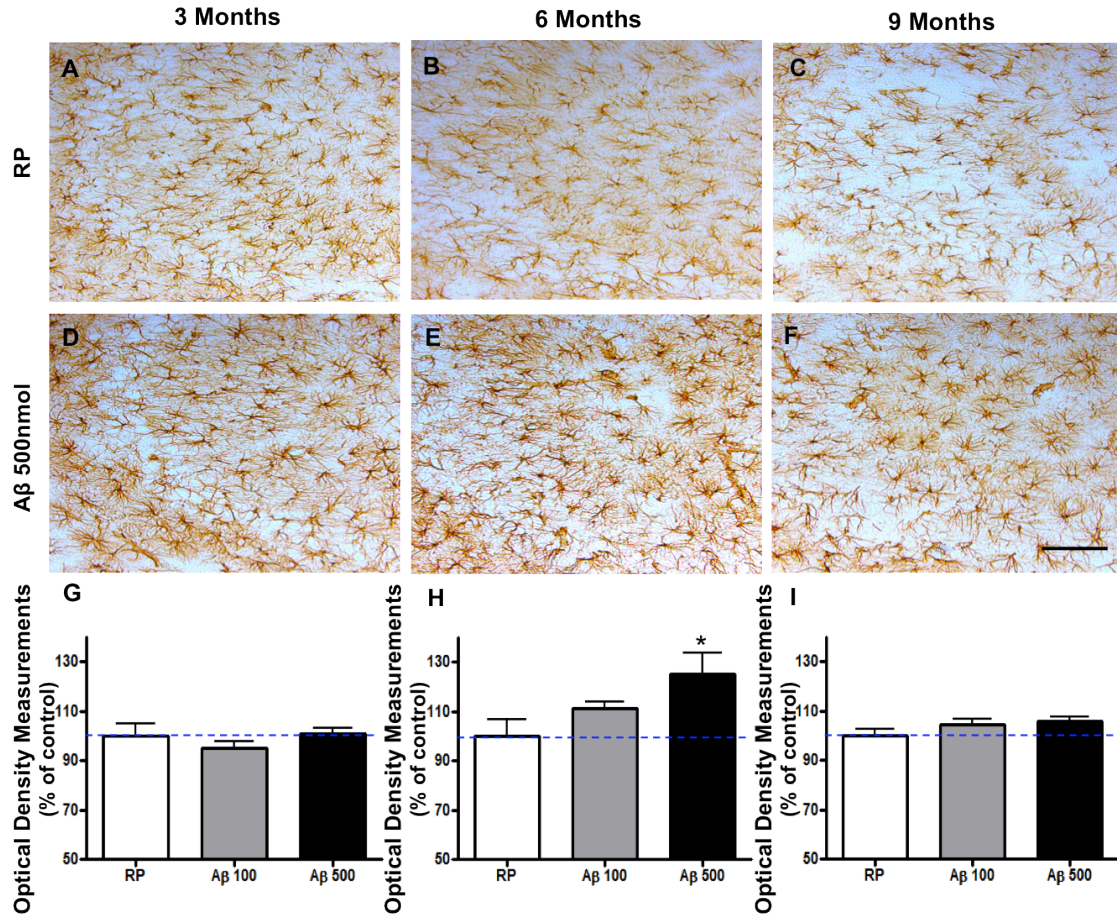


Figure 10. Astrocyte activation in the CA3 region of the hippocampus. (A-F) Representative photomicrographs of GFAP immunolabeled astrocytes in the CA3 subfield of the hippocampus in RP and A β_{25-35} 500nmol administered rats 3, 6 or 9 months of age. Scale bar 100 μ m **(G-I)** Optical density measurements of GFAP immunopositive astrocytes in the CA3 region of the hippocampus in 3, 6 or 9 month-old rats 21 days following icv administration of RP, A β_{25-35} 100nmol or A β_{25-35} 500nmol. Optical density measurements are shown as a percentage of the control, RP group within an age group. Data are presented as mean \pm SEM, * p <0.05 vs. RP group within an age-group (One-way ANOVA, Tukey's post-hoc).

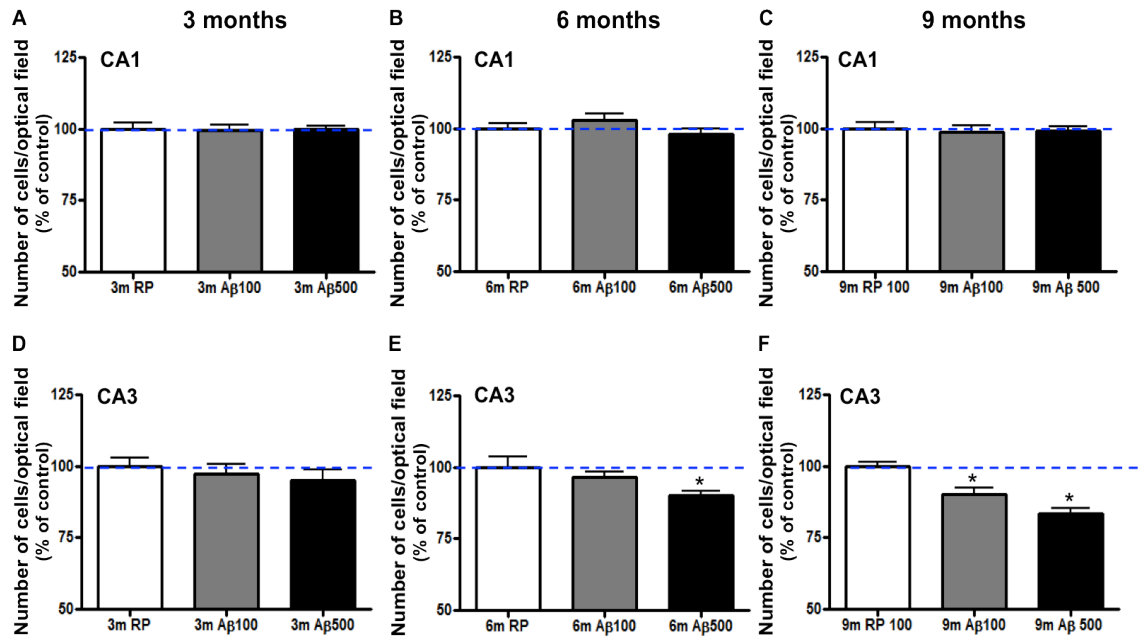


Figure 11. Neuronal numbers in the CA1 and CA3 subfields of the hippocampus. Variations in neuronal cell counts from Hematoxylin and Eosin stained sections in the (A-C) CA1 and (D-F) CA3 hippocampal regions determined 3 weeks after icv injection of RP, A β_{25-35} 100nmol or A β_{25-35} 500nmol in 3, 6 or 9 month old rats. Pyramidal cell counts are shown as a percentage of the control RP group within an age group. Data presented as mean \pm SEM, * p <0.05 vs. RP group within an age group (One-way ANOVA, Tukey's post-hoc).

neurons in the CA3 region of the hippocampus were determined, along with number of neurons identified as being irregular, giving the reported measure of percentage of irregular neurons. Irregular neurons were those identified as being severely misshapen and/or with changed nuclei (pyknosis, karyorrhexis and karyolysis). No differences in percentage of irregular neurons were identified between treatment groups for 3 months old animals (Figure 12G). Six-month $A\beta_{25-35}$ 500nmol administered animals had an increased number of irregular neurons in the CA3 region of the hippocampus compared to 6 month RP animal ($p < 0.01$; Figure 12N). Animals 9 month of age receiving icv injections of $A\beta_{25-35}$ 500nmol also showed an increase in irregular neurons compared to 9 month RP animals ($p < 0.05$; Figure 12U).

3.1.7 Leakiness of cerebrovasculature

Amyloid depositions in the vasculature, and disruption of the blood brain barrier (BBB) have been implicated as playing a role in AD. To determine whether age and $A\beta_{25-35}$ toxicity play a role in the susceptibility of the brain to vascular dysfunction dual-labeling for SMI71 & Dysferlin was used to assess leakiness of cerebrovasculature. SMI71 staining is a marker for endothelial proteins at the BBB and is localized to mature endothelial cells when the BBB is intact (Sternberger and Sternberger, 1987). Staining for SMI71 is lost when there is disruption of the BBB (Sternberger et al., 1989; Kim et al., 2012). Dysferlin expression is associated with vascular leakage of serum proteins, indicative of leaky blood vessels (Hochmeister et al., 2006). Qualitative analysis involving blinded assessment and ratings of extent of dysferlin staining and loss of SMI71 staining in defined regions was conducted.

Qualitative analysis of SMI71 & Dysferlin staining showed an age-dependent increase in BBB leakage in the thalamus, and hippocampus in response to $A\beta_{25-35}$ administration. Examination of cerebrovasculature was completed in the hippocampus of 3, 6 and 9 month RP, 100nmol $A\beta_{25-35}$ and 500nmol $A\beta_{25-35}$ icv injected animals. Three-month animals irregardless of

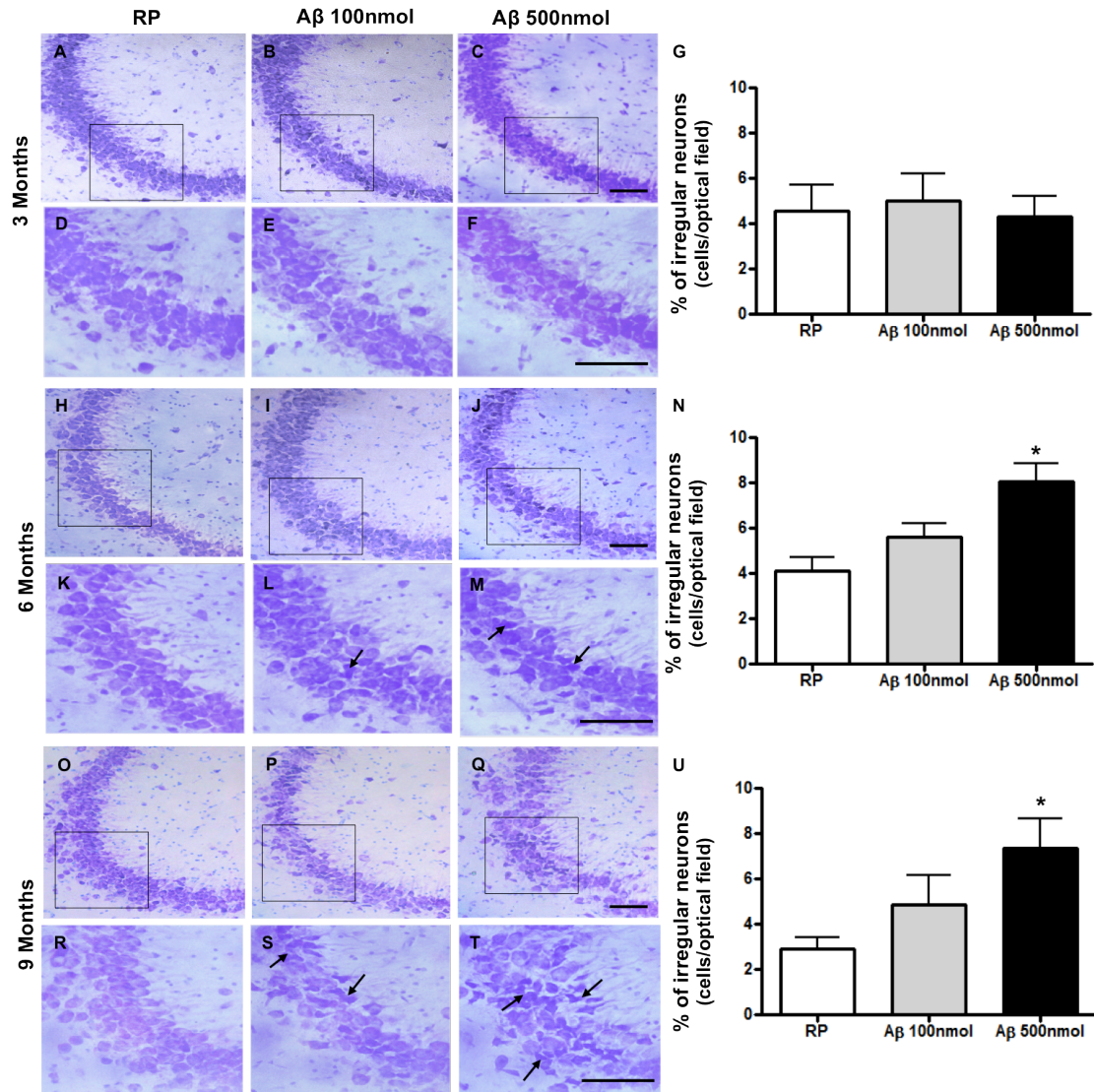


Figure 12. Thionin staining to evaluate neuronal integrity in the CA3 region of the hippocampus. Representative photomicrographs of thionin stained cells in the CA3 subfield of the hippocampus in RP, A β_{25-35} 100nmol, and A β_{25-35} 500nmol administered rats 3, 6 or 9 months of age. Areas boxed at lower power (20x) are shown at higher power (40x) in the corresponding panel below. Representative irregular neurons are indicated by arrows, scale bar 100 μ m. **(G,N,U)** The number of irregular neurons shown as a percentage of total neuronal counts in the hippocampal CA3 region for RP, A β_{25-35} 100nmol and A β_{25-35} 500nmol administered rats 3, 6 and 9 months of age. Data are presented as mean \pm SEM, * p <0.05 vs. RP group within an age group (One-way ANOVA, Tukey's post hoc).

treatment showed little to no dysferlin staining in the CA1 or CA3 subfields of the hippocampus (Figure 13A,B,E,F). Animals 9 months of age showed minimal dysferlin staining in the CA1 region of the hippocampus (Figure 13C,D). In the CA3 hippocampal region 500nmol $A\beta_{25-35}$ animals showed more dysferlin staining than RP animals, with all 9 month treatment groups showing more dysferlin staining than seen in the same regions in 3 months animals (Figure 13G-H).

The same thalamic nuclei imaged and analyzed for neuroinflammation was evaluated for vascular integrity, namely the posterior thalamic, ventral posteromedial and ventral posterolateral thalamic nuclei. At 3 months SMI71 staining was present throughout the thalamic region, and minimal dysferlin staining was observed regardless of treatment (Figure 14A-B). Nine-month animals showed dysferlin staining in the thalamic region in both RP and $A\beta_{25-35}$ administered animals (Figure 14C-D). However, $A\beta_{25-35}$ treated animals showed greater amounts of dysferlin staining, with longer lengths of vessels being stained for dysferlin. Animals six months of age showed an intermediate pathology between that seen in 3 and 9-month old animals (Images not shown).

3.2 CAT-SKL and $A\beta_{25-35}$ toxicity

In order to evaluate the potential of CAT-SKL treatment to reduce $A\beta_{25-35}$ toxicity similar analysis and quantification of the pathology as performed for the age and $A\beta_{25-35}$ toxicity study (Aim 1) was completed. All of these experiments were done with 6 months old rats.

3.2.1 Body Weight Changes

Rats were weighed on the day of $A\beta_{25-35}$ or RP $A\beta_{35-25}$ icv administration and once weekly for the following 3 weeks. Change in body weight was determined based on weight on day 21 minus weight on day of icv $A\beta_{25-35}$ or RP administration. No significant changes in body weights were seen between treatment groups. However, those animals in both $A\beta$ and $A\beta$ +CAT-SKL groups lost more weight than those in the RP and RP+CAT-SKL groups (Figure 15).

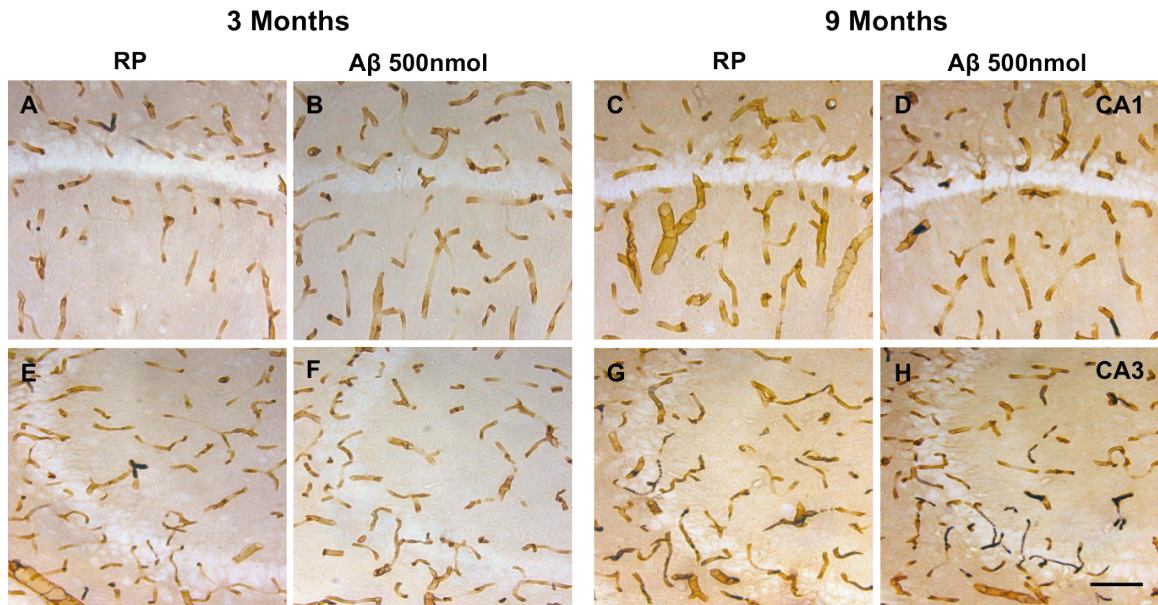


Figure 13. Cerebromicrovessels in the CA1 and CA3 subfields of the hippocampus. Photomicrographs of SMI71 & Dysferlin staining in (A-D) the CA1 and (E-H) CA3 regions of the hippocampus in 3 and 9 month old rats 3 weeks after icv administration of RP, or A β ₂₅₋₃₅ 500nmol. SMI71 (brown staining) is a marker for endothelial proteins at the blood brain barrier and dysferlin (black/dark brown staining), is a marker associated with vascular leakage of serum proteins. Scale bar 100 μ m.

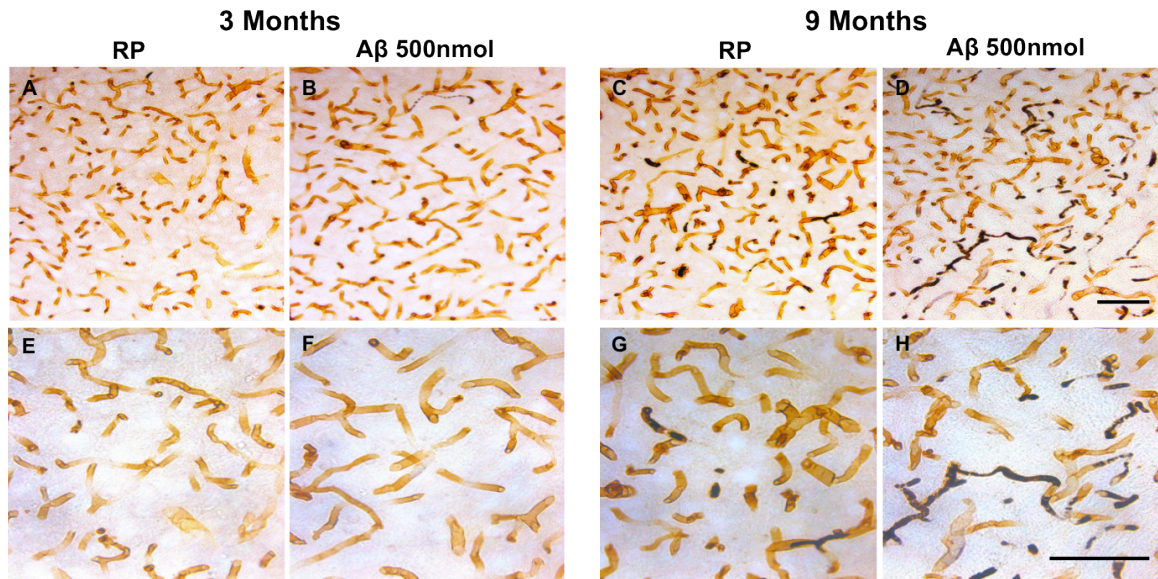


Figure 14. Age-dependent leakiness of cerebrovasculature in the thalamus. Representative photomicrographs of SMI71 & Dysferlin staining in the thalamus (posterior thalamic, ventral posteromedial and ventral posterolateral thalamic nuclei) of 3 and 9 months old RP and A β_{25-35} 500nmol administered rats. Areas shown in lower power (10x) photomicrographs (**A-D**) are shown at higher power (20x) in corresponding panels (**E-H**). SMI71 (brown staining) is a marker for endothelial proteins at the blood brain barrier co-labeled with dysferlin (black/dark brown staining), a marker associated with vascular leakage of serum proteins. Scale bar 100 μ m.

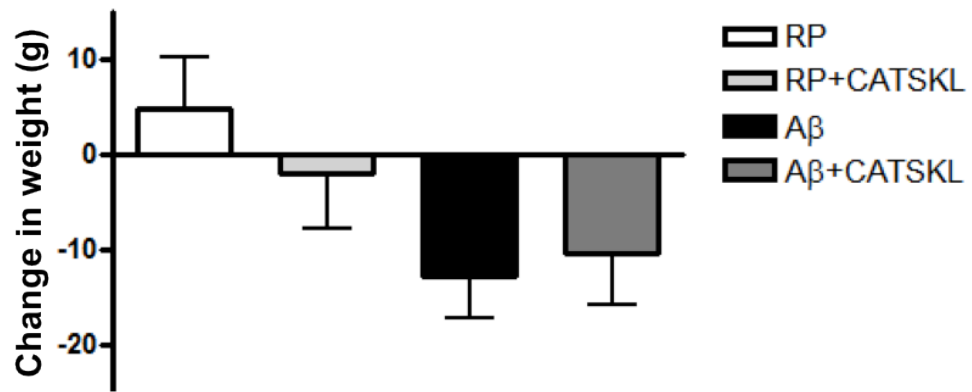


Figure 15. Body weight changes. Change in body weight in RP, RP+CAT-SKL, A β and A β +CAT-SKL rats was calculated as weight on day of perfusion minus weight on day of reverse peptide A β_{35-25} or A β_{25-35} icv administration.

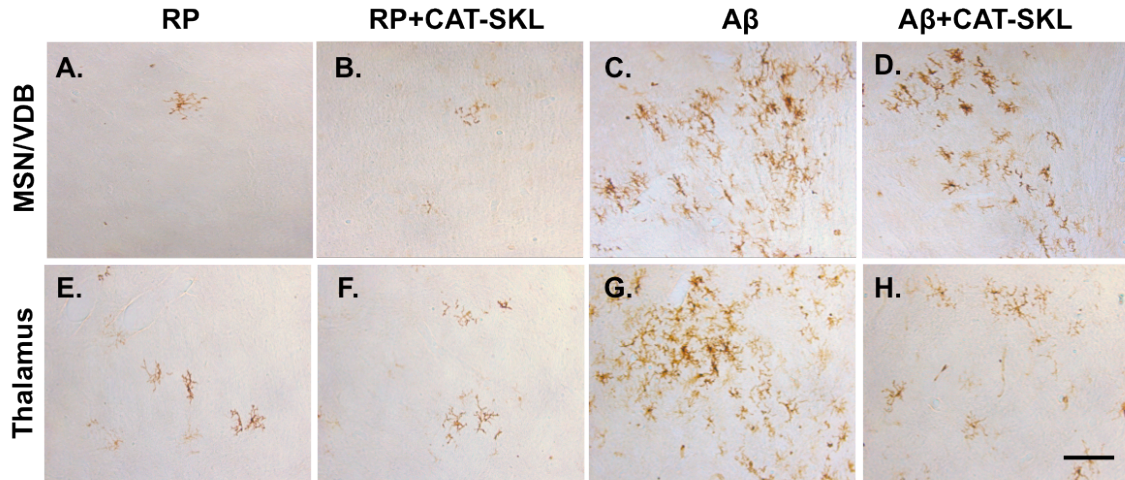
3.2.2 Neuroinflammation: Microglia expression in CAT-SKL treated animals

The significant activation of microglia in the MSN/VDB (Figure 6) and thalamus (Figure 8) identified in 6 month $A\beta_{25-35}$ injected rats lead to the investigation of whether CAT-SKL treatment could diminish this microglia response. The microglia marker OX-6 was used to evaluate microglia reactivity. There was a significant increase in activated microglia in the MSN/VDB of $A\beta_{25-35}$ icv injected rats when compared to the control RP ($p < 0.001$), and RP+CAT-SKL animals ($p < 0.001$). Microglia activation in $A\beta_{25-35}$ treated rats was effectively reduced by treatment with CAT-SKL, with $A\beta$ +CAT-SKL animals showing a significant decrease in microglia in the MSN/VDB when compared to $A\beta_{25-35}$ animals ($p < 0.05$; Figure 16I).

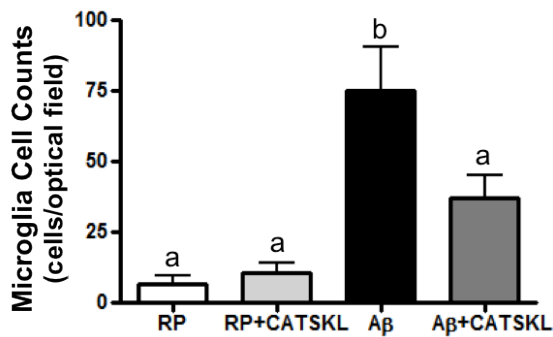
Microglia activation in the thalamus was significantly greater in $A\beta_{25-35}$ administered animals compared to the control RP group ($p < 0.05$). CAT-SKL treatment combined with $A\beta_{25-35}$ administration reduced microglia activation in the thalamus such that the microglia in the thalamus of $A\beta$ +CAT-SKL animals was not significantly different from both control groups (RP or RP+CAT-SKL) ($p > 0.05$; Figure 16J). However, this reduction in microglia was not significantly lower than the $A\beta_{25-35}$ treated animals.

3.2.3 Cholinergic neurons in the MSN/VDB in CAT-SKL treated animals

In accordance with the finding, described above, of decreased cholinergic neuronal numbers in the MSN/VDB in older $A\beta_{25-35}$ administered animals, the number of ChAT positive neurons in the MSN/VDB was evaluated. Anti-choline acetyltransferase antibody (ChAT) was used to stain cholinergic neurons in the MSN/VDB. The number of ChAT positive cholinergic neurons in the MSN/VDB was significantly reduced in $A\beta_{25-35}$ administered animals compared to RP and RP+CAT-SKL treated rats ($p < 0.05$). With CAT-SKL treatment this significant reduction induced by $A\beta_{25-35}$ administration was lost and there were no significant differences in cholinergic neuronal counts between $A\beta$ +CAT-SKL treated rats vs. RP and RP+CAT-SKL treated animals ($p > 0.05$; Figure 17).



I. MSN/VDB



J. Thalamus

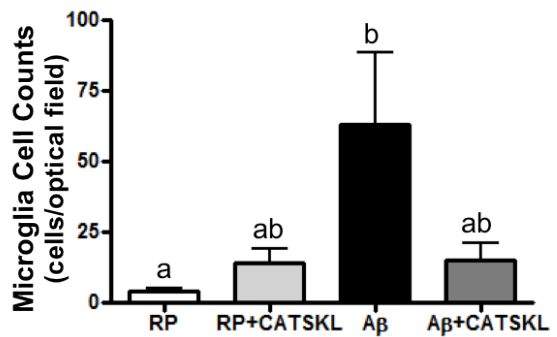


Figure 16. CAT-SKL reduces microglia activation in the MSN/VDB and thalamus. (A-D) Representative photomicrographs of microglia immunolabeled with OX-6 in the medial septal nucleus/vertical diagonal band (MSN/VDB) and (E-H) activated microglia in the thalamus of RP, RP+CATSKL, A β and A β +CATSKL treated rats respectively. Scale bar 100 μ m. (I) The number of OX-6 immunopositive microglia in the MSN/VDB and (J) the number of OX-6 immunolabeled in the thalamus of RP, RP+CATSKL, A β and A β +CATSKL treated rats. Data are presented as mean \pm SEM, means with different letters are significantly different (One-way ANOVA, Tukey's post-hoc, $p < 0.05$).

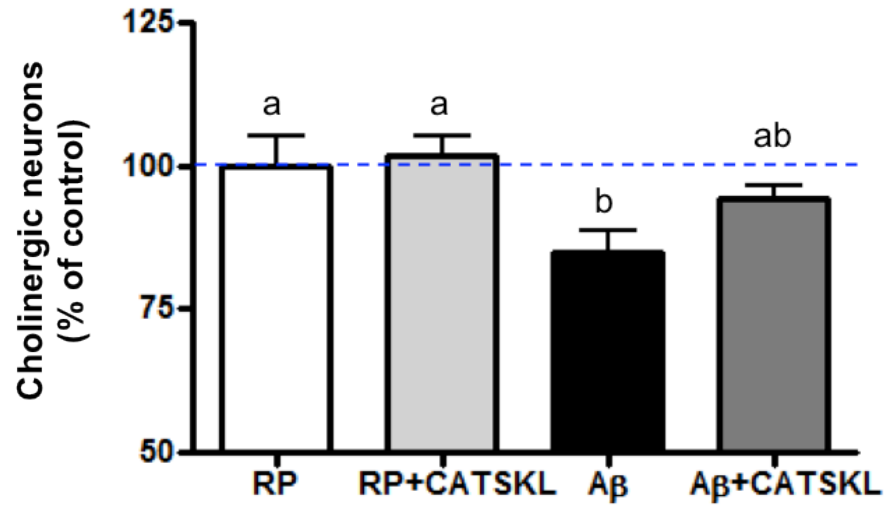


Figure 17. CAT-SKL prevents cholinergic loss in the MSN/VDB. The number of ChAT positive cholinergic neurons shown as a percentage of the RP group in the MSN/VDB of the basal forebrain in RP, RP+CAT-SKL, A β and A β +CAT-SKL treated rats. Data are presented as mean \pm S.E.M. Means with different letters signify significance (One-way ANOVA, Tukey's post-hoc, $p < 0.05$).

3.2.4 Astrocyte activation in the hippocampus of CAT-SKL treated animals

Optical density measurements of GFAP immunopositive astrocytes was taken as a measurement of astroglial reactivity. A β_{25-35} administered animals showed a significant increase in astrocyte density in the CA3 region of the hippocampus compared to RP and RP+CAT-SKL treated animals ($p < 0.05$ vs. RP, $p < 0.01$ vs. RP+CAT-SKL). CAT-SKL treatment reversed this increase in astrocyte density induced by A β_{25-35} in the CA3 ($p < 0.05$ A β vs. A β +CAT-SKL; (Figure 18). No differences in astrocyte density were detected in the CA1 region of the hippocampus between treatment groups (Data not shown).

3.2.5 Neuronal integrity in the hippocampus following A β_{25-35} administration and CAT-SKL treatment

The known vulnerability of hippocampal neurons to A β_{25-35} toxicity lead to the examination of neuronal integrity in the CA1 and CA3 subfields of the hippocampus. The number of pyramidal neurons in the CA1 and CA3 region of the hippocampus were determined using H&E and thionin staining 3 weeks after icv injections of RP or A β_{25-35} . Counts of H&E stained pyramidal neurons in the CA1 region of the hippocampus revealed no differences in neuronal numbers between treatment groups (Figure 19I). There was a significant reduction in neuronal numbers in the CA3 region of the hippocampus in A β_{25-35} treated rats compared to RP treated animals ($p < 0.05$). With CAT-SKL treatment this significant reduction in neuronal numbers was no longer observed. There were no significant differences in pyramidal cell numbers between A β_{25-35} and RP+CAT-SKL or A β +CAT-SKL treated rats (Figure 19J).

In order to further examine neuronal morphology and changes in neuronal number in response to A β_{25-35} toxicity thionin staining was completed. The number of neurons identified as being irregular over the total number of neurons in the CA3 region of the hippocampus was determined, giving the reported measure of percentage of irregular neurons. There was a significant increase in percentage of irregular neurons in the CA3 region in A β_{25-35} administered animals

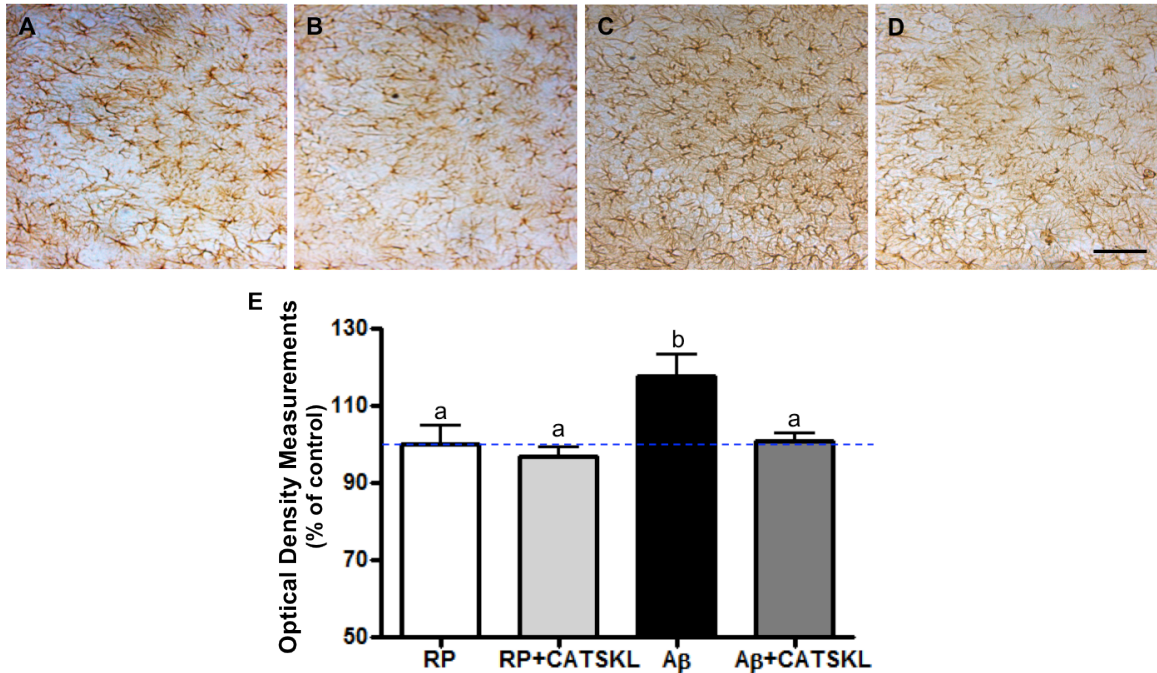


Figure 18. CAT-SKL reduces astrocyte activation in the CA3 region of the hippocampus. (A-D) Representative photomicrographs of GFAP immunolabeled astrocytes in the CA3 region of the hippocampus of RP, RP+CAT-SKL, A β and A β +CAT-SKL treated rats respectively. Scale bar 100 μ m. **(E)** Optical density measurements of GFAP immunopositive astrocytes in the CA3 region of the hippocampus shown as a percentage of the mean value of the RP group. Different letters represent statistically significant differences (One-way ANOVA, Tukey's post-hoc, $p < 0.05$).

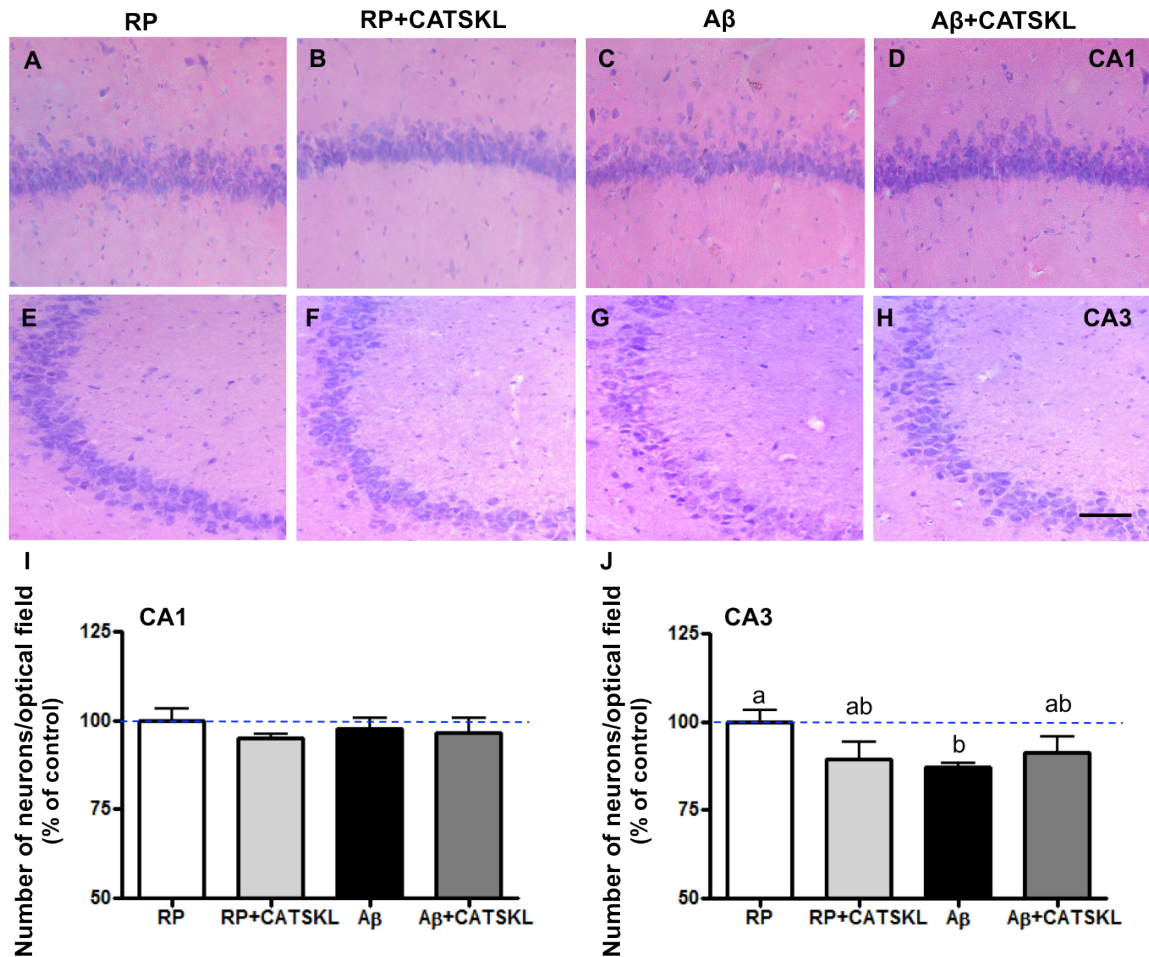


Figure 19. Neuronal integrity in the CA1 and CA3 regions of the hippocampus. Representative photomicrographs of Hematoxylin and Eosin stained cells in (A-D) the CA1 and (E-H) CA3 region of the hippocampus in RP, RP+CAT-SKL, A β and A β +CAT-SKL treated rats respectively. Scale bar 100 μ m. (I-J) Pyramidal cell numbers in the CA1 and CA3 subfields of the hippocampus shown as a percentage of the control RP group. Different letters represent statistically significant differences (One-way ANOVA, Tukey's post hoc, $p < 0.05$)

compared to RP ($p < 0.01$), RP+CAT-SKL ($p < 0.05$) and A β +CAT-SKL ($p < 0.05$) administered animals. This increase in irregular neurons was prevented by CAT-SKL treatment. No differences in counts were seen between RP, RP+CATSKL, or A β +CAT-SKL treated rats (Figure 20).

3.2.6 Behavior Testing: Morris Water Maze

To determine whether A β_{25-35} toxicity resulted in learning and memory deficits and to also examine if CAT-SKL treatment was able to alleviate memory or learning impairments animals were trained on a spatial learning task in the Morris water maze (MWM), followed by two probe trials. The spatial task was used to assess learning and the probe trials were used to assess reference memory. Reference memory was determined based on animals' preference for the platform area when the platform was absent. Probe trial 1 took place on day 12 (D12), to assess short-term reference memory retention and probe trial 2 was completed on day 19 (D19) to assess long-term reference memory retention.

Latency, path length and swimming speed during spatial learning

Rats were trained in the MWM 8 days after icv administration of A β_{25-35} or RP. Rats were subject to a total of 16 spatial learning trials over a period of 4 days, with 4 trials per day. During the training days, latency (s) to reach the platform, distance traveled (m) to reach the platform and average swimming speed (m/s) were measured and analyzed. Latency and distance travelled to find the platform decreased significantly over the course of acquisition training for all treatment groups ($p < 0.001$ Day 4 vs. Day 1), indicative of successful learning of the task. There were no differences in latency or distance travelled to find the platform between treatment groups, suggesting A β_{25-35} toxicity did not impair spatial learning (Figure 21A-B). Average swimming speed appeared to decrease over the training period for all groups, however this was not significant except for the RP+CAT-SKL group who showed a significant reduction in mean swimming speed over the course of the spatial learning trials ($p < 0.05$ Day 1 vs. Day 4).

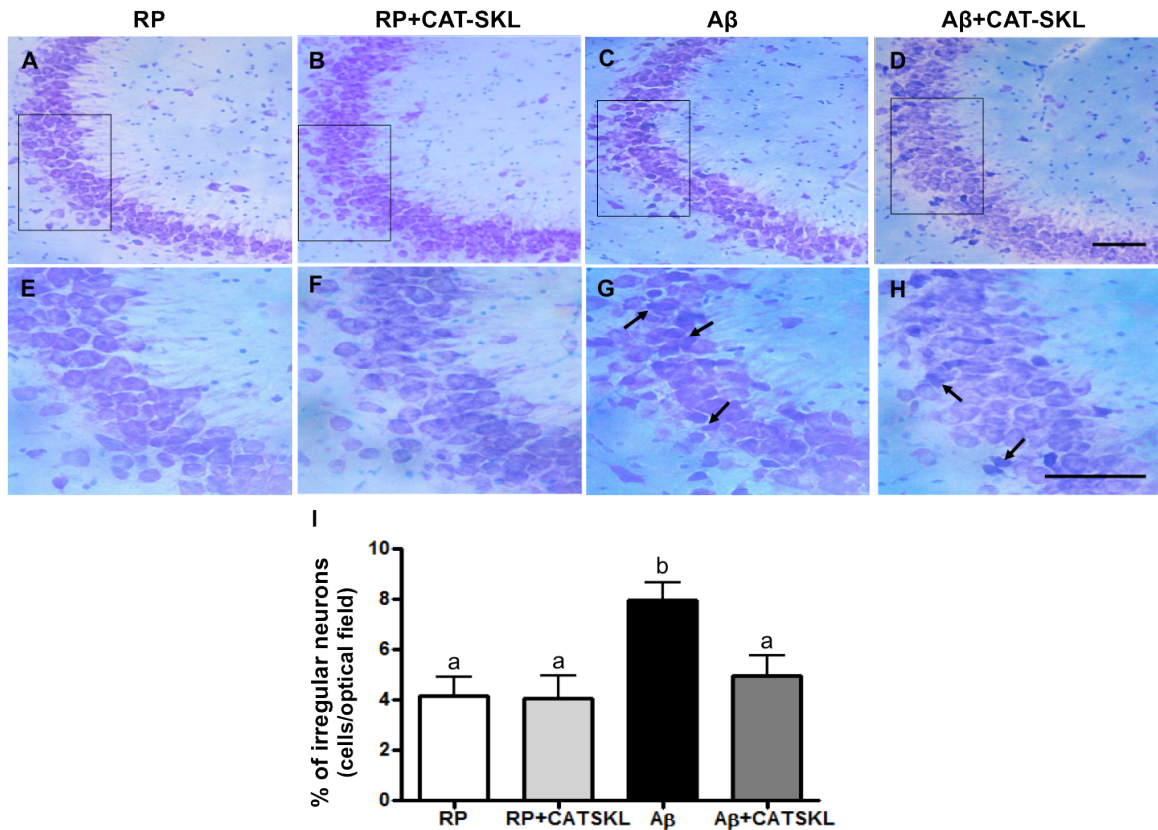


Figure 20. Thionin staining in the hippocampus. Representative photomicrographs of thionin stained cells in the CA3 subfield of the hippocampus in RP, RP+CAT-SKL, A β and A β +CAT-SKL treatment groups. Areas boxed at lower power (20x) (A-D) are shown at higher power (40x) in the panel below (E-H). Representative irregular neurons are indicated by arrows, scale bar 100 μ m. (I) The number of irregular neurons shown as a percentage of total neuronal counts in the hippocampal CA3 region. Data are presented as mean \pm SEM, means with different letters are significantly different (One-way ANOVA, Tukey's post hoc, $p < 0.05$).

There were no differences in mean swimming speed between treatment groups across training days (Figure 21C).

Probe Trial 1 on Day 12 (D12): Short-term memory retention

On day 12, 24 hours following the last spatial learning trial, rats were subject to their first probe trial. The percentage of time spent and the percentage of distance travelled in the target zone and average of the adjacent zones was determined for the probe trial. The time spent and distance travelled in the target quadrant was taken as an index of rats' memory capacity. All treatment groups spent significantly more time in the target zone than in the adjacent zones during the D12 probe trial ($p < 0.05$ for RP and RP+CAT-SKL, $p < 0.001$ for A β and $p < 0.01$ for A β +CAT-SKL; Figure 22A). RP+CATSKL, A β and A β +CAT-SKL also travelled a significantly greater distance in the target zone than in the adjacent zones ($p < 0.05$, $p < 0.01$, $p < 0.01$ respectively; Figure 22B). The greater time spent and distance travelled in the target zone over the adjacent zones indicates rats remembered the platform location and sought it out during the D12 probe trial. No differences in percentage of time spent or distance travelled in the target zone was identified between treatment groups (Figure 22A-B).

Probe Trial 2 on Day 19 (D19): Long-term memory retention

On day 19, 7 days after the first probe trial, rats were subjected to a second probe trial to assess long-term reference memory retention. As was done for the first probe trial the percentage of time spent and the percentage of distance travelled in the target zone and average of the adjacent zones was measured and analyzed. There were no significant differences in percentage of time spent in the target zone versus the adjacent zones across treatment groups. However, RP+CAT-SKL, and A β +CAT-SKL treated animals all spent a significantly greater percentage of time in the target zone than A β administered animals ($p < 0.01$ for RP+CAT-SKL vs. A β , $p < 0.05$ for A β +CAT-SKL vs A β) (Figure 22C). Animals from all treatment groups showed no significant differences in distance travelled in the target zone compared to the adjacent

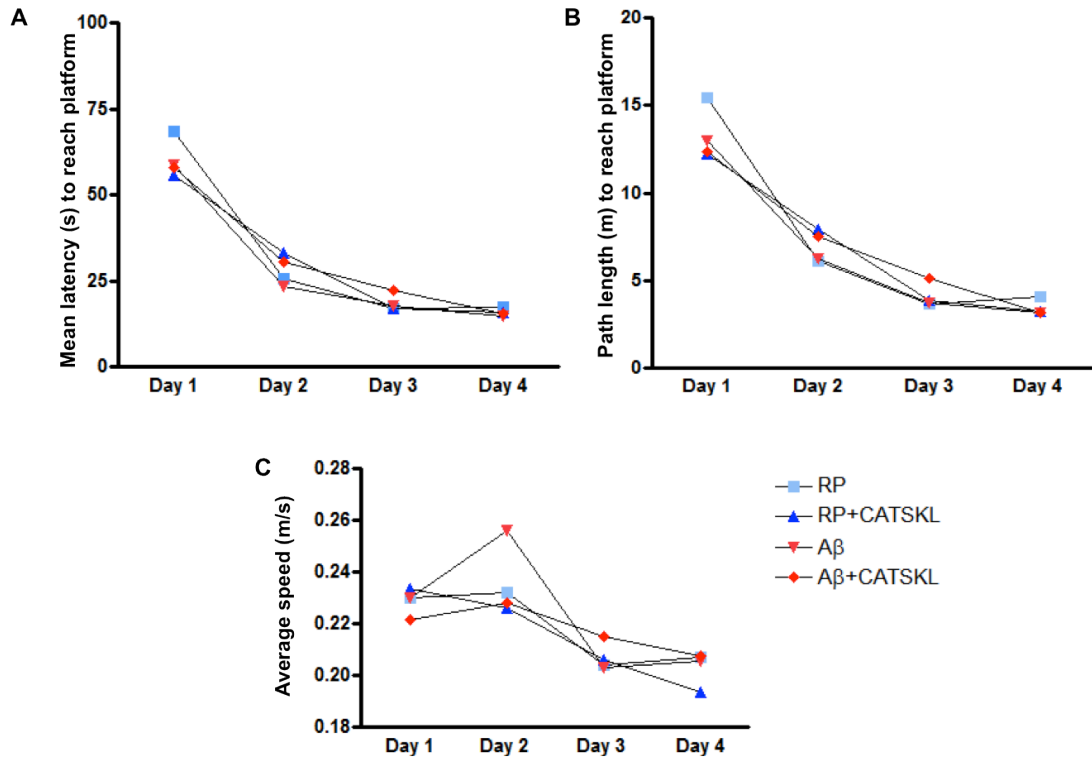


Figure 21. Spatial learning during the hidden platform Morris Water Maze (MWM) task. (A) Mean latency and **(B)** Path length to find the hidden platform in the MWM during four consecutive days of training for RP, RP+CAT-SKL, A β and A β +CAT-SKL treatment groups. Rats received 4 training trials per day with an inter-trial interval of 20 minutes. Animals from all groups showed a reduction in the mean latency and distance traveled to reach the hidden platform across training days. **(C)** Average swimming speed for all treatment groups for each of the training days during the spatial learning phase. No differences in mean speed were seen between treatment groups (Two-way ANOVA, Bonferroni posttest, $p < 0.05$).

zones except for RP+CAT-SKL treated animals who travelled a greater distance in the target zone than in adjacent zones ($p < 0.05$; Figure 22D). RP, RP+CAT-SKL, and A β +CAT-SKL animals all travelled a greater distance in the target zone than A β only animals ($p < 0.05$ for RP vs. A β , $p < 0.001$ for RP+CAT-SKL vs. A β , $p < 0.01$ for A β +CAT-SKL vs A β).

Comparison between probe trial on D12 and D19

The percentage of time spent and percentage of distance travelled in the target zone on D12 (Probe 1) and D19 (Probe 2) were compared to determine if there were any changes in reference memory across probe trials. A β administered animals spent significantly less time and travelled significantly less distance in the target zone on D19 compared to D12 ($p < 0.01$). No significant differences in time spent or distance travelled in the target quadrant between D12 and D19 were found for RP, RP+CAT-SKL and A β +CAT-SKL treated rats ($p > 0.05$; Figure 23 A-B). The reduction in time spent and distance traveled in the target quadrant on D19 compared to D12 for A β ₂₅₋₃₅ animals indicates long-term reference memory deficits, which was effectively ameliorated in A β animals treated with CAT-SKL.

Cued learning

On days 20-21 rats under went cued platform learning. Cued learning was used as a control procedure in order to determine if any differences observed in the MWM could be attributed to either a difference in motivation to escape the water, or an inability to use cues to locate the hidden platform. A cue directly attached to the platform was used to indicate the platforms position. Animals were subjected to a total of 8 cued learning trials and data are presented as the mean of the 8 trials. Animals across treatment groups showed no significant differences in the time it took them to locate the platform, or distance travelled to find the platform (Figure 24A-B). Average swimming speed was not significantly different between treatment groups (Figure 24C). Thus, rats across treatment groups demonstrated similar motivation and abilities to escape the water.

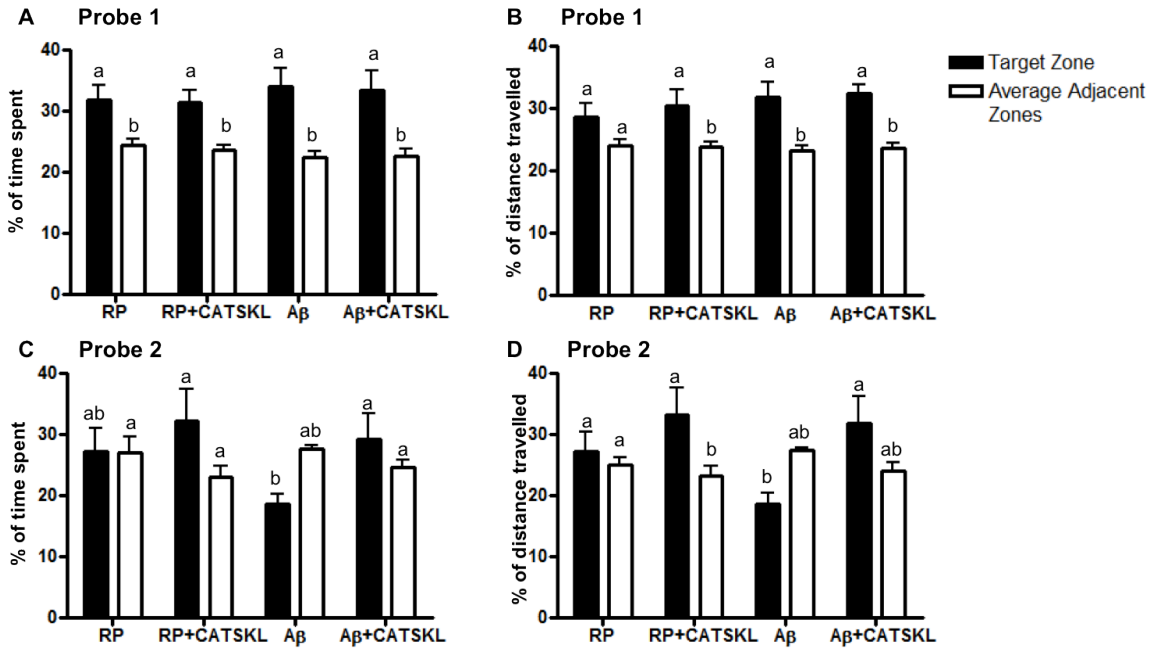


Figure 22. Probe trials: Short and long term memory retention. The percentage of time spent and percentage of distance travelled in the target zone and the average of the adjacent zones for RP, RP+CAT-SKL, A β and A β +CAT-SKL treated groups for **(A-B)** Probe trial 1, day 12 and **(C-D)** Probe trial 2, day 19. Means with different letters signify significance (Two-way ANOVA, Bonferroni post-test, $p < 0.05$).

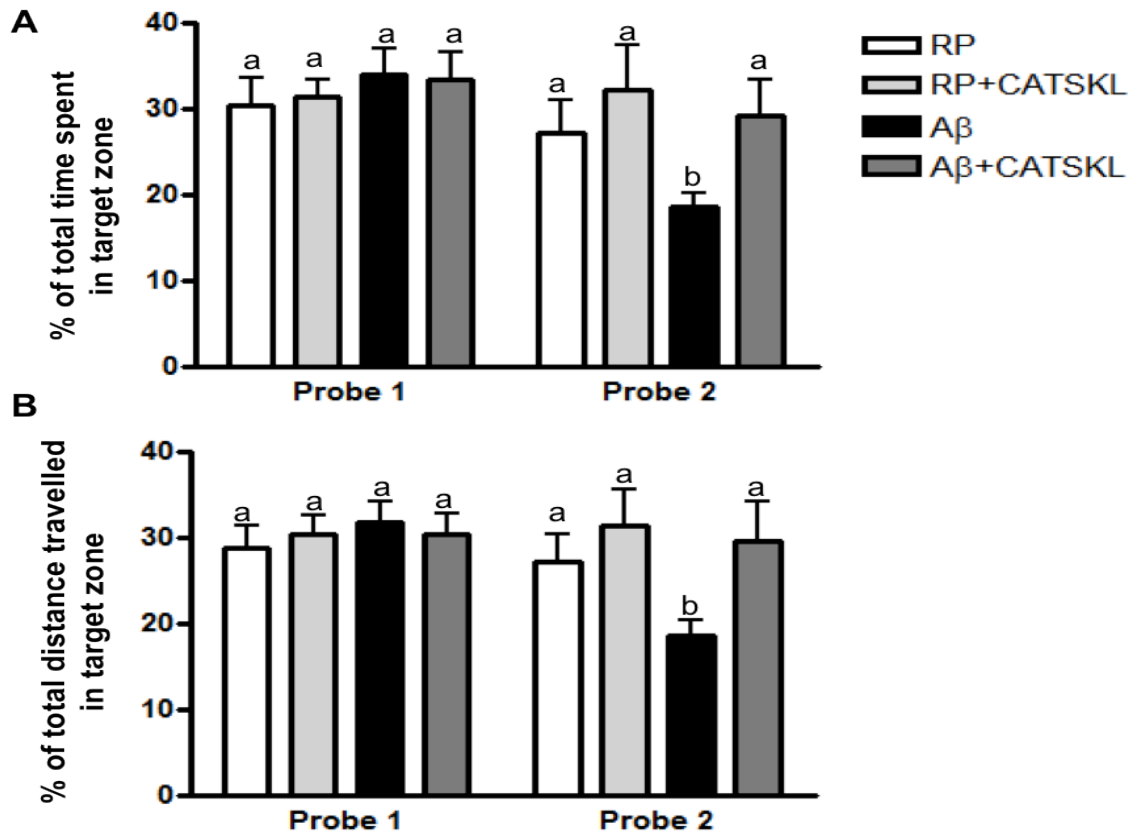


Figure 23. CAT-SKL reduces A β_{25-35} induced impairments in long-term reference memory. (A) The percentage of total time spent and **(B)** percentage of total distance travelled in the quadrant where the platform was located 24 hours following the last spatial learning trial (Probe 1) and 8 days after the last spatial training trial (Probe 2) for RP, RP+CAT-SKL, A β and A β +CAT-SKL treatment groups. Data are presented as mean \pm S.E.M. Different letters indicate significance (Two-way ANOVA, Bonferoni post hoc, $p < 0.05$).

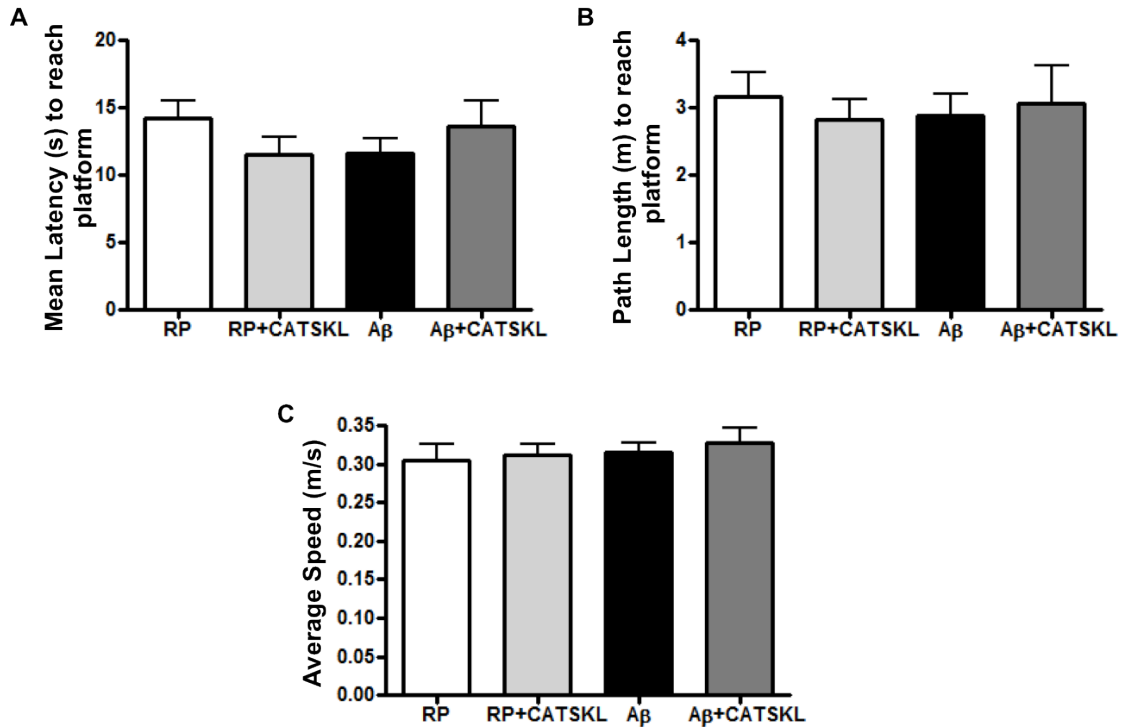


Figure 24. Cued learning during the Morris Water Maze (MWM). (A) Mean latency and (B) mean path length to find the cued platform in the MWM averaged over 8 trials for RP, RP+CAT-SKL, A β and A β +CAT-SKL treated rats. No differences in mean latency or distance traveled to reach the platform were seen between treatment groups. (C) Average swimming speed for all treatment groups over 8 cued learning trials. There were no differences in mean swimming speed between treatment groups. Data are presented as the mean \pm SEM of the 8 cued learning trials (One-way ANOVA, Tukey's post hoc, $p < 0.05$).

Section 4
DISCUSSION

The results of this investigation in a rat model of amyloid toxicity revealed two important findings. Firstly, the age of the animal plays a major role in the development of pathological changes in response to A β ₂₅₋₃₅ toxicity. Secondly, we have demonstrated for the first time that the targeted antioxidant CAT-SKL, a genetically modified catalase molecule, is effective in preventing the pathological, inflammatory and cognitive deficits induced by amyloid toxicity. In accordance with previous findings this study showed that a single icv injection of A β ₂₅₋₃₅ in male Wistar rats resulted in pathological changes in the brain 3 weeks after injection (Whitehead et al., 2005ab; Cheng et al., 2006; Zussy et al., 2011; 2013). Specifically, increased inflammation in the basal forebrain and thalamus, cholinergic loss in the MSN/VDB and loss of neuronal integrity in the hippocampus were shown. Moreover, this pathological response to A β ₂₅₋₃₅ toxicity was shown to be greater in 6 and 9 months old animals than in 3 months old animals. This suggests that at the ages of 6 and 9 months, the rodent brain is already more vulnerable to A β ₂₅₋₃₅ toxicity than it was at 3 months. Additionally, this study was the first to use and demonstrate the beneficial effects of the targeted antioxidant CAT-SKL in reducing A β ₂₅₋₃₅ toxicity in an animal model. CAT-SKL was able to reduce cholinergic neuronal loss, decrease neuroinflammation and attenuate long-term memory deficits induced by A β ₂₅₋₃₅ toxicity (Summarized in Figure 25).

4.1 Neuroinflammation

It has been well established that neuroinflammation plays a role in the pathogenesis of AD, and that A β in particular contributes to the neuroinflammatory response (Akiyama et al., 2000). The cellular mediators of inflammation, microglia and astrocytes, were detected using OX-6 and GFAP antibodies respectively, with increased microgliosis and astrogliosis being taken as correlates of inflammation in the brain. Astrocyte activation in response to A β toxicity has been repeatedly reported in cell culture and in animal models of AD (Glass et al., 2010). This study showed an increase in astrocyte density in the CA3 region of the hippocampus in A β ₂₅₋₃₅ administered 6 months old rats.

However, no differences, using optical density measurements, in astrocyte density were identified in the thalamus or CA1 subfield of the hippocampus in rats regardless of treatment or age. The lack of differences seen in astrocyte activation could in part be due to the inefficiency of optical density measurements to detect changes in astrocyte reactivity. Astrocytes only occupy a portion of the area from which optical density measurements were taken. Thus, even a large increase in astrocytes would only result in a small change in optical density measurements. Additionally, work by Zussy et al., reported increased GFAP levels in the frontal cortex, amygdala and hypothalamus in response to A β injection, however no changes in GFAP levels were identified in the hippocampus (Zussy et al., 2013). Therefore, it may be that activation and proliferation of astrocytes did not occur in the regions of the brain (thalamus, hippocampus) examined in this study.

Six and 9 months old animals showed a significant increase in microglia in the thalamus in response to A β_{25-35} administration compared to 3 months old animals. The involvement of the thalamus in AD has not received the same amount of attention as other brain structures. However, amyloid deposits and neurofibrillary tangles have been shown to occur in almost all thalamic nuclei in the human AD brain (Braak and Braak, 1990). Moreover, structural imaging studies have shown reductions in thalamic volume in the brains of AD patients, with thalamic atrophy correlating with impaired cognitive performance (de Jong et al., 2008; Zarei et al., 2009). In animal models of the disease A β deposition, neuroinflammation and neurodegeneration have been shown to occur in the thalamus. Work by Miao et al., have shown in a transgenic mouse model of AD that with increasing age there is extensive deposition of A β in the thalamic microvasculature and that regions of the thalamus showing A β accumulation also demonstrate enhanced levels of inflammatory cells (Miao et al., 2005; Fan et al., 2007). Thus, the increased microglia activation in this region is in accordance with the reported susceptibility of this region to AD pathology.

A β -induced toxicity elicited an age and dose-dependent increase in microglia in the MSN/VDB of the basal forebrain. Higher doses of A β ₂₅₋₃₅ administration resulted in a significant increase in microglia in the MSN/VDB in 3, 6 and 9 months old rats. Additionally, 6 and 9 months old rats had an increase in microglia activation in this region when compared to 3 months old treatment matched animals. This is in accordance with other studies in rodents that have demonstrated administration of A β ₁₋₄₀ and A β ₂₅₋₃₅ results in increased levels of reactive astrocytes and microglia in the basal forebrain (Scali et al., 1999, Giovannini et al., 2002). The MSN and VDB are part of the basal forebrain cholinergic system, which provides major cholinergic inputs to the hippocampus and neocortex (D'Hooge and De Deyn, 2001; Auld et al., 2002). Neuroinflammation has been shown to occur in susceptible regions of the AD brain, and basal forebrain cholinergic cells have been shown to be selectively vulnerable to AD pathology (Auld et al., 2002). Furthermore, these A β -induced inflammatory responses are thought to contribute to cholinergic hypofunction, which is a well described change associated with human AD pathogenesis.

4.2 The basal forebrain cholinergic system

A significant decrease in the number of chAT immunolabeled cholinergic neurons in the MSN/VDB of the basal forebrain was seen in A β ₂₅₋₃₅ 500nmol administered animals 6 and 9 months of age. This is in agreement with previous studies that have demonstrated both single injection or prolonged exposure to A β peptides, including A β ₁₋₄₀, A β ₁₋₄₂ and A β ₂₅₋₃₅, induces degeneration of cholinergic neurons and results in memory impairment in rodents (Harkany et al., 1995; Terranova et al., 1996; Vaucher et al., 2001; Colom et al., 2010;). Most of the studies examining cholinergic loss in response to A β toxicity however, have directly injected A β peptides into various basal forebrain structures including the MSN and nucleus basalis of Meynert (Terranova et al., 1996; Colom et al., 2010). This study was able to demonstrate cholinergic hypofunction in the MSN/VDB in response to icv A β ₂₅₋₃₅ administration, better demonstrating the selective vulnerability of this cholinergic neuronal population to A β toxicity, as amyloid was

not directly injected into this region. Zussy et al., have shown similar results with icv A β_{25-35} injections resulting in a decrease in cholinergic neurons in the basal forebrain when examined at 3 weeks and 6 weeks post icv A β administration (Zussy et al., 2011; 2013). Demonstrating a loss of cholinergic neurons in the basal forebrain is of significance since it is believed to be one of the earliest pathological events in AD and may contribute to the cognitive impairment associated with the disease process (Auld et al., 2002).

The interplay between neuroinflammation and cholinergic neuronal loss in the basal forebrain has not been extensively studied. However, the A β -induced increase in microglia activation in this region accompanied by a decrease in cholinergic neuronal numbers demonstrated in this study suggests inflammation and cholinergic loss may be linked. The contribution of neuroinflammation to cholinergic degeneration is supported by *in vitro* work that showed brain inflammation, and in particular excessive microglia activation, selectively damages cholinergic neurons in primary rat basal forebrain mixed neuronal/glial cultures (McMillian et al., 1995). Additionally, infusion of lipopolysaccharide, a potent inflammatory molecule, into the basal forebrain of young rats has been shown to induce an extensive inflammatory response accompanied by a significant loss of cholinergic neurons (Wenk et al., 2000). It is thought that inflammatory processes that activate microglia and astrocytes results in the release of cytokines and ROS, which in excess can be detrimental to cellular functioning. Cholinergic neurons in the basal forebrain appear to be particularly susceptible to the damaging effects of such molecules. Therefore, the increase in microglia in the MSN/VDB in response to A β_{25-35} injection could be contributing to cholinergic dysfunction in this region.

4.3 Neuronal integrity

A β_{25-35} induced toxicity was also associated with histopathological changes in the hippocampus. The histological stains H&E and thionin revealed a loss of pyramidal cells in the CA3 region of the hippocampus in A β_{25-35} administered 6 and 9-month-old animals. However, no changes in hippocampal

cell numbers were identified in the CA1 hippocampal subfield. Similar results have been demonstrated by other groups showing decreases in cell numbers in the CA1, CA2 and CA3 regions of the hippocampus (Stepanichev et al., 2004; Zussy et al., 2011; 2013). The loss of hippocampal cells as shown by histological stains suggests impairments in neuronal integrity, however cell counts alone do not confirm cell death. Work by others on the toxicity of the A β ₂₅₋₃₅ fragment indicates that hippocampal cell loss is most likely the result of apoptotic processes (Castro et al., 2010; Guo et al., 2013; Zussy et al., 2013). Cell death, and more specifically apoptosis, could be more thoroughly analyzed using alternative approaches including the labeling of apoptotic cells through dUTP nick end-labeling (TUNEL), or through examination of caspase-3 and caspase-6 expression, both of which play a role in the execution phase of cell apoptosis. Alternatively, necrosis could be examined. Evaluation of apoptosis and necrotic cellular markers could confirm neurodegeneration in the regions examined, and furthermore delineate the way in which cells are dying.

4.4 CAT-SKL

This study was the first to use the targeted antioxidant CAT-SKL to try to reduce the toxicity induced by A β ₂₅₋₃₅ in the mature rat brain. CAT-SKL is a genetically engineered derivative of the antioxidant enzyme catalase. The SKL targeting sequence enables catalase to be more effectively targeted to peroxisomes, where its main function is to metabolize H₂O₂ to oxygen and water. Metabolism of H₂O₂ is critical, because it can react with Fe²⁺ to generate hydroxyl radicals, which are highly reactive species capable of inducing protein, lipid and DNA damage (Markesbery and Carney, 1999; Milton, 2004; Trippier et al., 2013). A β ₂₅₋₃₅ toxicity was induced in 6 months old male Wistar rats. Animals 6 months of age were used based on the findings from aim 1 of this study that demonstrated significantly greater pathology and inflammation in 6 months old A β ₂₅₋₃₅ administered animals in comparison to 3 months old treatment matched animals.

In the present experiments, CAT-SKL was shown to reduce microglia activation in the MSN/VDB and thalamus of 6 months old A β ₂₅₋₃₅ administered

rats. Reduction in microglia activation is likely a secondary consequence of the anti-oxidant properties of the CAT-SKL molecule. By decreasing ROS production, the toxicity induced by A β would be lessened thereby decreasing the activation and proliferation of inflammatory microglia and astrocytes. CAT-SKL may also have aided in reducing the production of inflammatory molecules. Previous studies *in vitro* have demonstrated the ability of CAT-SKL supplementation to reduce the expression of the inflammatory cytokine TNF- α in a human cell model of psoriasis (Young, 2008). Moreover, CAT-SKL has been shown to protect rat myocytes from hypoxia-reoxygenation and ischemia reperfusion injury via reduction of oxidative stress in cell culture (Undyala et al., 2011).

The demonstrated ability of CAT-SKL to reduce oxidative stress and inflammatory molecules is of particular relevance since A β is believed to exert its toxicity in part by increasing ROS production. This has been demonstrated in neuronal and astrocyte cell cultures where addition of A β results in increased levels of ROS, and in particular H₂O₂ levels (Behl et al., 1994; Goodman et al., 1994; Manelli and Puttfarcken, 1995; Harris et al., 1996). Moreover, *in vivo* continuous infusion of A β ₁₋₄₀ has been shown to increase H₂O₂ formation, reduce the activity of H₂O₂ degrading enzymes and increase the activity of H₂O₂ generating enzymes in the rat brain (Kaminsky and Kosenko, 2008). Thus, the ability of CAT-SKL to specifically metabolize H₂O₂ may be of importance in reducing A β mediated toxicity. A β is also known to upregulate the production of inflammatory molecules, and activate microglia and astrocytes. Thus, CAT-SKL may be exerting its beneficial effect by reducing A β -induced production of ROS and inflammatory molecules, which in turn results in decreased microglia activation and an overall reduction in the inflammatory response.

Treatment with CAT-SKL was also able to decrease cholinergic neuronal loss in the MSN/VDB of the basal forebrain, and promoted neuronal survival in the CA3 region of the hippocampus. Presumably this reduction in neuronal loss is related to the decreased inflammation seen following CAT-SKL treatment. A β , inflammation and ROS work in a self-propagating cycle, with the result being

excessive neuroinflammation and oxidative damage that can disrupt normal cellular functioning and ultimately lead to neuronal death. Stimulation of ROS production and activation of inflammatory molecules in culture has been shown to induce neuronal death. Moreover, A β has been shown to mediate cell death via its production of ROS (Kadowaki et al., 2005). Therefore, the protective effect of CAT-SKL on neuronal functioning and survival could be via CAT-SKL mediated reduction in ROS and inflammation.

Previous studies have investigated the role of catalase in maintaining oxidative equilibrium. Addition of catalase to neuronal cultures challenged with A β has been shown to reduce H₂O₂ levels and improve neuronal survival (Behl et al., 1994; Manelli and Puttfracken, 1995; Zhang et al., 1996). Moreover, inhibition of catalase activity has been shown to enhance the cytotoxicity of A β in neuronal cultures (by increasing ROS levels), indicating an important role of this antioxidant enzyme in maintaining oxidative balance (Behl et al., 1994; Milton, 2001). Work in a transgenic mouse model of AD has demonstrated the beneficial effects of using a superoxide dismutase/catalase mimetic, EUK-207, to reduce A β pathology. EUK-207 was shown to reduce oxidation of nucleic acids and lipid peroxidation, and was able to decrease A β and tau accumulation (Clausen et al., 2012). Moreover, the impact of ROS, and in particular H₂O₂ levels on longevity has been examined in a transgenic mouse line overexpressing human catalase. The study demonstrated a significant enhancement in murine lifespan in mice overexpressing catalase when compared to wild type controls. This increased longevity was attributed in part to the reduction in H₂O₂ levels and oxidative stress (Schriner et al., 2005). Taken together these studies provide evidence for the protective role of catalase in aging, and in reducing A β toxicity. The CAT-SKL molecule may be of further benefit due to its unique targeting signal that directs it to the organelle where it can carry out its function- the peroxisome. A model of A β associated free radical oxidative stress, and the proposed interference of CAT-SKL in the pathway are outlined in Figure 25.

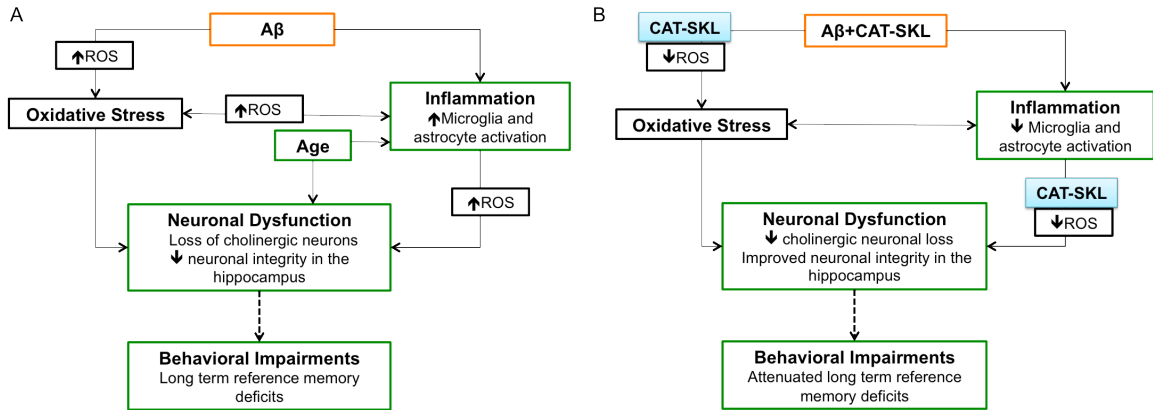


Figure 25. Summary of pathology induced by $A\beta_{25-35}$ toxicity with and without CAT-SKL treatment (A) Outline of pathology induced by $A\beta_{25-35}$ icv administration in rats (B) Pathology in rats administered $A\beta_{25-35}$ and treated with CAT-SKL. Boxes outlined in green were demonstrated in this study.

4.5 Behavior Testing: Morris Water Maze

Spatial learning and reference memory was evaluated in rats using the MWM (D'Hooge and De Deyn 2001; Vorhees and Williams, 2006). No differences in performance were identified between RP, RP+CATSKL, A β and A β +CATSKL treatment groups during the spatial learning task in the MWM, indicating animals from all groups learned the task to the same degree. Other groups examining the learning capabilities of rats in the MWM following icv injection of A β peptides, including A β_{25-35} , have shown deficits in spatial learning (Nabeshima and Nitta, 1994; Chen et al., 1996; Delobette et al., 1997; Guo et al., 2013). The discrepancy between our finding and that of others could be attributed to differences in the time at which behavior testing was started, and/or due to the aggregation state of the A β peptide injected. Work by Delobette et al., showed that the physical state of the peptide, whether aggregated or soluble, at the time of injection influences animals performance in the spatial acquisition phase of the MWM (Delobette et al., 1997). Moreover, a study examining the time course based changes in response to A β_{25-35} toxicity showed that spatial acquisition in rats starting behavioral testing one-week post A β_{25-35} injection did not demonstrate spatial learning deficits. However, those animals beginning testing 2 or 3 weeks following A β_{25-35} administration showed spatial acquisition impairments in the MWM (Zussy et al., 2011). Our study began spatial training 8 days after A β_{25-35} injection, and thus the short time frame may not have been sufficient to allow for A β_{25-35} toxicity to impair spatial learning.

Reference memory was assessed during the probe trials, with probe trial 1 being used to evaluate short-term reference memory retention and probe trial 2 as an assessment of long-term reference memory (Patil et al., 2009). Animals from all treatment groups successfully remembered the platform location during the first probe trial, as indicated by their preference for the target zone over adjacent zones. Additionally, no differences in performance between treatment groups was identified, indicating at this time point A β_{25-35} toxicity did not result in impairments in reference memory. During the second probe trial, 19 days after

$A\beta_{25-35}$ injection, animals showed a significantly decreased preference for the target zone than animals from other treatment groups. $A\beta_{25-35}$ injected animals also spent less time and travelled a shorter distance in the target zone during the second probe trial compared to the first probe trial. This decreased preference for the target zone during the second probe trial was not seen in $A\beta_{25-35}$ administered animals treated with CAT-SKL. Taken together this indicates that $A\beta_{25-35}$ icv administration induces long-term reference memory deficits, and moreover treatment with CAT-SKL is able to attenuate $A\beta_{25-35}$ induced long-term reference memory impairments. These results confirm that cognitive impairment develops approximately 3 weeks after the administration of amyloid peptides in rats (Zussy et al., 2011).

During cued learning no differences in swimming speed, path length, or latency to reach the cued platform location were identified between treatment groups. Cued learning served as an important control procedure, as the task requires many of the same basic abilities (intact eyesight, swimming ability) basic strategies (learning to swim away from the wall, learning to climb on the platform) and the same motivation (escape from the water) as the spatial version of the task. If animals are not capable of performing the cued task it casts doubt on the ability of animals to learn using distal cues in the spatial task (Vorhees and Williams, 2006). Since animals from all treatment groups were found equally competent at completing the cued task, differences in memory retention can more reliably be attributed to differences in treatment.

The deficits seen in long-term reference memory could be a consequence of cholinergic neuronal loss in the MSN/VDB of the basal forebrain induced by $A\beta_{25-35}$ toxicity. Moreover, the ability of CAT-SKL to reduce long-term reference memory deficits in $A\beta_{25-35}$ injected rats could be due in part to the ability of CAT-SKL to rescue cholinergic neurons. Previous studies have demonstrated that lesions of the MSN and/or nucleus basalis of the basal forebrain impair MWM performance in rodents (D'Hooge and De Deyn, 2001). Intracerebroventricular injection of $A\beta_{25-35}$ in mice has also been shown to induce MWM memory

impairments that were reversed by the cholinergic agents tacrine and nicotine. Tacrine is an acetylcholinesterase inhibitor, and nicotine is an acetylcholine receptor agonist, both of which exert their effects by promoting cholinergic functioning. The ability of tacrine and nicotine to reverse the behavioral deficits induced by $A\beta_{25-35}$ administration suggests that cholinergic dysfunction contributes to spatial learning and reference memory impairments (Maurice et al., 1996). The $A\beta_{25-35}$ induced cholinergic deficits accompanied by impairments in long term reference memory seem to be in accordance with the well-described cholinergic dysfunction and memory impairments reported in AD.

4.6 Limitations and Future Directions

There are several limitations to this study, most of which are likely to be resolved with further investigation. This study only examined the pathology induced by $A\beta$ -toxicity 21 days following icv administration. Evaluation of pathology at additional time points would allow for a better understanding of the time course of $A\beta_{25-35}$ induced pathological changes in the brain and moreover could help determine if $A\beta$ -induced pathology is progressive in this model. Additionally, this model only replicates some of the $A\beta$ -induced pathological changes associated with AD pathogenesis. AD is a complex disease and the sequence of events causing it is not fully understood. Thus, no animal model is able to fully simulate all aspects of the human AD condition. This does not negate the usefulness of modeling aspects of the human disease in animals as investigations in such models can help dissect out the complexity of the human condition and provide useful information on the pathogenic impact and underlying mechanisms of specific components of the disease process. Intracerebroventricular administration of $A\beta_{25-35}$ in older animals provides an adult-onset model of $A\beta$ toxicity that demonstrates pathological changes representative of the early stages of the disease process. Such a model is of particular use when evaluating co-morbid conditions as has been done in our lab in the past (Whitehead et al., 2005ab; 2007ab).

This study was able to demonstrate the beneficial effect of CAT-SKL in reducing A β ₂₅₋₃₅ toxicity in the rat brain, however numerous questions remain unanswered and warrant further investigation in regards to the mechanism by which CAT-SKL is reducing A β toxicity. Ongoing work in our lab is currently investigating lipid peroxidation and DNA oxidation levels, both indicators of oxidative stress, in the brains of rats treated with and without CAT-SKL. This combined with more rigorous analysis of oxidative damage in the brain via the use of biochemical assays will help elucidate whether CAT-SKL is exerting its effect by reducing oxidative stress and increasing catalase levels in the rat brain. Furthermore, since this was one of the first studies to use CAT-SKL *in vivo* and information regarding the pharmacokinetics and pharmacodynamics of CAT-SKL are limited, the optimal quantity and dosages of CAT-SKL are uncertain and warrants further investigation. Finally, this was a proof-of principle study with CAT-SKL administration beginning a week prior to A β ₂₅₋₃₅ icv injection; therefore, the neuroprotective effects of CAT-SKL may be due to prevention rather than treatment of A β ₂₅₋₃₅ toxicity. Future studies are needed to elucidate whether CAT-SKL would be beneficial in reducing pre-existing A β -induced pathology.

Section 5

SUMMARY AND CONCLUSIONS

This study demonstrated the importance of considering the age of the animal when modeling A β toxicity. Intracerebroventricular administration of A β ₂₅₋₃₅ in animals 6 and 9 months of age resulted in increased pathology compared to A β ₂₅₋₃₅ induced pathology in 3 months old animals. Older animals showed increased microglia activation in the thalamus and MSN/VDB, decreased number of cholinergic neurons in the basal forebrain, and loss of neuronal integrity in the hippocampus. The majority of studies investigating A β toxicity in non-transgenic models of the disease administer A β in 2-3 month old animals. However, AD is a disease of the elderly, with the most important non-genetic risk factor for late-onset AD being age. A number of changes occur in the brain with age, including increased levels of ROS, increased production of inflammatory mediators, reduced functioning of antioxidant enzymes, and accumulation of modified lipids and proteins. While these changes alone may not manifest themselves as impairments, the progressive accumulation of them over time may alter the brain in such a way that renders it vulnerable to age-associated disease processes. Interestingly, even at 6 and 9 months we were able to show increased A β induced pathology, speaking to the important role that even these ages plays in rendering the brain vulnerable to insult. Although 6 and 9 months is not considered old for a rat, these ages provide a more physiologically relevant equivalent to an adult brain than that of a 3 month animal (Quinn, 2005; Sengupta, 2011). Therefore, icv administration of A β in animals 6 or 9 months of age provides a model for adult-onset A β toxicity with pathological changes that reflect the early stages of AD pathogenesis.

Using this adult-onset model of A β ₂₅₋₃₅ toxicity, we then investigated whether the targeted antioxidant, CAT-SKL could reduce A β ₂₅₋₃₅ induced pathology. Treatment with CAT-SKL decreased A β -induced microglia activation and reduced cholinergic loss in the MSN/VDB of the basal forebrain. Moreover, it decreased astrocyte activation and promoted neuronal survival in the CA3 region of the hippocampus. CAT-SKL treatment also attenuated long-term reference memory deficits induced by A β ₂₅₋₃₅ administration. The precise mechanism by which CAT-SKL was able to reduce A β toxicity *in vivo* is unknown; however, the

neuroprotective effects of the molecule are likely attributed to its antioxidant and anti-inflammatory properties. This preclinical data provides support for the use of CAT-SKL in reducing neuroinflammation and long-term reference memory deficits induced by A β ₂₅₋₃₅.

Substantial evidence exists implicating oxidative stress and neuroinflammation in the pathogenesis of AD. However, whether oxidative stress is an initiator of AD pathogenesis or is a mediator of the disease process remains to be answered. Nonetheless, oxidative stress appears to occur during the early stages of the disease process, before the appearance of amyloid plaques and neurofibrillary tangles in both humans and in animals models of the disease (Dumont and Beal, 2011). Therapeutics aimed at restoring or maintaining the homeostatic balance between production and elimination of ROS, and thus reducing oxidative stress and inflammation during the early stages of the disease may help in slowing disease progression and may aide in the protection of at-risk individuals from the development of AD. The antioxidant molecule, CAT-SKL, may therefore be a viable therapeutic approach for reducing oxidative stress and neuroinflammation during the beginning stages of AD pathogenesis.

References

Abramowski D, Rabe S, Upadhaya AR, Reichwald J, Danner S, Staab D, Capetillo-Zarate E, Yamaguchi H, Saido TC, Wiederhold KH, Thal DR, Staufenbiel M (2012) Transgenic expression of intraneuronal Abeta42 but not Abeta40 leads to cellular abeta lesions, degeneration, and functional impairment without typical alzheimer's disease pathology. *J Neurosci (United States)* 32:1273-1283.

Aizenstein HJ, Nebes RD, Saxton JA, Price JC, Mathis CA, Tsopelas ND, Ziolkowski SK, James JA, Snitz BE, Houck PR, Bi W, Cohen AD, Lopresti BJ, DeKosky ST, Halligan EM, Klunk WE (2008) Frequent amyloid deposition without significant cognitive impairment among the elderly. *Arch Neurol (United States)* 65:1509-1517.

Akiyama H et al (2000) Inflammation and alzheimer's disease. *Neurobiol Aging (United States)* 21:383-421.

Alper G, Sozmen E, Kanit L, Menten G, Ersoz G and Kutay F (1998). Age-related alterations in superoxide dismutase and catalase activities in rat brain. *Tr. J of Medical Sciences (Turkey)* 26:491-494.

Alzheimer A, Stelzmann RA, Schnitzlein HN, Murtagh FR (1995) An english translation of alzheimer's 1907 paper, "uber eine eigenartige erkankung der hirnrinde". *Clin Anat (United States)* 8:429-431.

Ashe KH, Zahs KR (2010) Probing the biology of alzheimer's disease in mice. *Neuron (United States)* 66:631-645.

Auld DS, Kornecook TJ, Bastianetto S, Quirion R (2002) Alzheimer's disease and the basal forebrain cholinergic system: Relations to beta-amyloid peptides, cognition, and treatment strategies. *Prog Neurobiol (England)* 68:209-245.

Bamberger ME, Landreth GE (2002) Inflammation, apoptosis, and alzheimer's disease. *Neuroscientist (United States)* 8:276-283.

Behl C, Davis JB, Lesley R, Schubert D (1994) Hydrogen peroxide mediates amyloid beta protein toxicity. *Cell (United States)* 77:817-827.

Bell RD, Zlokovic BV (2009) Neurovascular mechanisms and blood-brain barrier disorder in alzheimer's disease. *Acta Neuropathol (Germany)* 118:103-113.

Bentahir M, Nyabi O, Verhamme J, Tolia A, Horre K, Wiltfang J, Esselmann H, De Strooper B (2006) Presenilin clinical mutations can affect gamma-secretase activity by different mechanisms. *J Neurochem (England)* 96:732-742.

Braak H, Braak E (1991) Alzheimer's disease affects limbic nuclei of the thalamus. *Acta Neuropathol (Germany)* 81:261-268.

Brookmeyer R, Johnson E, Ziegler-Graham K, Arrighi HM (2007) Forecasting the global burden of alzheimer's disease. *Alzheimers Dement (United States)* 3:186-191.

Bruce-Keller AJ, Li YJ, Lovell MA, Kraemer PJ, Gary DS, Brown RR, Markesbery WR, Mattson MP (1998) 4-hydroxynonenal, a product of lipid peroxidation, damages cholinergic neurons and impairs visuospatial memory in rats. *J Neuropathol Exp Neurol (United States)* 57:257-267.

Butterfield DA, Drake J, Pocernich C, Castegna A (2001) Evidence of oxidative damage in alzheimer's disease brain: Central role for amyloid beta-peptide. *Trends Mol Med (England)* 7:548-554.

Cai H, Wang Y, McCarthy D, Wen H, Borchelt DR, Price DL, Wong PC (2001) BACE1 is the major beta-secretase for generation of abeta peptides by neurons. *Nat Neurosci (United States)* 4:233-234.

Cai XD, Golde TE, Younkin SG (1993) Release of excess amyloid beta protein from a mutant amyloid beta protein precursor. *Science (United States)* 259:514-516.

Calhoun ME, Burgermeister P, Phinney AL, Stalder M, Tolnay M, Wiederhold KH, Abramowski D, Sturchler-Pierrat C, Sommer B, Staufenbiel M, Jucker M (1999) Neuronal overexpression of mutant amyloid precursor protein results in prominent deposition of cerebrovascular amyloid. *Proc Natl Acad Sci U S A (United States)* 96:14088-14093.

Campion D, Dumanchin C, Hannequin D, Dubois B, Belliard S, Puel M, Thomas-Anterion C, Michon A, Martin C, Charbonnier F, Raux G, Camuzat A, Penet C, Mesnage V, Martinez M, Clerget-Darpoux F, Brice A, Frebourg T (1999) Early-onset autosomal dominant alzheimer disease: Prevalence, genetic heterogeneity, and mutation spectrum. *Am J Hum Genet (United States)* 65:664-670.

Castro RE, Santos MM, Gloria PM, Ribeiro CJ, Ferreira DM, Xavier JM, Moreira R, Rodrigues CM (2010) Cell death targets and potential modulators in alzheimer's disease. *Curr Pharm Des (Netherlands)* 16:2851-2864.

Chen SY, Wright JW, Barnes CD (1996) The neurochemical and behavioral effects of beta-amyloid peptide(25-35). *Brain Res (Netherlands)* 720:54-60.

Cheng G, Whitehead SN, Hachinski V, Cechetto DF (2006) Effects of pyrrolidine dithiocarbamate on beta-amyloid (25-35)-induced inflammatory responses and memory deficits in the rat. *Neurobiol Dis (United States)* 23:140-151.

Cimini A, Moreno S, D'Amelio M, Cristiano L, D'Angelo B, Falone S, Benedetti E, Carrara P, Fanelli F, Cecconi F, Amicarelli F, Ceru MP (2009) Early biochemical and morphological modifications in the brain of a transgenic mouse model of

alzheimer's disease: A role for peroxisomes. *J Alzheimers Dis (Netherlands)* 18:935-952.

Citron M, Oltersdorf T, Haass C, McConlogue L, Hung AY, Seubert P, Vigo-Pelfrey C, Lieberburg I, Selkoe DJ (1992) Mutation of the beta-amyloid precursor protein in familial alzheimer's disease increases beta-protein production. *Nature (England)* 360:672-674.

Clausen A, Xu X, Bi X, Baudry M (2012) Effects of the superoxide dismutase/catalase mimetic EUK-207 in a mouse model of alzheimer's disease: Protection against and interruption of progression of amyloid and tau pathology and cognitive decline. *J Alzheimers Dis (Netherlands)* 30:183-208.

Collerton D (1986) Cholinergic function and intellectual decline in alzheimer's disease. *Neuroscience (England)* 19:1-28.

Colom LV, Castaneda MT, Banuelos C, Puras G, Garcia-Hernandez A, Hernandez S, Mounsey S, Benavidez J, Lehker C (2010) Medial septal beta-amyloid 1-40 injections alter septo-hippocampal anatomy and function. *Neurobiol Aging (United States)* 31:46-57.

Corder EH, Saunders AM, Strittmatter WJ, Schmechel DE, Gaskell PC, Small GW, Roses AD, Haines JL, Pericak-Vance MA (1993) Gene dose of apolipoprotein E type 4 allele and the risk of alzheimer's disease in late onset families. *Science (United States)* 261:921-923.

Coyle JT, Price DL, DeLong MR (1983) Alzheimer's disease: A disorder of cortical cholinergic innervation. *Science (United States)* 219:1184-1190.

de Jong LW, van der Hiele K, Veer IM, Houwing JJ, Westendorp RG, Bollen EL, de Bruin PW, Middelkoop HA, van Buchem MA, van der Grond J (2008) Strongly reduced volumes of putamen and thalamus in alzheimer's disease: An MRI study. *Brain (England)* 131:3277-3285.

De Strooper B (2003) Aph-1, pen-2, and nicastrin with presenilin generate an active gamma-secretase complex. *Neuron (United States)* 38:9-12.

Delobette S, Privat A, Maurice T (1997) In vitro aggregation facilitates beta-amyloid peptide-(25-35)-induced amnesia in the rat. *Eur J Pharmacol (Netherlands)* 319:1-4.

Deshpande A, Mina E, Glabe C, Busciglio J (2006) Different conformations of amyloid beta induce neurotoxicity by distinct mechanisms in human cortical neurons. *J Neurosci (United States)* 26:6011-6018.

D'Hooge R, De Deyn PP (2001) Applications of the morris water maze in the study of learning and memory. *Brain Res Brain Res Rev (Netherlands)* 36:60-90.

Dickson DW, Crystal HA, Mattiace LA, Masur DM, Blau AD, Davies P, Yen SH, Aronson MK (1992) Identification of normal and pathological aging in prospectively studied nondemented elderly humans. *Neurobiol Aging (United States)* 13:179-189.

Dickstein DL, Walsh J, Brautigam H, Stockton SD, Jr, Gandy S, Hof PR (2010) Role of vascular risk factors and vascular dysfunction in alzheimer's disease. *Mt Sinai J Med (United States)* 77:82-102.

Donev R, Kolev M, Millet B, Thome J (2009) Neuronal death in alzheimer's disease and therapeutic opportunities. *J Cell Mol Med (England)* 13:4329-4348.

Dumont M, Beal MF (2011) Neuroprotective strategies involving ROS in alzheimer disease. *Free Radic Biol Med (United States)* 51:1014-1026.

Eckman CB, Eckman EA (2007) An update on the amyloid hypothesis. *Neurol Clin (United States)* 25:669-82, vi.

Esch FS, Keim PS, Beattie EC, Blacher RW, Culwell AR, Oltersdorf T, McClure D, Ward PJ (1990) Cleavage of amyloid beta peptide during constitutive processing of its precursor. *Science (United States)* 248:1122-1124.

Fan R, DeFilippis K, Van Nostrand WE (2007) Induction of complement proteins in a mouse model for cerebral microvascular A beta deposition. *J Neuroinflammation (England)* 4:22.

Forstl H, Kurz A (1999) Clinical features of alzheimer's disease. *Eur Arch Psychiatry Clin Neurosci (Germany)* 249:288-290.

Gallagher M, Nicolle MM (1993) Animal models of normal aging: Relationship between cognitive decline and markers in hippocampal circuitry. *Behav Brain Res (Netherlands)* 57:155-162.

Genin E et al (2011) APOE and alzheimer disease: A major gene with semi-dominant inheritance. *Mol Psychiatry (England)* 16:903-907.

Giovannini MG, Scali C, Prospero C, Bellucci A, Vannucchi MG, Rosi S, Pepeu G, Casamenti F (2002) Beta-amyloid-induced inflammation and cholinergic hypofunction in the rat brain in vivo: Involvement of the p38MAPK pathway. *Neurobiol Dis (United States)* 11:257-274.

Glass CK, Saijo K, Winner B, Marchetto MC, Gage FH (2010) Mechanisms underlying inflammation in neurodegeneration. *Cell (United States)* 140:918-934.

Glenner GG, Wong CW (1984) Alzheimer's disease: Initial report of the purification and characterization of a novel cerebrovascular amyloid protein. *Biochem Biophys Res Commun (United States)* 120:885-890.

- Goodman Y, Steiner MR, Steiner SM, Mattson MP (1994) Nordihydroguaiaretic acid protects hippocampal neurons against amyloid beta-peptide toxicity, and attenuates free radical and calcium accumulation. *Brain Res (Netherlands)* 654:171-176.
- Gotz J, Eckert A, Matamales M, Ittner LM, Liu X (2011) Modes of abeta toxicity in alzheimer's disease. *Cell Mol Life Sci (Switzerland)* 68:3359-3375.
- Gotz J, Streffer JR, David D, Schild A, Hoerndli F, Pennanen L, Kurosinski P, Chen F (2004) Transgenic animal models of alzheimer's disease and related disorders: Histopathology, behavior and therapy. *Mol Psychiatry (England)* 9:664-683.
- Grammas P (2011) Neurovascular dysfunction, inflammation and endothelial activation: Implications for the pathogenesis of alzheimer's disease. *J Neuroinflammation (England)* 8:26.
- Grammas P, Yamada M, Zlokovic B (2002) The cerebrovasculature: A key player in the pathogenesis of alzheimer's disease. *J Alzheimers Dis (Netherlands)* 4:217-223.
- Guo LL, Guan ZZ, Huang Y, Wang YL, Shi JS (2013) The neurotoxicity of beta-amyloid peptide toward rat brain is associated with enhanced oxidative stress, inflammation and apoptosis, all of which can be attenuated by scutellarin. *Exp Toxicol Pathol (Germany)* 65:579-584.
- Haass C, Selkoe DJ (1993) Cellular processing of beta-amyloid precursor protein and the genesis of amyloid beta-peptide. *Cell (United States)* 75:1039-1042.
- Haass C, Schlossmacher MG, Hung AY, Vigo-Pelfrey C, Mellon A, Ostaszewski BL, Lieberburg I, Koo EH, Schenk D, Teplow DB (1992) Amyloid beta-peptide is produced by cultured cells during normal metabolism. *Nature (England)* 359:322-325.
- Habib LK, Lee MT, Yang J (2010) Inhibitors of catalase-amyloid interactions protect cells from beta-amyloid-induced oxidative stress and toxicity. *J Biol Chem (United States)* 285:38933-38943.
- Hardy J, Selkoe DJ (2002) The amyloid hypothesis of alzheimer's disease: Progress and problems on the road to therapeutics. *Science (United States)* 297:353-356.
- Hardy J, Allsop D (1991) Amyloid deposition as the central event in the aetiology of alzheimer's disease. *Trends Pharmacol Sci (England)* 12:383-388.
- Hardy JA, Higgins GA (1992) Alzheimer's disease: The amyloid cascade hypothesis. *Science (United States)* 256:184-185.

Harkany T, De Jong GI, Soos K, Penke B, Luiten PG, Gulya K (1995) Beta-amyloid (1-42) affects cholinergic but not parvalbumin-containing neurons in the septal complex of the rat. *Brain Res (Netherlands)* 698:270-274.

Harris ME, Wang Y, Pedigo NW, Jr, Hensley K, Butterfield DA, Carney JM (1996) Amyloid beta peptide (25-35) inhibits Na^+ -dependent glutamate uptake in rat hippocampal astrocyte cultures. *J Neurochem (United States)* 67:277-286.

Hayakawa N, Kato H, Araki T (2007) Age-related changes of astrocytes, oligodendrocytes and microglia in the mouse hippocampal CA1 sector. *Mech Ageing Dev (Ireland)* 128:311-316.

Herrup K (2010) Reimagining alzheimer's disease--an age-based hypothesis. *J Neurosci (United States)* 30:16755-16762.

Hochmeister S, Grundtner R, Bauer J, Engelhardt B, Lyck R, Gordon G, Korosec T, Kutzelnigg A, Berger JJ, Bradl M, Bittner RE, Lassmann H (2006) Dysferlin is a new marker for leaky brain blood vessels in multiple sclerosis. *J Neuropathol Exp Neurol (United States)* 65:855-865.

Hoshi M, Sato M, Matsumoto S, Noguchi A, Yasutake K, Yoshida N, Sato K (2003) Spherical aggregates of beta-amyloid (amylospheroid) show high neurotoxicity and activate tau protein kinase I/glycogen synthase kinase-3beta. *Proc Natl Acad Sci U S A (United States)* 100:6370-6375.

Huang Y, Mucke L (2012) Alzheimer mechanisms and therapeutic strategies. *Cell (United States)* 148:1204-1222.

Humpel C (2011) Chronic mild cerebrovascular dysfunction as a cause for alzheimer's disease? *Exp Gerontol (England)* 46:225-232.

Jacobsen KT, Iverfeldt K (2009) Amyloid precursor protein and its homologues: A family of proteolysis-dependent receptors. *Cell Mol Life Sci (Switzerland)* 66:2299-2318.

Jucker M (2010) The benefits and limitations of animal models for translational research in neurodegenerative diseases. *Nat Med (United States)* 16:1210-1214.

Kadowaki H, Nishitoh H, Urano F, Sadamitsu C, Matsuzawa A, Takeda K, Masutani H, Yodoi J, Urano Y, Nagano T, Ichijo H (2005) Amyloid beta induces neuronal cell death through ROS-mediated ASK1 activation. *Cell Death Differ (England)* 12:19-24.

Kaminsky YG, Kosenko EA (2008) Effects of amyloid-beta peptides on hydrogen peroxide-metabolizing enzymes in rat brain in vivo. *Free Radic Res (England)* 42:564-573.

Kaneko I, Morimoto K, Kubo T (2001) Drastic neuronal loss in vivo by beta-

amyloid racemized at ser(26) residue: Conversion of non-toxic [D-ser(26)]beta-amyloid 1-40 to toxic and proteinase-resistant fragments. *Neuroscience (United States)* 104:1003-1011.

Kim JE, Ryu HJ, Choi SY, Kang TC (2012) Tumor necrosis factor-alpha-mediated threonine 435 phosphorylation of p65 nuclear factor-kappaB subunit in endothelial cells induces vasogenic edema and neutrophil infiltration in the rat piriform cortex following status epilepticus. *J Neuroinflammation (England)* 9:6-2094-9-6.

Koepke JI, Nakrieko KA, Wood CS, Boucher KK, Terlecky LJ, Walton PA, Terlecky SR (2007) Restoration of peroxisomal catalase import in a model of human cellular aging. *Traffic (Denmark)* 8:1590-1600.

Kou J, Kovacs GG, Hoftberger R, Kulik W, Brodde A, Forss-Petter S, Honigschnabl S, Gleiss A, Brugger B, Wanders R, Just W, Budka H, Jungwirth S, Fischer P, Berger J (2011) Peroxisomal alterations in alzheimer's disease. *Acta Neuropathol (Germany)* 122:271-283.

Kowall NW, McKee AC, Yankner BA, Beal MF (1992) In vivo neurotoxicity of beta-amyloid [beta(1-40)] and the beta(25-35) fragment. *Neurobiol Aging (United States)* 13:537-542.

Krafft GA, Klein WL (2010) ADDLs and the signaling web that leads to alzheimer's disease. *Neuropharmacology (England)* 59:230-242.

Kubo T, Nishimura S, Kumagae Y, Kaneko I (2002) In vivo conversion of racemized beta-amyloid ([D-ser 26]A beta 1-40) to truncated and toxic fragments ([D-ser 26]A beta 25-35/40) and fragment presence in the brains of alzheimer's patients. *J Neurosci Res (United States)* 70:474-483.

Lambert MP, Barlow AK, Chromy BA, Edwards C, Freed R, Liosatos M, Morgan TE, Rozovsky I, Trommer B, Viola KL, Wals P, Zhang C, Finch CE, Krafft GA, Klein WL (1998) Diffusible, nonfibrillar ligands derived from Abeta1-42 are potent central nervous system neurotoxins. *Proc Natl Acad Sci U S A (United States)* 95:6448-6453.

Landfield PW (1988) Hippocampal neurobiological mechanisms of age-related memory dysfunction. *Neurobiol Aging (UNITED STATES)* 9:571-579.

Leuner K, Muller WE, Reichert AS (2012) From mitochondrial dysfunction to amyloid beta formation: Novel insights into the pathogenesis of alzheimer's disease. *Mol Neurobiol (United States)* 46:186-193.

Lizard G, Rouaud O, Demarquoy J, Cherkaoui-Malki M, Iuliano L (2012) Potential roles of peroxisomes in alzheimer's disease and in dementia of the alzheimer's type. *J Alzheimers Dis (Netherlands)* 29:241-254.

Lovell MA, Xie C, Markesbery WR (2001) Acrolein is increased in alzheimer's disease brain and is toxic to primary hippocampal cultures. *Neurobiol Aging (United States)* 22:187-194.

Lovell MA, Ehmann WD, Butler SM, Markesbery WR (1995) Elevated thiobarbituric acid-reactive substances and antioxidant enzyme activity in the brain in alzheimer's disease. *Neurology (United States)* 45:1594-1601.

Lublin AL, Gandy S (2010) Amyloid-beta oligomers: Possible roles as key neurotoxins in alzheimer's disease. *Mt Sinai J Med (United States)* 77:43-49.

Lue LF, Brachova L, Civin WH, Rogers J (1996) Inflammation, A beta deposition, and neurofibrillary tangle formation as correlates of alzheimer's disease neurodegeneration. *J Neuropathol Exp Neurol (United States)* 55:1083-1088.

Manelli AM, Puttfarcken PS (1995) Beta-amyloid-induced toxicity in rat hippocampal cells: In vitro evidence for the involvement of free radicals. *Brain Res Bull (United States)* 38:569-576.

Mao P, Manczak M, Calkins MJ, Truong Q, Reddy TP, Reddy AP, Shirendeb U, Lo HH, Rabinovitch PS, Reddy PH (2012) Mitochondria-targeted catalase reduces abnormal APP processing, amyloid beta production and BACE1 in a mouse model of alzheimer's disease: Implications for neuroprotection and lifespan extension. *Hum Mol Genet (England)* 21:2973-2990.

Marcello E, Epis R, Di Luca M (2008) Amyloid flirting with synaptic failure: Towards a comprehensive view of alzheimer's disease pathogenesis. *Eur J Pharmacol (Netherlands)* 585:109-118.

Mark RJ, Lovell MA, Markesbery WR, Uchida K, Mattson MP (1997) A role for 4-hydroxynonenal, an aldehydic product of lipid peroxidation, in disruption of ion homeostasis and neuronal death induced by amyloid beta-peptide. *J Neurochem (United States)* 68:255-264.

Markesbery WR, Carney JM (1999) Oxidative alterations in alzheimer's disease. *Brain Pathol (Switzerland)* 9:133-146.

Markesbery WR, Lovell MA (1998) Four-hydroxynonenal, a product of lipid peroxidation, is increased in the brain in alzheimer's disease. *Neurobiol Aging (United States)* 19:33-36.

Massaad CA (2011) Neuronal and vascular oxidative stress in alzheimer's disease. *Curr Neuropharmacol (United Arab Emirates)* 9:662-673.

Maurice T, Lockhart BP, Privat A (1996) Amnesia induced in mice by centrally administered beta-amyloid peptides involves cholinergic dysfunction. *Brain Res (Netherlands)* 706:181-193.

- Mawuenyega KG, Sigurdson W, Ovod V, Munsell L, Kasten T, Morris JC, Yarasheski KE, Bateman RJ (2010) Decreased clearance of CNS beta-amyloid in alzheimer's disease. *Science (United States)* 330:1774.
- McMillian M, Kong LY, Sawin SM, Wilson B, Das K, Hudson P, Hong JS, Bing G (1995) Selective killing of cholinergic neurons by microglial activation in basal forebrain mixed neuronal/gliial cultures. *Biochem Biophys Res Commun (United States)* 215:572-577.
- Merlini M, Meyer EP, Ulmann-Schuler A, Nitsch RM (2011) Vascular beta-amyloid and early astrocyte alterations impair cerebrovascular function and cerebral metabolism in transgenic arcAbeta mice. *Acta Neuropathol (Germany)* 122:293-311.
- Miao J, Xu F, Davis J, Otte-Holler I, Verbeek MM, Van Nostrand WE (2005) Cerebral microvascular amyloid beta protein deposition induces vascular degeneration and neuroinflammation in transgenic mice expressing human vasculotropic mutant amyloid beta precursor protein. *Am J Pathol (United States)* 167:505-515.
- Millucci L, Raggiaschi R, Franceschini D, Terstappen G, Santucci A (2009) Rapid aggregation and assembly in aqueous solution of A beta (25-35) peptide. *J Biosci (India)* 34:293-303.
- Milton NG (2004) Role of hydrogen peroxide in the aetiology of alzheimer's disease: Implications for treatment. *Drugs Aging (New Zealand)* 21:81-100.
- Milton NG (2001) Inhibition of catalase activity with 3-amino-triazole enhances the cytotoxicity of the alzheimer's amyloid-beta peptide. *Neurotoxicology (Netherlands)* 22:767-774.
- Milton NG (1999) Amyloid-beta binds catalase with high affinity and inhibits hydrogen peroxide breakdown. *Biochem J (England)* 344 Pt 2:293-296.
- Minger SL, Esiri MM, McDonald B, Keene J, Carter J, Hope T, Francis PT (2000) Cholinergic deficits contribute to behavioral disturbance in patients with dementia. *Neurology (United States)* 55:1460-1467.
- Mohsenzadegan M, Mirshafiey A (2012) The immunopathogenic role of reactive oxygen species in alzheimer disease. *Iran J Allergy Asthma Immunol (Iran)* 11:203-216.
- Morishima-Kawashima M, Oshima N, Ogata H, Yamaguchi H, Yoshimura M, Sugihara S, Ihara Y (2000) Effect of apolipoprotein E allele epsilon4 on the initial phase of amyloid beta-protein accumulation in the human brain. *Am J Pathol (United States)* 157:2093-2099.
- Murray IV, Proza JF, Sohrabji F, Lawler JM (2011) Vascular and metabolic

dysfunction in alzheimer's disease: A review. *Exp Biol Med* (Maywood) (England) 236:772-782.

Nabeshima T, Nitta A (1994) Memory impairment and neuronal dysfunction induced by beta-amyloid protein in rats. *Tohoku J Exp Med* (Japan) 174:241-249.

Nalivaeva NN, Turner AJ (2013) The amyloid precursor protein: A biochemical enigma in brain development, function and disease. *FEBS Lett* (Netherlands) 587:2046-2054.

Nunomura A, Perry G, Pappolla MA, Wade R, Hirai K, Chiba S, Smith MA (1999) RNA oxidation is a prominent feature of vulnerable neurons in alzheimer's disease. *J Neurosci* (United States) 19:1959-1964.

Oda T, Wals P, Osterburg HH, Johnson SA, Pasinetti GM, Morgan TE, Rozovsky I, Stine WB, Snyder SW, Holzman TF (1995) Clusterin (apoJ) alters the aggregation of amyloid beta-peptide (A beta 1-42) and forms slowly sedimenting A beta complexes that cause oxidative stress. *Exp Neurol* (United States) 136:22-31.

Pagani L, Eckert A (2011) Amyloid-beta interaction with mitochondria. *Int J Alzheimers Dis* (England) 2011:925050.

Pappolla MA, Omar RA, Kim KS, Robakis NK (1992) Immunohistochemical evidence of oxidative [corrected] stress in alzheimer's disease. *Am J Pathol* (United States) 140:621-628.

Patil SS, Sunyer B, Hoyer H, Lubec G (2009) Evaluation of spatial memory of C57BL/6J and CD1 mice in the barnes maze, the multiple T-maze and in the morris water maze. *Behav Brain Res* (Netherlands) 198:58-68.

Paxinos G, Watson C (1986) *The Rat Brain in Stereotaxic Coordinates*, 2nd ed. London: Academic Press Inc.

Pearson RC, Sofroniew MV, Cuello AC, Powell TP, Eckenstein F, Esiri MM, Wilcock GK (1983) Persistence of cholinergic neurons in the basal nucleus in a brain with senile dementia of the alzheimer's type demonstrated by immunohistochemical staining for choline acetyltransferase. *Brain Res* (Netherlands) 289:375-379.

Perry EK, Tomlinson BE, Blessed G, Bergmann K, Gibson PH, Perry RH (1978) Correlation of cholinergic abnormalities with senile plaques and mental test scores in senile dementia. *Br Med J* (England) 2:1457-1459.

Pike CJ, Walencewicz AJ, Glabe CG, Cotman CW (1991) In vitro aging of beta-amyloid protein causes peptide aggregation and neurotoxicity. *Brain Res* (Netherlands) 563:311-314.

- Pike CJ, Walencewicz-Wasserman AJ, Kosmoski J, Cribbs DH, Glabe CG, Cotman CW (1995) Structure-activity analyses of beta-amyloid peptides: Contributions of the beta 25-35 region to aggregation and neurotoxicity. *J Neurochem (United States)* 64:253-265.
- Price M, Terlecky SR, Kessel D (2009) A role for hydrogen peroxide in the proapoptotic effects of photodynamic therapy. *Photochem Photobiol (United States)* 85:1491-1496.
- Querfurth HW, LaFerla FM (2010) Alzheimer's disease. *N Engl J Med (United States)* 362:329-344.
- Quinn R (2005) Comparing rat's to human's age: How old is my rat in people years? *Nutrition (United States)* 21:775-777.
- Resende R, Moreira PI, Proenca T, Deshpande A, Busciglio J, Pereira C, Oliveira CR (2008) Brain oxidative stress in a triple-transgenic mouse model of alzheimer disease. *Free Radic Biol Med (United States)* 44:2051-2057.
- Ruan CJ, Zhang L, Chen DH, Li Z, Du GH, Sun L (2010) Effects of trans-2,4-dimethoxystibene against the neurotoxicity induced by abeta(25-35) both in vitro and in vivo. *Neurosci Res (Ireland)* 67:209-214.
- Sagara Y, Dargusch R, Klier FG, Schubert D, Behl C (1996) Increased antioxidant enzyme activity in amyloid beta protein-resistant cells. *J Neurosci (United States)* 16:497-505.
- Santos MJ, Quintanilla RA, Toro A, Grandy R, Dinamarca MC, Godoy JA, Inestrosa NC (2005) Peroxisomal proliferation protects from beta-amyloid neurodegeneration. *J Biol Chem (United States)* 280:41057-41068.
- Sayre LM, Zelasko DA, Harris PL, Perry G, Salomon RG, Smith MA (1997) 4-hydroxynonenal-derived advanced lipid peroxidation end products are increased in alzheimer's disease. *J Neurochem (United States)* 68:2092-2097.
- Scali C, Prospero C, Giovannelli L, Bianchi L, Pepeu G, Casamenti F (1999) Beta(1-40) amyloid peptide injection into the nucleus basalis of rats induces microglia reaction and enhances cortical gamma-aminobutyric acid release in vivo. *Brain Res (Netherlands)* 831:319-321.
- Schliebs R (2005) Basal forebrain cholinergic dysfunction in alzheimer's disease-interrelationship with beta-amyloid, inflammation and neurotrophin signaling. *Neurochem Res (United States)* 30:895-908.
- Schrader M, Fahimi HD (2006) Peroxisomes and oxidative stress. *Biochim Biophys Acta (Netherlands)* 1763:1755-1766.
- Schriner SE, Linford NJ, Martin GM, Treuting P, Ogburn CE, Emond M, Coskun

PE, Ladiges W, Wolf N, Van Remmen H, Wallace DC, Rabinovitch PS (2005) Extension of murine life span by overexpression of catalase targeted to mitochondria. *Science (United States)* 308:1909-1911.

Selkoe DJ (2001) Alzheimer's disease: Genes, proteins, and therapy. *Physiol Rev (United States)* 81:741-766.

Sengupta P, (2011) A scientific review of age determination for a laboratory rat: how old is it in comparison with human age? *Biomed Int* 2:81-89.

Smetanin P, Kobak P, Briante C, Stiff, D, Sherman G, Ahmad, S (2009). Rising Tide: The Impact of Dementia in Canada 2008 to 2038. RiskAnalytica, Alzheimer's society.

Seubert P, Oltersdorf T, Lee MG, Barbour R, Blomquist C, Davis DL, Bryant K, Fritz LC, Galasko D, Thal LJ (1993) Secretion of beta-amyloid precursor protein cleaved at the amino terminus of the beta-amyloid peptide. *Nature (England)* 361:260-263.

Seubert P, Vigo-Pelfrey C, Esch F, Lee M, Dovey H, Davis D, Sinha S, Schlossmacher M, Whaley J, Swindlehurst C (1992) Isolation and quantification of soluble alzheimer's beta-peptide from biological fluids. *Nature (England)* 359:325-327.

Sheikh FG, Pahan K, Khan M, Barbosa E, Singh I (1998) Abnormality in catalase import into peroxisomes leads to severe neurological disorder. *Proc Natl Acad Sci U S A (United States)* 95:2961-2966.

Shoji M, Golde TE, Ghiso J, Cheung TT, Estus S, Shaffer LM, Cai XD, McKay DM, Tintner R, Frangione B (1992) Production of the alzheimer amyloid beta protein by normal proteolytic processing. *Science (United States)* 258:126-129.

Sisodia SS (1992) Beta-amyloid precursor protein cleavage by a membrane-bound protease. *Proc Natl Acad Sci USA (United States)* 89:6075-6079.

Stepanichev MY, Zdobnova IM, Zarubenko II, Moiseeva YV, Lazareva NA, Onufriev MV, Gulyaeva NV (2004) Amyloid-beta(25-35)-induced memory impairments correlate with cell loss in rat hippocampus. *Physiol Behav (United States)* 80:647-655.

Sternberger NH, Sternberger LA (1987) Blood-brain barrier protein recognized by monoclonal antibody. *Proc Natl Acad Sci USA (United States)* 84:8169-8173.

Sternberger NH, Sternberger LA, Kies MW, Shear CR (1989) Cell surface endothelial proteins altered in experimental allergic encephalomyelitis. *J Neuroimmunol (Netherlands)* 21:241-248.

Su B, Wang X, Nunomura A, Moreira PI, Lee HG, Perry G, Smith MA, Zhu X

(2008) Oxidative stress signaling in alzheimer's disease. *Curr Alzheimer Res (United Arab Emirates)* 5:525-532.

Swerdlow RH (2011) Brain aging, alzheimer's disease, and mitochondria. *Biochim Biophys Acta (Netherlands)* 1812:1630-1639.

Tabner BJ, El-Agnaf OM, German MJ, Fullwood NJ, Allsop D (2005) Protein aggregation, metals and oxidative stress in neurodegenerative diseases. *Biochem Soc Trans (England)* 33:1082-1086.

Terlecky SR, Terlecky LJ, Giordano CR (2012) Peroxisomes, oxidative stress, and inflammation. *World J Biol Chem (China)* 3:93-97.

Terlecky SR, Koepke JI, Walton PA (2006) Peroxisomes and aging. *Biochim Biophys Acta (Netherlands)* 1763:1749-1754.

Terlecky SR and Walton PA. (Inventors); Wayne State University (Owner). Promotion of Peroxisomal Catalase Function in Cells. United States patent issued in 2009 (#7601366). Patent approved in European Union, Singapore, New Zealand and Israel.

Terranova JP, Kan JP, Storme JJ, Perreaut P, Le Fur G, Soubrie P (1996) Administration of amyloid beta-peptides in the rat medial septum causes memory deficits: Reversal by SR 57746A, a non-peptide neurotrophic compound. *Neurosci Lett (Ireland)* 213:79-82.

Titorenko VI, Terlecky SR (2011) Peroxisome metabolism and cellular aging. *Traffic (Denmark)* 12:252-259.

Trippier PC, Jansen Labby K, Hawker DD, Mataka JJ, Silverman RB (2013) Target- and mechanism-based therapeutics for neurodegenerative diseases: Strength in numbers. *J Med Chem (United States)* 56:3121-3147.

Tuppo EE, Arias HR (2005) The role of inflammation in alzheimer's disease. *Int J Biochem Cell Biol (England)* 37:289-305.

Undyala V, Terlecky SR, Vander Heide RS (2011) Targeted intracellular catalase delivery protects neonatal rat myocytes from hypoxia-reoxygenation and ischemia-reperfusion injury. *Cardiovasc Pathol (United States)* 20:272-280.

Varadarajan S, Yatin S, Aksenova M, Butterfield DA (2000) Review: Alzheimer's amyloid beta-peptide-associated free radical oxidative stress and neurotoxicity. *J Struct Biol (United States)* 130:184-208.

Vaucher E, Aumont N, Pearson D, Rowe W, Poirier J, Kar S (2001) Amyloid beta peptide levels and its effects on hippocampal acetylcholine release in aged, cognitively-impaired and -unimpaired rats. *J Chem Neuroanat (Netherlands)* 21:323-329.

Venkateshappa C, Harish G, Mahadevan A, Srinivas Bharath MM, Shankar SK (2012) Elevated oxidative stress and decreased antioxidant function in the human hippocampus and frontal cortex with increasing age: Implications for neurodegeneration in alzheimer's disease. *Neurochem Res (United States)* 37:1601-1614.

Vorhees CV, Williams MT (2006) Morris water maze: Procedures for assessing spatial and related forms of learning and memory. *Nat Protoc (England)* 1:848-858.

Walsh DM, Selkoe DJ (2007) A beta oligomers - a decade of discovery. *J Neurochem (England)* 101:1172-1184.

Wenk GL, McGann K, Mencarelli A, Hauss-Wegrzyniak B, Del Soldato P, Fiorucci S (2000) Mechanisms to prevent the toxicity of chronic neuroinflammation on forebrain cholinergic neurons. *Eur J Pharmacol (Netherlands)* 402:77-85.

West MJ (1993) Regionally specific loss of neurons in the aging human hippocampus. *Neurobiol Aging (United States)* 14:287-293.

West MJ, Kawas CH, Stewart WF, Rudow GL, Troncoso JC (2004) Hippocampal neurons in pre-clinical alzheimer's disease. *Neurobiol Aging (United States)* 25:1205-1212.

Whitehead S, Cheng G, Hachinski V, Cechetto DF (2005) Interaction between a rat model of cerebral ischemia and beta-amyloid toxicity: II. effects of triflusal. *Stroke (United States)* 36:1782-1789.

Whitehead SN, Hachinski VC, Cechetto DF (2005) Interaction between a rat model of cerebral ischemia and beta-amyloid toxicity: Inflammatory responses. *Stroke (United States)* 36:107-112.

Whitehead SN, Cheng G, Hachinski VC, Cechetto DF (2007) Progressive increase in infarct size, neuroinflammation, and cognitive deficits in the presence of high levels of amyloid. *Stroke (United States)* 38:3245-3250.

Whitehead SN, Bayona NA, Cheng G, Allen GV, Hachinski VC, Cechetto DF (2007) Effects of triflusal and aspirin in a rat model of cerebral ischemia. *Stroke (United States)* 38:381-387.

Whitehouse PJ, Price DL, Struble RG, Clark AW, Coyle JT, Delon MR (1982) Alzheimer's disease and senile dementia: Loss of neurons in the basal forebrain. *Science (United States)* 215:1237-1239.

Wood CS, Koepke JI, Teng H, Boucher KK, Katz S, Chang P, Terlecky LJ, Papanayotou I, Walton PA, Terlecky SR (2006) Hypocatalasemic fibroblasts accumulate hydrogen peroxide and display age-associated pathologies. *Traffic*

(Denmark) 7:97-107.

Wyss-Coray T, Mucke L (2002) Inflammation in neurodegenerative disease--a double-edged sword. *Neuron (United States)* 35:419-432.

Yamada K, Nabeshima T (2000) Animal models of alzheimer's disease and evaluation of anti-dementia drugs. *Pharmacol Ther (England)* 88:93-113.

Yankner BA, Dawes LR, Fisher S, Villa-Komaroff L, Oster-Granite ML, Neve RL (1989) Neurotoxicity of a fragment of the amyloid precursor associated with alzheimer's disease. *Science (United States)* 245:417-420.

Young CN, Koepke JI, Terlecky LJ, Borkin MS, Boyd Savoy L, Terlecky SR (2008) Reactive oxygen species in tumor necrosis factor-alpha-activated primary human keratinocytes: Implications for psoriasis and inflammatory skin disease. *J Invest Dermatol (United States)* 128:2606-2614.

Zarei M, Patenaude B, Damoiseaux J, Morgese C, Smith S, Matthews PM, Barkhof F, Rombouts SA, Sanz-Arigita E, Jenkinson M (2010) Combining shape and connectivity analysis: An MRI study of thalamic degeneration in alzheimer's disease. *Neuroimage (United States)* 49:1-8.

Zhang Z, Rydel RE, Drzewiecki GJ, Fuson K, Wright S, Wogulis M, Audia JE, May PC, Hyslop PA (1996) Amyloid beta-mediated oxidative and metabolic stress in rat cortical neurons: No direct evidence for a role for H₂O₂ generation. *J Neurochem (United States)* 67:1595-1606.

Zussy C, Brureau A, Keller E, Marchal S, Blayo C, Delair B, Ixart G, Maurice T, Givalois L (2013) Alzheimer's disease related markers, cellular toxicity and behavioral deficits induced six weeks after oligomeric amyloid-beta peptide injection in rats. *PLoS One (United States)* 8:e53117.

Zussy C, Brureau A, Delair B, Marchal S, Keller E, Ixart G, Naert G, Meunier J, Chevallier N, Maurice T, Givalois L (2011) Time-course and regional analyses of the physiopathological changes induced after cerebral injection of an amyloid beta fragment in rats. *Am J Pathol (United States)* 179:315-334.

Appendix



Nov. 01, 2011

This is the 3rd Renewal for this protocol
A Full Protocol submission will be required in 2012

Dear Dr. Cechetto:

Your Animal Use Protocol form entitled:
Mechanisms of Vascular Cognitive Impairment and Prevention of Stroke and Its Consequences
Funding Agency: Kardiatech Inc.

has been approved by the University Council on Animal Care. This approval is valid from **Nov. 01, 2011 to Nov. 30, 2012**. The protocol number for this project is **#2008-113**.

1. This number must be indicated when ordering animals for this project.
2. Animals for other projects may not be ordered under this number.
3. If no number appears please contact this office when grant approval is received.
If the application for funding is not successful and you wish to proceed with the project, request that an internal scientific peer review be performed by the Animal Use Subcommittee office.
4. Purchases of animals other than through this system must be cleared through the ACVS office. Health certificates will be required.

ANIMALS APPROVED FOR 4 Years

| Species | Strain | Other Detail | Pain Level | Animal # Total for 4 Years |
|---------|--------|----------------|------------|----------------------------|
| Rat | Wistar | 250-300 G Male | D | 800 |

REQUIREMENTS/COMMENTS

Please ensure that individual(s) performing procedures on live animals, as described in this protocol, are familiar with the contents of this document.

e.g. Approved Protocol - D. Cechetto, N. McLeod, Z. Amtul, W. Lagerwerf
Approval Letter - N. McLeod, Z. Amtul, W. Lagerwerf

The University of Western Ontario
Animal Use Subcommittee / University Council on Animal Care
Health Sciences Centre, • London, Ontario • CANADA – N6A 5C1
PH: 519-661-2111 ext. 86770 • FL 519-661-2028 • www.uwo.ca/animal



AUP Number: 2008-113

PI Name: Cechetto, David

AUP Title: Mechanisms Of Vascular Cognitive Impairment And Prevention Of Stroke And Its Consequences

Approval Date: 05/06/2013

Official Notice of Animal Use Subcommittee (AUS) Approval: Your new Animal Use Protocol (AUP) entitled "Mechanisms Of Vascular Cognitive Impairment And Prevention Of Stroke And Its Consequences" has been APPROVED by the Animal Use Subcommittee of the University Council on Animal Care. This approval, although valid for four years, and is subject to annual Protocol Renewal.2008-113::5

1. This AUP number must be indicated when ordering animals for this project.
2. Animals for other projects may not be ordered under this AUP number.
3. Purchases of animals other than through this system must be cleared through the ACVS office. Health certificates will be required.

The holder of this Animal Use Protocol is responsible to ensure that all associated safety components (biosafety, radiation safety, general laboratory safety) comply with institutional safety standards and have received all necessary approvals. Please consult directly with your institutional safety officers.

CURRICULUM VITAE

Hayley J Nell

Academic Background:

Master of Science 2011-present
University of Western Ontario, Canada
Anatomy and Cell Biology: Neurobiology
Supervisors: Dr. David Cechetto & Dr. Shawn Whitehead

Bachelor of Medical Science 2007-2011
University of Western Ontario, Canada
Honors Specialization in Medical Science

Academic Awards & Funding:

- Western Graduate Research Scholarship—University of Western Ontario (2011-2013)
- Gabriel G. Altmann Poster Award, Masters in Biological Research—University of Western Ontario (2012)
- Academic Canadian Honour Roll (2008-2012)
- Dean's Honour List (2008-2012)
- Western Scholarship of Excellence—University of Western Ontario (2007-2008)

Related Experience:

Teaching Assistant 2012-2013
University of Western Ontario, Medical Sciences 4900F/G

Presentations:

Poster Presentation: Investigating pathological response to beta-amyloid toxicity in rats; the role of age and inflammation. **H.Nell**, S.Whitehead, D.Cechetto. London Health Research Day 2012, London, ON.

Poster Presentation: Investigating age-related pathological response to beta-amyloid toxicity in rats. **H.Nell**, S.Whitehead, L.Wang, D.Cechetto. Society for Neuroscience conference 2012, New Orleans, LA.

Poster Presentation: Investigating age-related pathological response to beta-amyloid toxicity in rats. **H.Nell**, S.Whitehead, L.Wang, D.Cechetto. 19th Annual Anatomy and Cell Biology Research day 2012, London, ON.

Poster Presentation: The targeted antioxidant, CAT-SKL, reduces beta-amyloid toxicity in the rat brain. **H.Nell**, L.Wang, Q.Liu, C.Giordano, S.Terlecky, P.Walton, S.Whitehead, D.Cechetto. 33rd annual SONA meeting 2013, Waterloo, ON

Published Abstract: D.Cechetto, S.Whitehead, **H.Nell**, L.Wang, H.Pei, E.Lui. Effect of Ginseng extracts in a non-transgenic rat model of A β toxicity. Natural Health Research Conference 2013, Windsor, ON.

Extracurricular Activities & Accomplishments:

Western University Swimming Team 2007-2012

- Member of Western's varsity swimming team, competing at the provincial, national and international level
- Women's team captain 2009-2011

OUA Women of Influence Award; Ontario Scholar Athlete 2010-2011

- Awarded to female student athletes excelling in their chosen sport, field of study, and community involvement

F.W.P Jones Award; Female Athlete of the Year 2010-2011

- Awarded to the female student-athlete who in the opinion of the selection committee made the greatest contribution to athletics within Western university